Chemistry–A European Journal

Supporting Information

Iridium-Catalyzed Domino Hydroformylation/Hydrogenation of Olefins to Alcohols: Synergy of Two Ligands

Weiheng Huang, Xinxin Tian, Haijun Jiao,* Ralf Jackstell,* and Matthias Beller*

1.Analytical Methods

NMR spectra were recorded on Bruker Avance 300 (300 MHz) and Bruker Avance 400(400 MHz) NMR spectrometers. Chemical shifts δ (ppm) are given relative to solvent: references for CDCl3 were 7.26 ppm (^{1}H-NMR) and 77.16 ppm (^{13}C-NMR). ^{13}C-NMR spectra were acquired on a broad band decoupled mode. Multiplets were assigned as s (singlet), d (doublet), t (triplet), dd (doublet of doublet), m (multiplet) and br. s (broad singlet). All measurements were carried out at room temperature unless otherwise stated. Electron impact (EI) mass spectra were recorded on AMD 402 mass spectrometer (70 eV). High resolution mass spectra (HRMS) were recorded on Agilent 6210 Time-of-Flight LC/MS (Agilent) with electrospray ionization (ESI). The data are given as mass units per charge (*m/z*) and intensities of signals are given in brackets. For GC analyses, HP 6890 chromatograph with a 29 m HP5 column was used. The products were isolated from the mixture by following column chromatography on silica gel 60, 0.064-0.2 mm, 70-230 mesh (Merk). Linear to branched ratios were determined by GC analysis of the crude reaction mixture.

2.Materials and Methods

All commercial reagents were ordered from Acros Organics, Alfa Aesar, Aldrich or Strem. Dry solvents were prepared according to standard procedures.[1] Air- and moisture-sensitive syntheses were performed under argon atmosphere in heat gun vacuum dried glassware. Non-commercial ligands were prepared according to literature.[2] Analytical data of literature known compounds were in accord with reported data.

3.Procedure of Ligand Synthesis

Bis(4-methoxyphenyl)(phenyl)phosphane (L1) Dried 1-Bromo-4-methoxybenzene (2.6 mL, 20 mmol) was added slowly to a 100 mL flask with Mg (0.50 g, 24 mmol) in THF (20 mL) under argon atmosphere at room temperature. After stirring for 5 hours, the mixture was cooled to -78 °C, dichlorophenylphosphine (1.36 mL, 10 mmol) in THF (20 mL) solution was added dropwise to the mixture over 30 minutes. Then the mixture was warmed up to room temperature and stirred for 18 hours. The reaction was quenched by saturated NH_4Cl aqueous solution (50 mL). The mixture was extracted by ethylacetate three times (20 mL each), the organic layer was collected, and dried by anhydrous Na_2SO_4. Filtrated then all the volatiles were removed under vacuum. White powder crude product was obtained. The product was recrystallized with warm dried methanol and 1.56 g (52%) product was obtained.

1,2-bis(bis(4-(trifluoromethyl)phenyl)phosphaneyl)ethane (L10) The preparation procedure followed the literature.[3] Dried 1-bromo-4-(trifluoromethyl)benzene (1.68 mL, 12 mmol) was added slowly to a 100 mL flask with Mg (0.32 g, 15 mmol) in THF (20 mL) under argon atmosphere at room temperature. After stirring for 5 hours, the mixture was cooled to -78 °C, 1,2-bis(dichlorophosphaneyl)ethane (0.45 mL, 3 mmol) in THF (10 mL) solution was added to the mixture over 30 minutes. Then the mixture was warmed up to room temperature and stirred for 18 hours. The reaction was quenched by saturated NH_4Cl aqueous solution (50 mL). The mixture was extracted by ethylacetate three times (20 mL each), the organic layer was collected, and dried by anhydrous Na_2SO_4. Filtrated then all the volatiles were removed under vacuum. Orange powder crude product was obtained. The product was recrystallized with warm dried methanol and 0.92 g pale yellow product (46%) was obtained.

1,2-bis(bis(4-fluorophenyl)phosphaneyl)ethane (L11) and **1,2-bis(bis(3,5-bis(trifluoromethyl)phenyl)phosphaneyl)ethane (L12)** The procedure followed the same method above.

4.General Procedure for the Hydroformylation/reduction of Olefins

Hydroformylation/reduction experiments were carried out in a 300 mL autoclave which can be placed with six 4 mL vials or five 12 mL vials. Generally, exact amount of Iridium precursor, ligands and PTSA·H_2O or other additives were weighed and added into the vials with a small stirring bar. Solvent, water and olefin were added by syringe under argon atmosphere. The autoclave was flushed by nitrogen gas three times and then twice with carbon monoxide. 40 bar of carbon monoxide was pressurized at room temperature then the autoclave was heated to 140 ℃ for 20 hours with 600 rpm stirring speed. To terminate the reaction, the autoclave was cooled by 0 ℃ ice water. Dioxane was added to dilute and homogenize the reaction solution then isooctane was added as internal standard. The solution was analyzed by gas chromatography.

5.Supplemental experiments

Table S1. Iridium-Catalyzed Hydroformylation/Reduction of 1-Octene: Phosphine ligand free experiments under syn gas. [a]

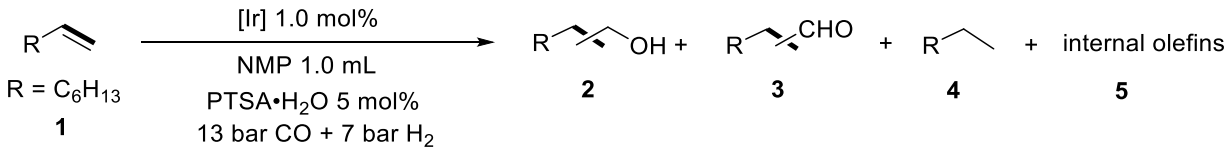

Entry	Iridium precursor	Temp.	Yield (%)[b]			
			2 (n:iso)[c]	**3** (n:iso)	**4**	**5**
1	$[Ir(cod)Cl]_2$	60 ℃	n.d.	12 (52:48)	4	2
2	$[Ir(cod)_2]BF_4$	60 ℃	n.d.	9 (51:49)	3	1
3	$Ir(acac)(CO)_2$	60 ℃	n.d.	2	2	<1
4	$[Ir(cyclooctene)_2Cl_2]_2$	60 ℃	n.d.	13 (59:41)	5	2
5	$IrCl_3$	60 ℃	n.d.	2	<1	<1
6	$[Ir(cod)Cl]_2$	80 ℃	n.d.	29 (69:31)	10	7
7	$[Ir(cod)_2]BF_4$	80 ℃	n.d.	27 (69:31)	13	8
8	$Ir(acac)(CO)_2$	80 ℃	n.d.	13 (62:38)	8	3
9	$[Ir(cyclooctene)_2Cl_2]_2$	80 ℃	n.d.	33 (70:30)	15	11
10	$IrCl_3$	80 ℃	n.d.	2	<1	<1
11	$[Ir(cod)Cl]_2$	100 ℃	n.d.	15 (60:40)	18	7
12	$[Ir(cod)_2]BF_4$	100 ℃	n.d.	16 (63:27)	15	8
13	$Ir(acac)(CO)_2$	100 ℃	n.d.	2	<1	3
14	$[Ir(cyclooctene)_2Cl_2]_2$	100 ℃	n.d.	37 (70:30)	27	22
15	$IrCl_3$	100 ℃	n.d.	2	<1	2
16	$[Ir(cod)Cl]_2$	120 ℃	n.d.	35 (56:44)	45	18
17	$[Ir(cod)_2]BF_4$	120 ℃	n.d.	34 (66:34)	40	21
18	$Ir(acac)(CO)_2$	120 ℃	n.d.	35 (62:38)	46	17
19	$[Ir(cyclooctene)_2Cl_2]_2$	120 ℃	n.d.	34 (56:44)	47	15
20	$IrCl_3$	120 ℃	n.d.	6 (54:46)	8	8

[a] Rection conditions: 1.0 mmol of 1-Octene, 1.0 mol% of [Ir], NMP 1.0 mL, PTSA·H_2O 5 mol%, 20 h. [b] Determined by GC using isooctane (57 mg) as internal standard. [c] n:iso is the ratio of linear product to all branched products.

Table S2. Iridium-Catalyzed Hydroformylation/Reduction of 1-Octene: Phosphine ligand free experiments under WGSR. [a]

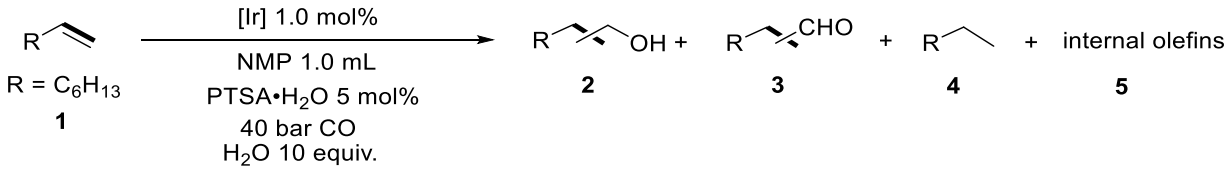

Entry	Iridium precursor	Temp.	Yield (%)[b]			
			2 (n:iso)[c]	**3** (n:iso)	**4**	**5**
1	$[Ir(cod)Cl]_2$	80 ℃	n.d.	7 (81:19)	<1	1
2	$[Ir(cod)_2]BF_4$	80 ℃	n.d.	n.d.	<1	<1
3	$Ir(acac)(CO)_2$	80 ℃	n.d.	n.d.	<1	<1
4	$[Ir(cyclooctene)_2Cl_2]_2$	80 ℃	n.d.	8 (79:21)	<1	2
5	$IrCl_3$	80 ℃	n.d.	12 (76:24)	<1	4
6	$[Ir(cod)Cl]_2$	100 ℃	n.d.	30 (65:35)	34	23
7	$[Ir(cod)_2]BF_4$	100 ℃	n.d.	30 (65:35)	38	29
8	$Ir(acac)(CO)_2$	100 ℃	n.d.	16 (63:37)	20	12
9	$[Ir(cyclooctene)_2Cl_2]_2$	100 ℃	n.d.	16 (73:27)	<1	22
10	$IrCl_3$	100 ℃	n.d.	27 (72:28)	<1	33
11	$[Ir(cod)Cl]_2$	120 ℃	n.d.	10 (66:34)	<1	52
12	$[Ir(cod)_2]BF_4$	120 ℃	n.d.	16 (74:26)	<1	70
13	$Ir(acac)(CO)_2$	120 ℃	n.d.	12 (82:28)	<1	41
14	$[Ir(cyclooctene)_2Cl_2]_2$	120 ℃	n.d.	18 (81:29)	2	72
15	$IrCl_3$	120 ℃	n.d.	17 (57:43)	5	74
16	$[Ir(cod)Cl]_2$	140 ℃	n.d.	9 (26:74)	34	54
17	$[Ir(cod)_2]BF_4$	140 ℃	n.d.	1	31	66
18	$Ir(acac)(CO)_2$	140 ℃	n.d.	1	28	67
19	$[Ir(cyclooctene)_2Cl_2]_2$	140 ℃	n.d.	3 (45:55)	37	57
20	$IrCl_3$	140 ℃	n.d.	12 (21:79)	42	45

[a] Rection conditions: 1.0 mmol of 1-Octene, 1.0 mol% of [Ir], NMP 1.0 mL, PTSA·H_2O 5 mol%, 40 bar CO, H_2O 10 equiv., 20 h. [b] Determined by GC using isooctane (57 mg) as internal standard. [c] n:iso is the ratio of linear product to all branched products.

Table S3. Iridium-Catalyzed Hydroformylation/Reduction of 1-Octene: WGSR alkaline promoters.[a]

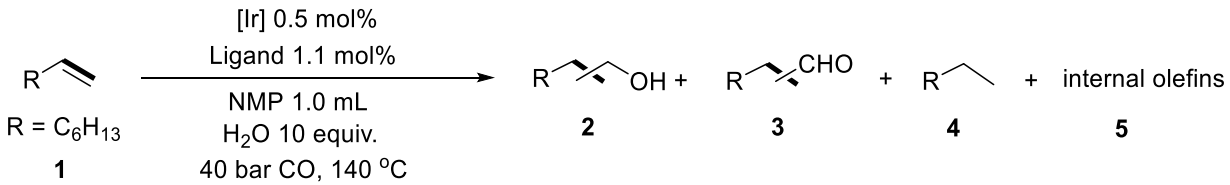

Entry	Ir precursor	Ligand	Base	Conv.	Yield (%)[b]			
					2 (n:iso)[c]	**3** (n:iso)	**4**	**5**
1	$[Ir(cod)Cl]_2$	PPh_3	-	96	n.d.	58 (75:25)	6	32
2	$[Ir(cod)Cl]_2$	PPh_3	NEt_3 10 mol%	0	0	0	0	0
3	$Ir_4(CO)_{12}$	PPh_3	NEt_3 10 mol%	59	n.d.	13 (84:26)	5	41
4	$Ir_4(CO)_{12}$	PCy_3	NEt_3 10 mol%	31	n.d.	3 (76:24)	2	26
5	$Ir_4(CO)_{12}$	PPh_2Py	NEt_3 10 mol%	66	n.d.	40 (77:23)	3	23
6	$Ir_4(CO)_{12}$	PPh_2Py	KOH 5 mol%	2	0	0	0	2
7[d]	$IrCl_3$	PPh_3	NEt_3 10 mol%	84	n.d.	25 (74:26)	8	51
8[d]	$IrCl_3$	**L7**	NEt_3 10 mol%	43	n.d.	23 (78:22)	3	17
9[d]	$IrCl_3$	**L8**	NEt_3 10 mol%	68	n.d.	50 (79:21)	2	16
10[e]	$IrCl_3$	**L10**	-	99	14 (73:27)	72 (63:37)	7	7

[a] Rection conditions: 1.0 mmol of 1-Octene, 0.5 mol% of [Ir], 1.1 mol% of ligand, NMP 1.0 mL, CO 40 bar, H_2O 10 equiv., 140 °C, 20 h. [b] Determined by GC using isooctane (57 mg) as internal standard. [c] n:iso is the ratio of linear product to all branched products. [d] 1.0 mol% of [Ir], 2.2 mol% of ligand. [e] 1.0 mol% of [Ir], 1.1 mol% of ligand.

Table S4. Iridium-Catalyzed Hydroformylation/Reduction of 1-Octene: Solvent.[a]

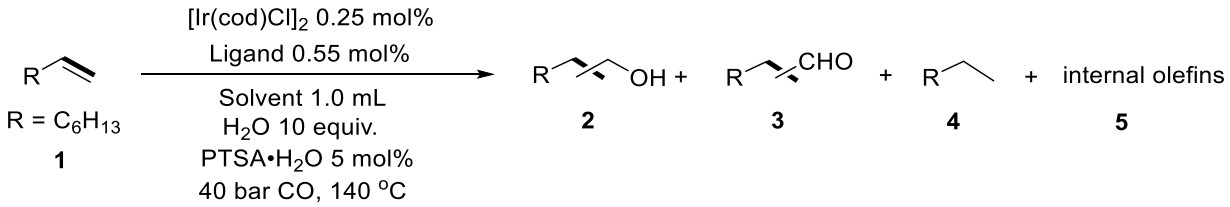

Entry	Solvent	Ligand	Conversion	Yield (%)[b]			
				2 (n:iso)[c]	**3** (n:iso)	**4**	**5**
1	Toluene	dppe	9	n.d.	n.d.	0	9
2	Dioxane	dppe	99	15 (77:23)	35 (45:55)	25	24
3[d]	THF	dppe	80	n.d.	15 (69:31)	29	36
4[d]	Anisole	dppe	0	0	0	0	0
5[d]	EtOH	dppe	0	0	0	0	0
6[d]	Acetonitrile	dppe	0	0	0	0	0
7	NMP	dppe	99	1	47 (58:42)	36	15
8	Toluene	**L10**	99	n.d.	33 (35:65)	32	34
9[e]	Dioxane	**L10**	99	9 (65:35)	22 (38:62)	54	13
10	THF	**L10**	99	55 (62:38)	8 (44:56)	26	6
11	Anisole	**L10**	99	18 (51:49)	54 (71:29)	24	2
12[d]	EtOH	**L10**	99	54 (55:45)	4	39	<1
13[d]	Acetonitrile	**L10**	0	0	0	0	0
14[d]	Water	**L10**	45	n.d.	8 (82:18)	4	33
15	NMP	**L10**	99	47 (66:33)	26 (46:54)	18	3

[a] Rection conditions: 1.0 mmol of 1-Octene, 0.25 mol% of $[Ir(cod)Cl]_2$, 0.55 mol% of ligand, solvent 1.0 mL, CO 40 bar, H_2O 10 equiv., PTSA·H_2O 5 mol%, 140 °C, 20 h. [b] Determined by GC using isooctane (57 mg) as internal standard. [c] n:iso is the ratio of linear product to all branched products. [d] $IrCl_3$ as precursor. [e] $[Ir(cyclooctene)_2Cl]_2$ as precursor.

Table S5. Iridium-Catalyzed Hydroformylation/Reduction of 1-Octene: Precursors.[a]

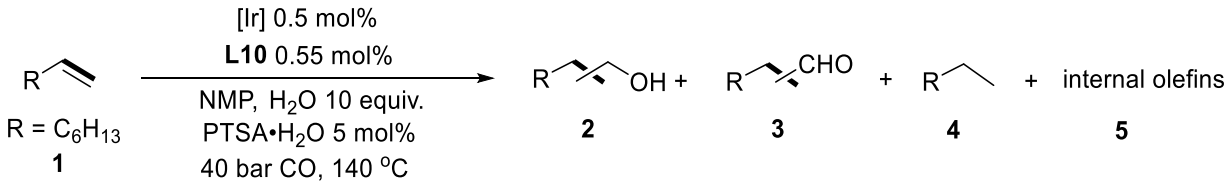

Entry	Catalyst	Yield (%)[b]			
		2 (n:iso)[c]	**3** (n:iso)	**4**	**5**
1	$[Ir(cod)Cl]_2$	47 (66:33)	26 (46:54)	18	3
2[d]	$[Ir(cod)Cl]_2$	62 (63:37)	16 (32:68)	19	3
3	$Ir(acac)(CO)_2$	n.d.	68 (72:28)	16	15
4	$Ir_4(CO)_{12}$	n.d.	52 (76:26)	6	36
5	$[Ir(cod)_2]BF_4$	14 (56:44)	61 (61:39)	15	10
6	$IrCl_3$	39 (57:43)	35 (45:55)	20	3
7[d]	$IrCl_3$	69 (63:37)	11 (27:73)	18	<1
8[e]	-	0	0	0	0

[a] Rection conditions: 1.0 mmol of 1-Octene, 0.5 mol% of [Ir], 0.55 mol% of **L10**, NMP 1.0 mL, CO 40 bar, H_2O 10 equiv., PTSA·H_2O 5 mol%, 140 °C, 20 h. [b] Determined by GC using isooctane (57 mg) as internal standard. [c] n:iso is the ratio of linear product to all branched products. [d] 1.0 mol% of [Ir] and 1.1 mol% of **L10** were used. [e] No iridium precursor.

Table S6. Iridium-Catalyzed Hydroformylation/Reduction of 1-Octene: LiCl.[a]

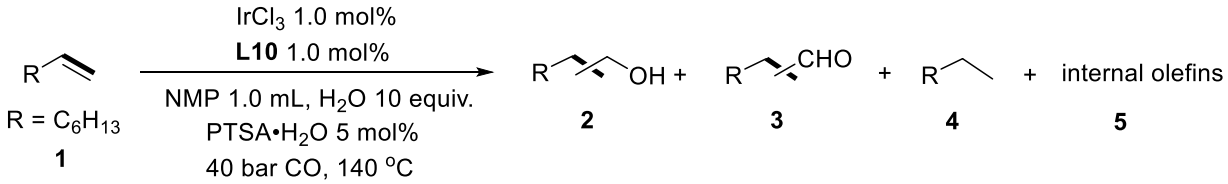

Entry	LiCl (mol%)	Conversion	Yield (%)[b]			
			2 (n:iso)[c]	**3** (n:iso)	**4**	**5**
1	0	99	69 (63:37)	11 (27:73)	18	<1
2	10	99	14 (70:30)	60 (68:32)	16	9
3	25	99	30 (60:40)	40 (48:52)	22	6
4[d]	25	28	10 (53:47)	<1	14	2

[a] Rection conditions: 1.0 mmol of 1-Octene, 1.0 mol% of $IrCl_3$, 1.0 mol% of **L10**, NMP 1.0 mL, 10 equiv. of H_2O, 5 mol% of PTSA·H_2O, 140 °C, 20 h. [b] Determined by GC using isooctane (57 mg) as internal standard. [c] n:iso is the ratio of linear product to all branched products. [d] Syn gas 40 bar ($CO:H_2$ = 1:1) was used instead of H_2O.

Table S7. Iridium-Catalyzed Hydroformylation/Reduction of 1-Octene: Pressuere.[a]

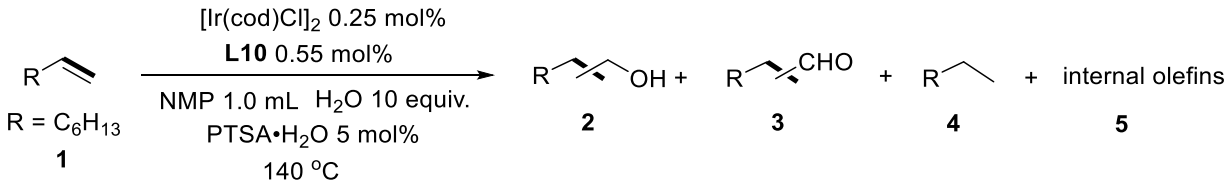

Entry	CO pressure	Yield (%)[b]			
		2 (n:iso)[c]	**3** (n:iso)	**4**	**5**
1[d]	10	13 (74:26)	59 (72:28)	19	8
2	20	10 (80:20)	62 (73:27)	15	10
3	40	47 (66:33)	26 (46:54)	18	3
4[e]	20	0	0	0	0

[a] Rection conditions: 1.0 mmol of 1-Octene, 0.25 mol% of $[Ir(cod)Cl]_2$, 0.55 mol% of **L10**, NMP 1.0 mL, H_2O 10 equiv., PTSA·H_2O 5 mol%, 140 ℃, 20 h. [b] Determined by GC using isooctane (57 mg) as internal standard. [c] n:iso is the ratio of linear product to all branched products. [d] 48 hours. [e] 20 bar CO + 20 bar CO_2.

Table S8. Iridium-Catalyzed Hydroformylation/Reduction of 1-Octene: Temperature.[a]

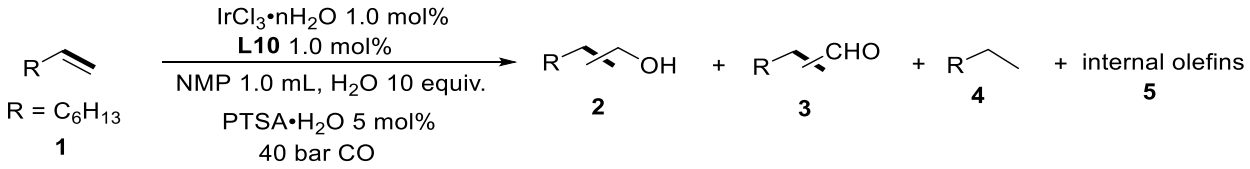

Entry	Temperature	Conversion	Yield (%)[b]			
			2 (n:iso)[c]	**3** (n:iso)	**4**	**5**
2	100 °C	49	n.d.	37 (73:27)	9	2
4	110 °C	98	n.d.	65 (71:29)	8	22
6	120 °C	95	10 (7:3)	65 (62:38)	10	9
8	140 °C	99	47 (66:33)	26 (46:54)	18	3

[a] Rection conditions: 1.0 mmol of 1-Octene, 1.0 mol% of $IrCl_3$, 1.1 mol% of ligand, NMP 1.0 mL, H_2O 10 equiv., PTSA·H_2O 5 mol%, 20 h. [b] Determined by GC using isooctane (57 mg) as internal standard. [c] n:iso is the ratio of linear product to all branched products.

Table S9. Iridium-Catalyzed Hydroformylation/Reduction of 1-Octene: Amount of water.[a]

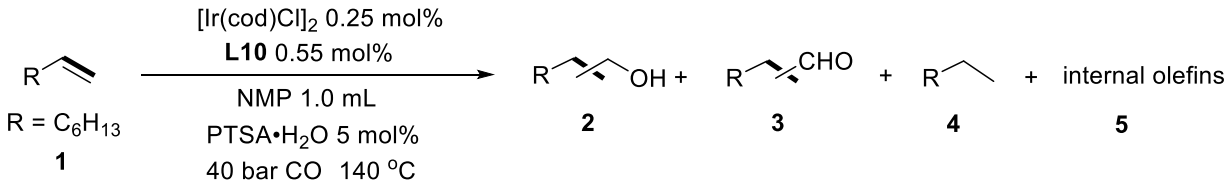

Entry	H_2O (equiv.)	Yield (%)[b]			
		2 (n:iso)[c]	**3** (n:iso)	**4**	**5**
1	5	3 (78:22)	72 (74:26)	9	7
2	10	47 (66:33)	26 (46:54)	18	3
3	20	19 (76:24)	42 (66:34)	38	2
4	50	6 (68:32)	27 (76:24)	56	5

[a] Rection conditions: 1.0 mmol of 1-Octene, 0.25 mol% of $[Ir(cod)Cl]_2$, 0.55 mol% of **L10**, NMP 1.0 mL, PTSA·H_2O 5 mol%, 140 °C, 20 h. [b] Determined by GC using isooctane (57 mg) as internal standard. [c] n:iso is the ratio of linear product to all branched products.

Table S10. Iridium-Catalyzed Hydroformylation/Reduction of 1-Octene: Control experiments.[a]

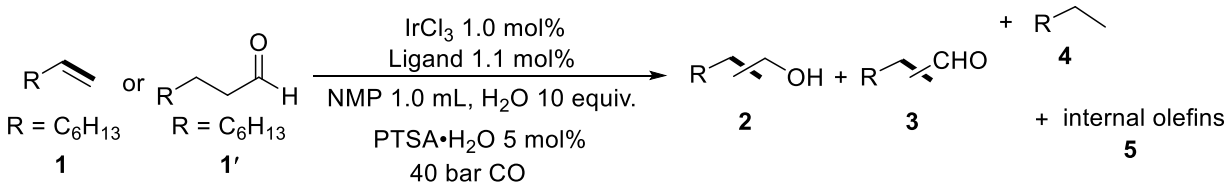

Entry	Temperature	Ligand	Substrate	Yield (%)[b]			
				2 (n:iso)[c]	**3** (n:iso)	**4**	**5**
1	100 ℃	**L1**	1-Octene	n.d.	17 (71:29)	2	22
2	100 ℃	**L10**	1-Octene	n.d.	37 (73:27)	9	2
3	100 ℃	**L1**	Nonanal	n.d.	72	0	0
4	100 ℃	**L10**	Nonanal	n.d.	70	0	0
5	110 ℃	**L1**	1-Octene	n.d.	15 (67:33)	2	23
6	110 ℃	**L10**	1-Octene	n.d.	65 (71:29)	8	22
7	110 ℃	**L1**	Nonanal	n.d.	70	0	0
8	110 ℃	**L10**	Nonanal	8	62	0	0
9	120 ℃	**L1**	1-Octene	n.d.	54 (60:40)	8	32
10	120 ℃	**L10**	1-Octene	10 (7:3)	65 (62:38)	10	9
11	120 ℃	**L1**	Nonanal	n.d.	72	0	0
12	120 ℃	**L10**	Nonanal	16	56	0	0
13[d]	140 ℃	**L1**	1-Octene	n.d.	96 (72:28)	2	1
14	140 ℃	**L10**	1-Octene	47 (66:33)	26 (46:54)	18	3
15	140 ℃	**L1**	Nonanal	n.d.	68	0	0
16	140 ℃	**L10**	Nonanal	28	44	0	0

[a] Rection conditions: 1.0 mmol of 1-Octene, 1.0 mol% of $IrCl_3$, 1.1 mol% of ligand, NMP 1.0 mL, H_2O 10 equiv., PTSA·H_2O 5 mol%, 20 h. [b] Determined by GC using isooctane (57 mg) as internal standard. [c] n:iso is the ratio of linear product to all branched products. [d] ligand : [Ir] = 2.2 : 1.

Table S11. Iridium-catalyzed Hydroformylation/Reduction of 1-octene: Influence of Ligand concentrations.[a]

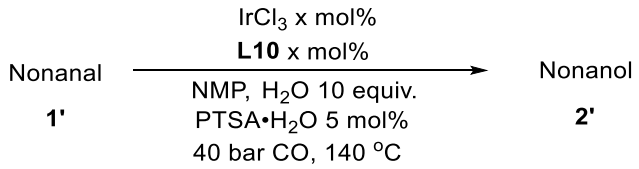

Entry	Mol%	Conversion and Yield (%)[b]		
	x	1' Conversion	2'	Aldol condensation
1[c]	0.8	61	27	17
2[c]	0.5	49	15	17
3[c]	0.3	44	8	18
4[d]	0.8	68	35	16
5[d]	0.5	57	20	18
6[d]	0.3	50	8	20

[a] Rection conditions: 1.0 mmol of 1-octene, x mol% of $IrCl_3$, x mol% of L10, NMP 1.0 mL, CO 40 bar, 10 equiv. of H_2O, 5 mol% of PTSA·H_2O, 140 °C. [b] Determined by GC using isooctane (57 mg) as internal standard. [c] 5 hours. [d] 10 hours.

Table S12. Iridium-Catalyzed Hydroformylation/Reduction of 1-octene: Control experiments (2).[a]

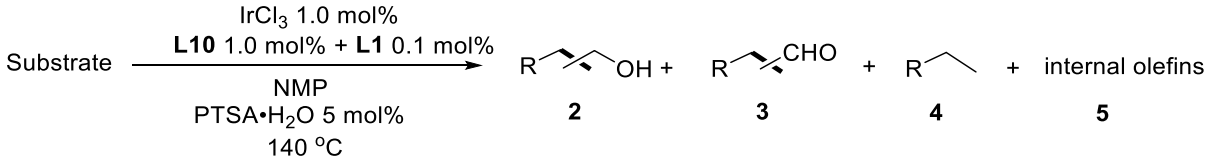

Entry	Substrate	Hydrogen source	Yield (%)[b]			
			2 (n:iso)[c]	**3** (n:iso)	**4**	**5**
1	1-octene	20 bar CO 20 bar H_2	33 (61:39)	1	51	9
2	1-octene	20 bar CO_2 20 bar H_2	n.d.	n.d.	99	0
3[f]	Nonanal	40 bar CO 10 mmol H_2O	25	48	0	0
4[f]	Nonanal	20 bar H_2	93	0	0	0
5[f, h]	Nonanal	20 bar H_2	0	72	0	0
6[f, i]	Nonanal	20 bar H_2	91	n.d.	0	0

[a] Rection conditions: 1.0 mmol of substrate, 1.0 mol% of $IrCl_3$, 1.0 mol% of **L10**, 0.1 mol% of **L1**, NMP 1.0 mL, PTSA·H_2O 5 mol%, 140 °C, 20 h. [b] Determined by GC using isooctane (57 mg) as internal standard. [c] n:iso is the ratio of linear product to all branched products. [g] Nonanal was used as substrate instead of 1-octene, H_2 (20 bar) was used without CO or H_2O. [f] Around 15 % of nonanal was transferred to condensation. [h] Only 1.0 mol% of **L1** was used. [i] Only 1.0 mol% of **L10** was used.

Table S13. Iridium-Catalyzed Hydroformylation/Reduction of 1-Octene: Temperature (mixed ligand).[a]

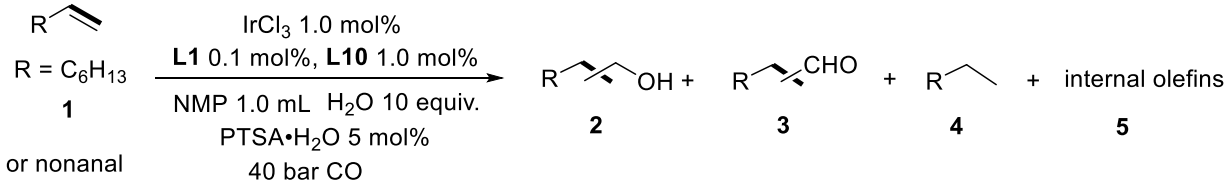

Entry	Substrate	Temperature	Yield (%)[b]			
			2 (n:iso)[c]	**3** (n:iso)	**4**	**5**
1	1-Octene	100	n.d.	33 (78:22)	2	14
2	1-Octene	110	<1	79 (76:24)	5	11
3	1-Octene	120	4 (50:50)	77 (68:32)	8	9
4	1-Octene	130	21 (57:43)	65 (55:45)	9	3
5	Nonanal	100	2	70	0	0
6	Nonanal	110	5	67	0	0
7	Nonanal	120	16	58	0	0
8	Nonanal	130	24	46	0	0

[a] Rection conditions: 1.0 mmol of 1-Octene, 1.0 mol% of $IrCl_3$, 0.1 mol% of **L1**, 1.0 mol% of **L10**, NMP 1.0 mL, CO 40 bar, H_2O 10 equiv., PTSA·H_2O 5 mol%, 20 h. [b] Determined by GC using isooctane (57 mg) as internal standard. [c] n:iso is the ratio of linear product to all branched products.

Table S14. Iridium-Catalyzed Hydroformylation/Reduction of 1-octene: Other metal precursors. [a]

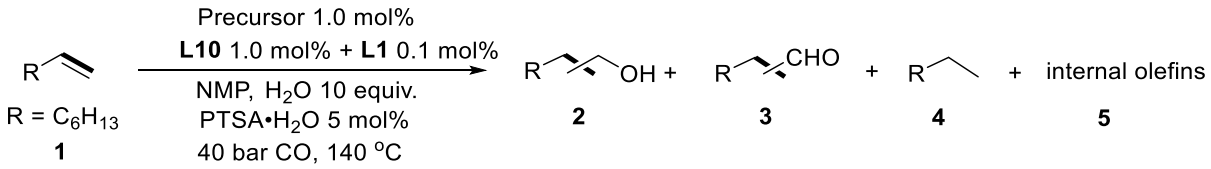

Entry	Precursors	Yield (%)[b]			
		2 (n:iso)[c]	**3** (n:iso)	**4**	**5**
1[d]	$PdCl_2$	n.d.	n.d.	6	59
2	$FeCl_3$	0	0	0	0
3	$CoCl_3$	0	0	0	0
4	$RuCl_3$	0	n.d.	0	32
5	$PtCl_2$	0	n.d.	0	69
6	$RhCl_3$	n.d.	54 (75:25)	8	30

[a] Rection conditions: 1.0 mmol of 1-octene, 1.0 mol% of catalyst, 1.0 mol% of **L10**, 0.1 mol% of **L1**, NMP 1.0 mL, CO 40 bar, 10 equiv. of H_2O, PTSA·H_2O 5 mol%, 140 °C, 20 h. [b] Determined by GC using isooctane (57 mg) as internal standard. [c] n:iso is the ratio of linear product to all branched products. [d] Carboxylic acids products.

Table S15. Iridium-Catalyzed Hydroformylation/Reduction of 1-Octene: Acid free experiments. [a]

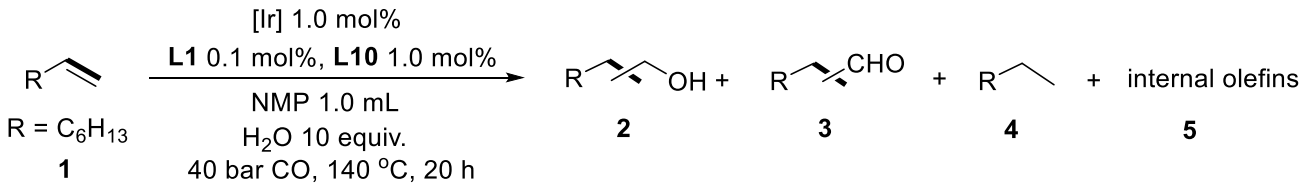

Entry	Iridium precursor	Yield (%)[b]			
		2 (n:iso)[c]	**3** (n:iso)	**4**	**5**
1	Ir_4CO_{12}	n.d.	2	<1	<1
2	$[Ir(cod)Cl]_2$	10 (77:23)	76 (64:36)	3	10
3	$Ir(cod)_2BF_4$	n.d.	21 (58:42)	<1	2
4	$Ir(acac)(CO)_2$	<1	62 (70:30)	2	35
5	$IrCl_3$	14 (73:27)	72 (63:37)	6	8

[a] Rection conditions: 1.0 mmol of 1-Octene, 1.0 mol% of [Ir], NMP 1.0 mL, H_2O 10 equiv., 20 h, CO 40 bar. [b] Determined by GC using isooctane (57 mg) as internal standard. [c] n:iso is the ratio of linear product to all branched products.

Table S16. Iridium-catalyzed Hydroformylation/Reduction of 1-octene: Influence of Ligand concentrations (3). [a]

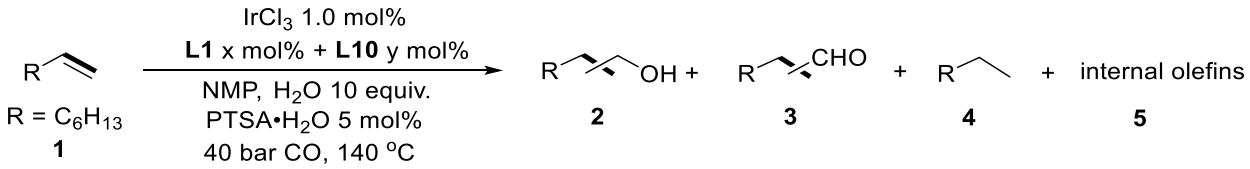

Entry	Mol%		Yield (%)[b]			
	x	Y	2 (n:iso) [c]	3 (n:iso)	4	5
1	0.05	1.0	46 (66:34)	37 (50:50)	16	1
2	0.1	0	n.d.	43 (35:65)	27	24
3[d]	2.0	2.0	72 (72:28)	19 (47:53)	6	<1
4[e]	1.0	1.0	3 (80:20)	78 (68:32)	10	8
5	0.5	1.0	52 (69:31)	41 (60:40)	5	1

[a] Rection conditions: 1.0 mmol of 1-octene, 1.0 mol% of $IrCl_3$, x mol% of L1, y mol% of L10, NMP 1.0 mL, CO 40 bar, 10 equiv. of H_2O, 5 mol% of PTSA·H_2O, 140 ℃, 20 h. [b] Determined by GC using isooctane (57 mg) as internal standard. [c] n:iso is the ratio of linear product to all branched products. [d] 2.0 mol% of $IrCl_3$. [e] 20 bar CO.

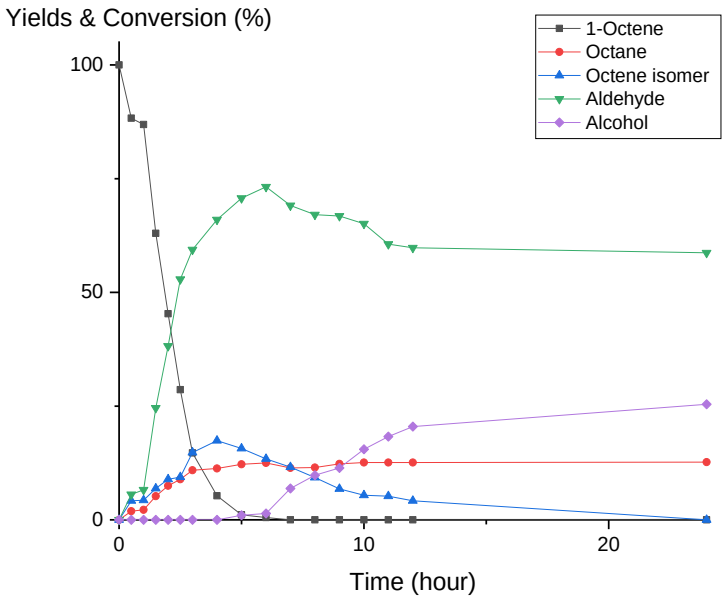

Figure S1. Kinetic profile: rection conditions: 20 mmol of 1-octene, 1.0 mol% of $IrCl_3$, 1.0 mol% of L10, NMP 20 mL, CO 40 bar, 10 equiv. of H_2O, 5 mol% of PTSA·H_2O, 140 °C.

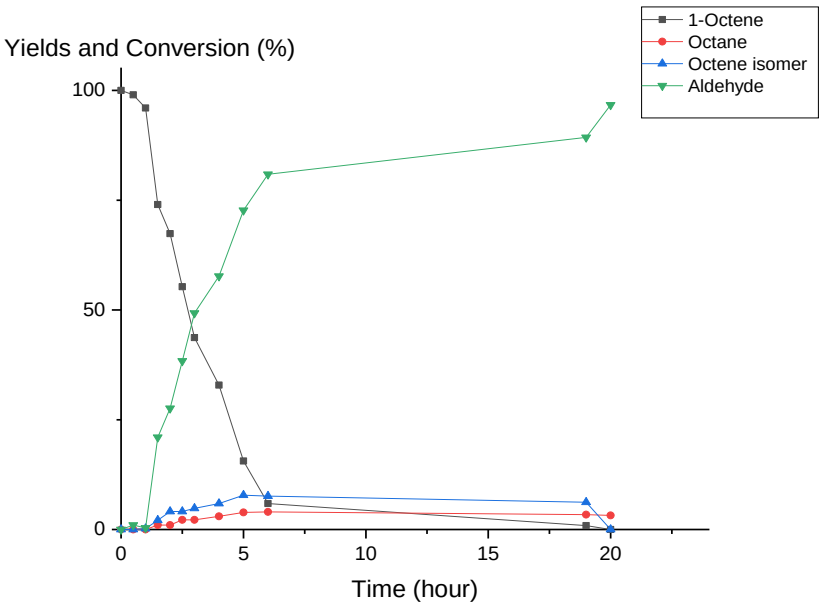

Figure S2. Kinetic profile: rection conditions: 20 mmol of 1-octene, 1.0 mol% of $IrCl_3$, 1.0 mol% of L1, NMP 20 mL, CO 40 bar, 10 equiv. of H_2O, 5 mol% of PTSA·H_2O, 140 °C.

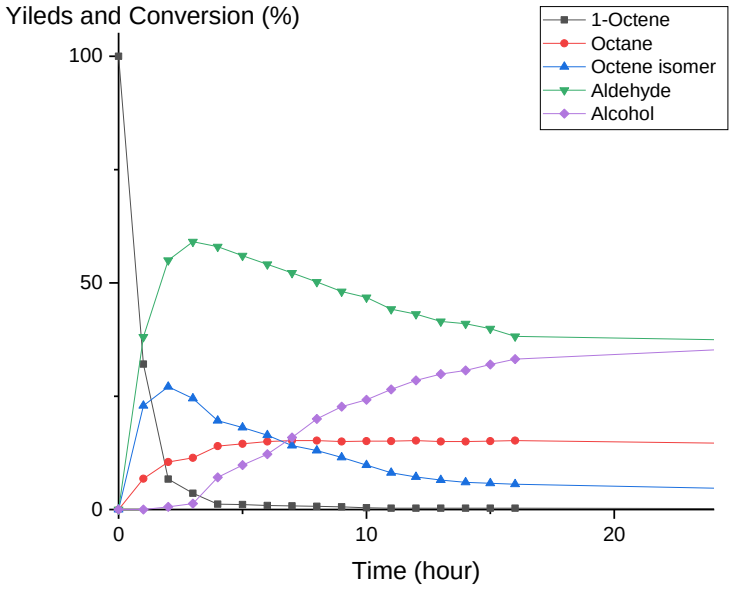

Figure S3. Kinetic profile: rection conditions: 20 mmol of 1-octene, 1.0 mol% of $IrCl_3$, 0.1 mol% of L1, 1.0 mol% of L10, NMP 20 mL, CO 40 bar, 10 equiv. of H_2O, 5 mol% of PTSA·H_2O, 140 °C, first 16 hours.

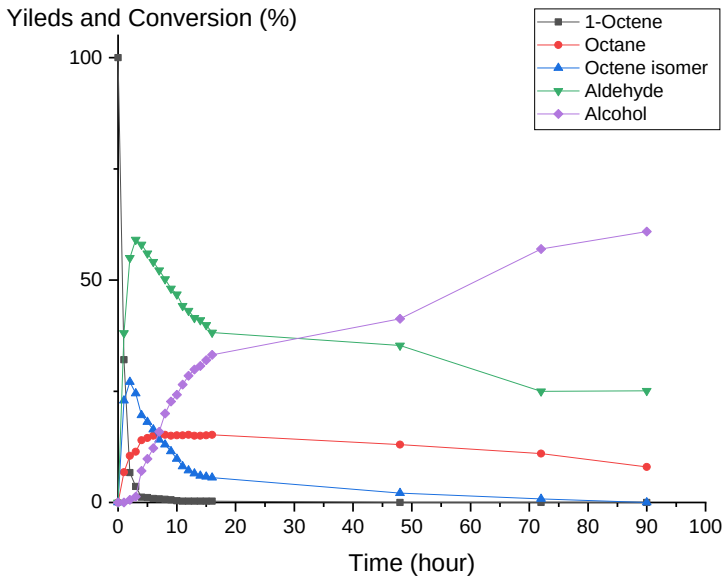

Figure S4. Kinetic profile: rection conditions: 20 mmol of 1-octene, 1.0 mol% of $IrCl_3$, 0.1 mol% of L1, 1.0 mol% of L10, NMP 20 mL, CO 40 bar, 10 equiv. of H_2O, 5 mol% of $PTSA{\cdot}H_2O$, 140 °C.

6.Charaterization of the Ligands

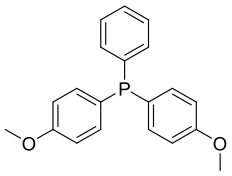

Bis(4-methoxyphenyl)(phenyl)phosphane (L1)

^{1}H NMR (400 MHz, $CDCl_3$) δ/ppm: 7.31-7.25 (m, 9H), 6.91-6.88 (dd, 4H), 3.80 (s, 6H).

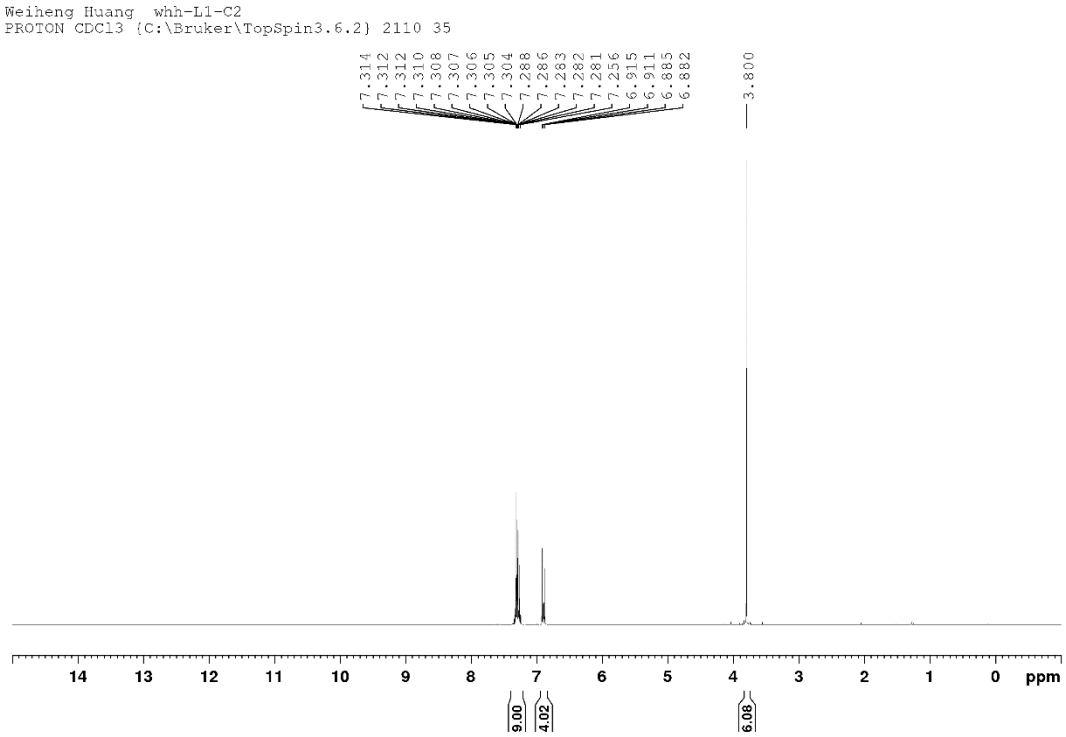

^{31}P NMR (162 MHz, $CDCl_3$) δ/ppm: -8.60.

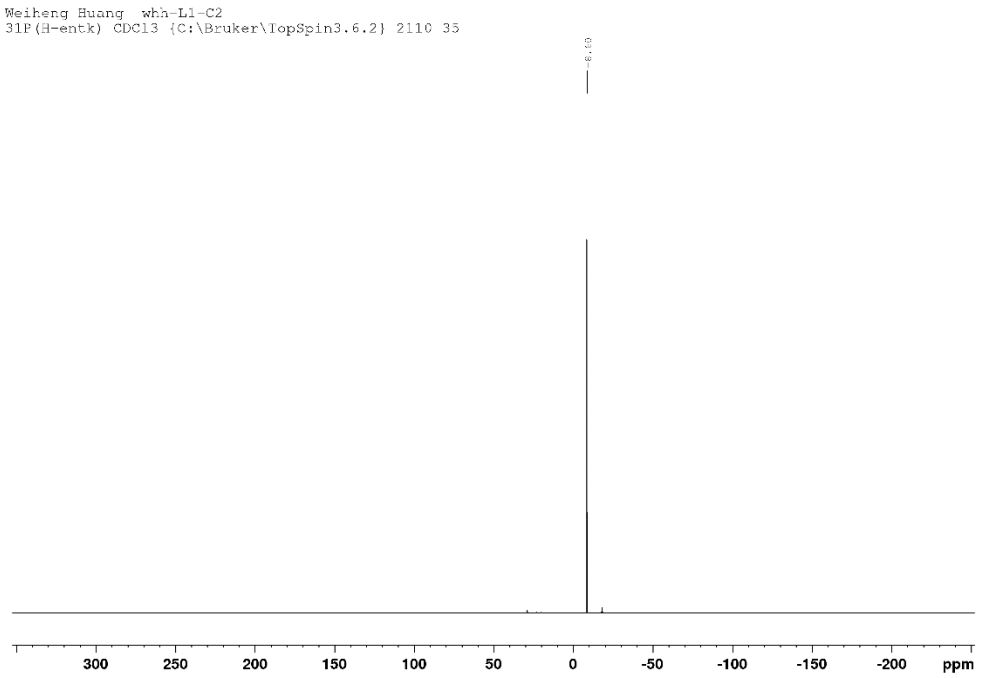

^{13}C NMR (75 MHz, $CDCl_3$) δ/ppm: 160.35, 135.60, 135.33, 133.41, 133.16, 128.71, 128.62, 128.53, 114.47, 114.37, 55.24.

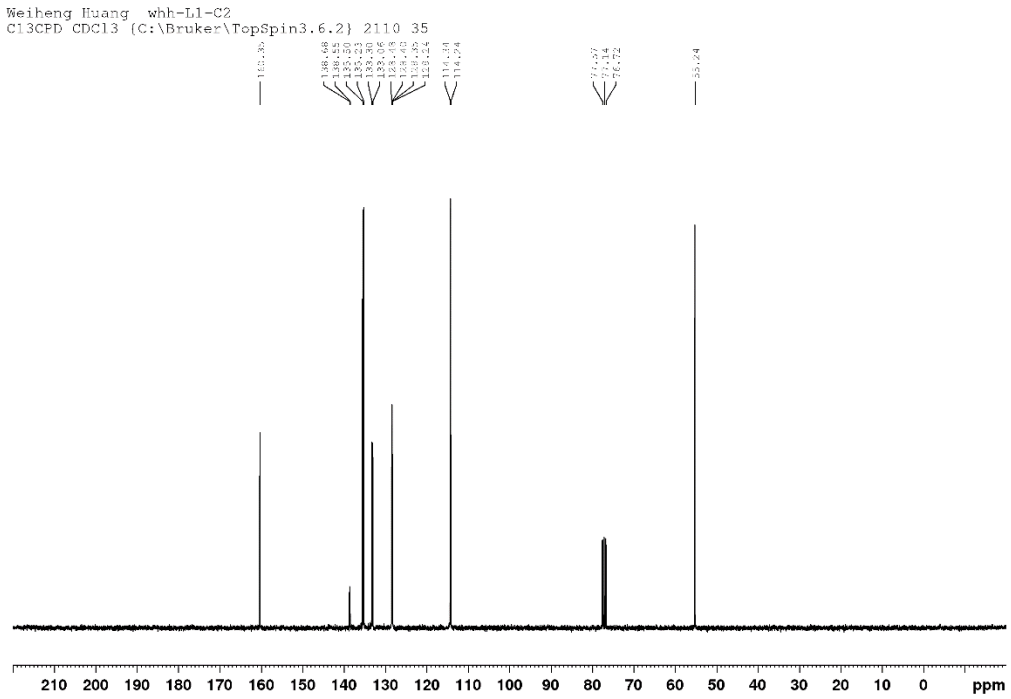

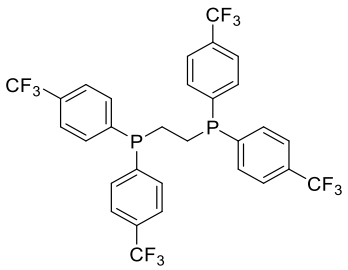

1,2-bis(bis(4-(trifluoromethyl)phenyl)phosphaneyl)ethane (L10)

^{1}H NMR (300 MHz, $CDCl_3$) δ/ppm: 7.58 (d, *J* = 7.92, 8H), 7.40 (d, *J* = 7.83, 8H), 2.13 (s, 4H). *THF: 3.49, 1.20.

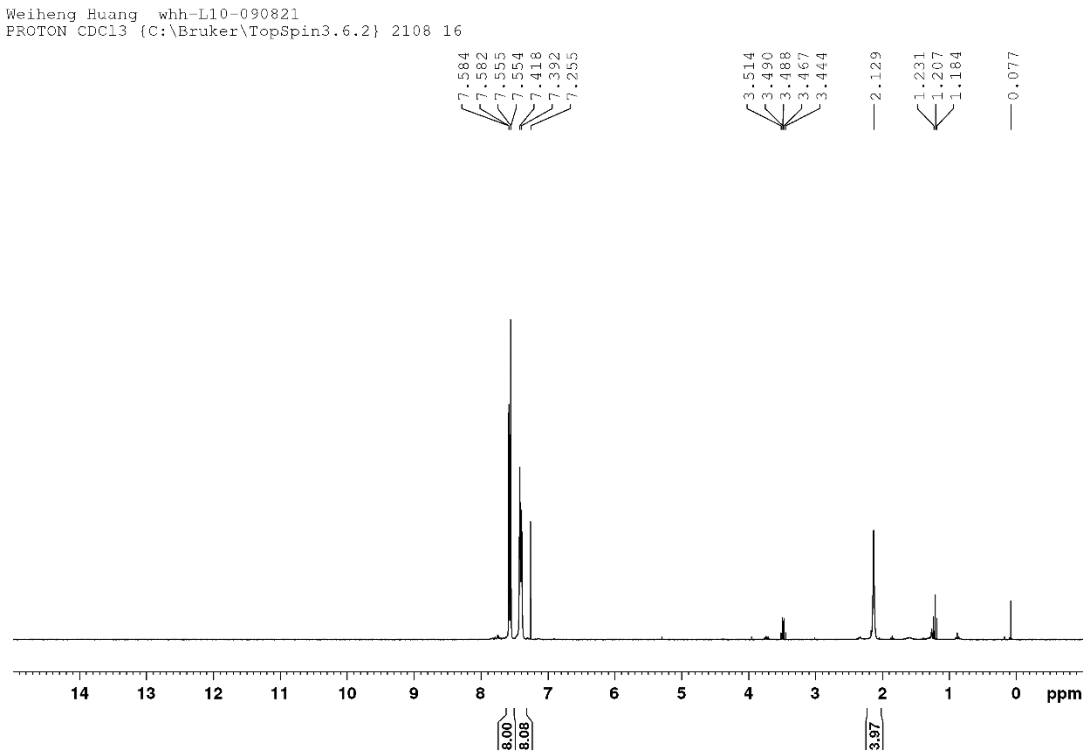

^{19}F NMR (282 MHz, $CDCl_3$) δ/ppm: -62.96.

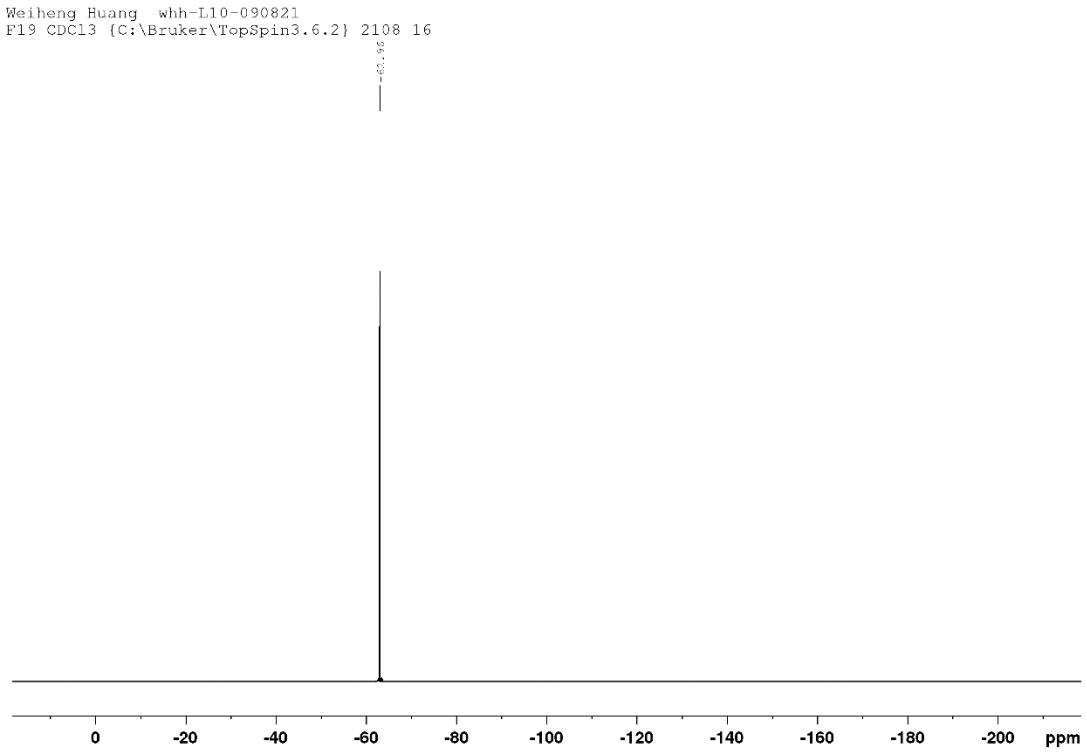

^{31}P NMR (121 MHz, $CDCl_3$) δ/ppm: -13.04.

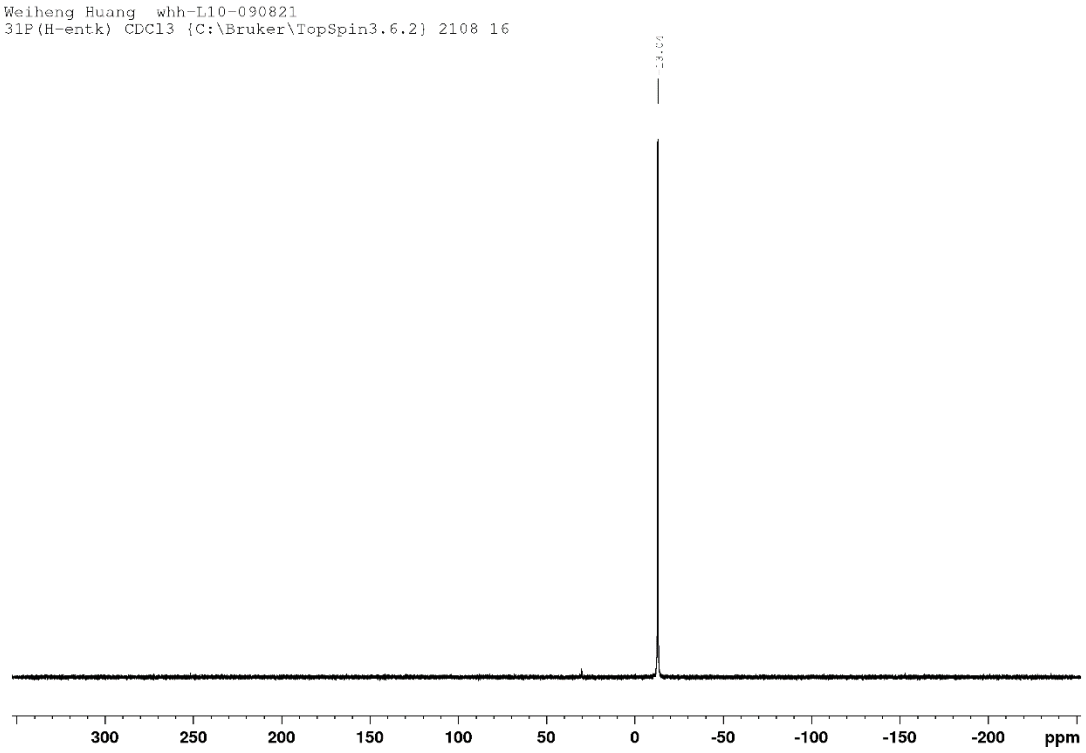

^{13}C NMR (75 MHz, $CDCl_3$) δ/ppm: 142.07, 133.09, 131.22, 125.58, 122.13, 23.61.

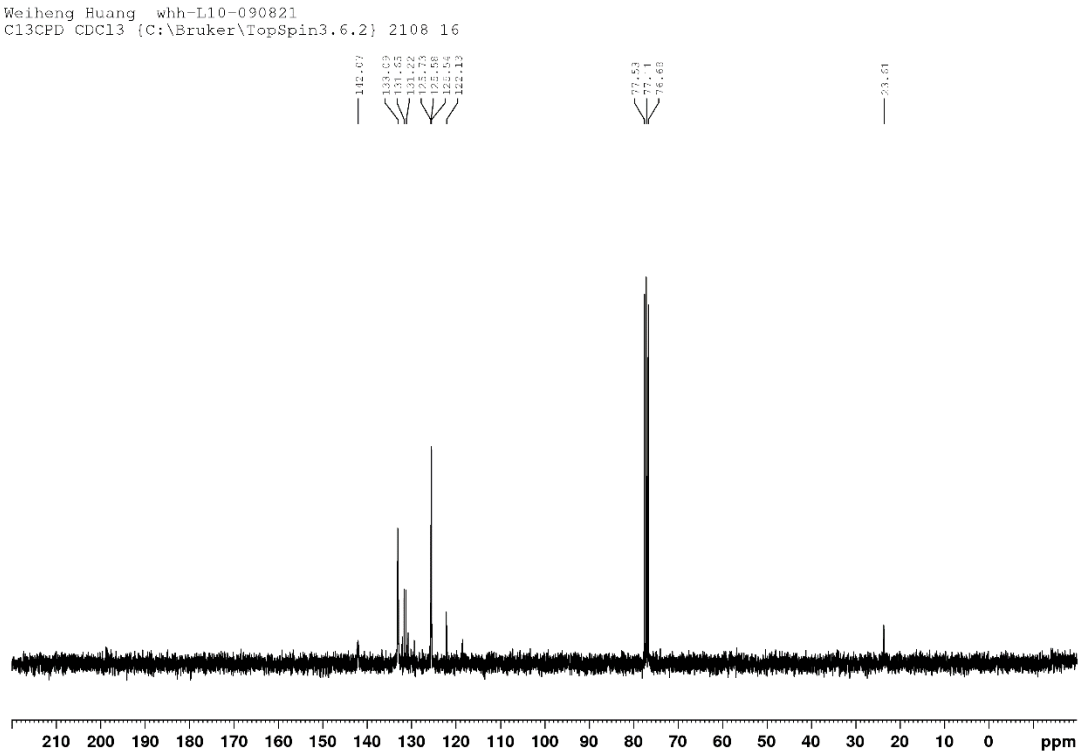

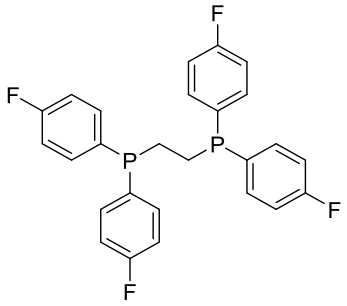

1,2-bis(bis(4-fluorophenyl)phosphaneyl)ethane (L11)

^{1}H NMR (300 MHz, $CDCl_3$) δ/ppm: 7.26-7.30 (m, 8H), 6.98 (t, *J* = 8.36, 8H), 2.00 (t, *J* = 4.18, 4H).
*THF: 3.76, 1.85; Et_2O: 1.21, 3.48.

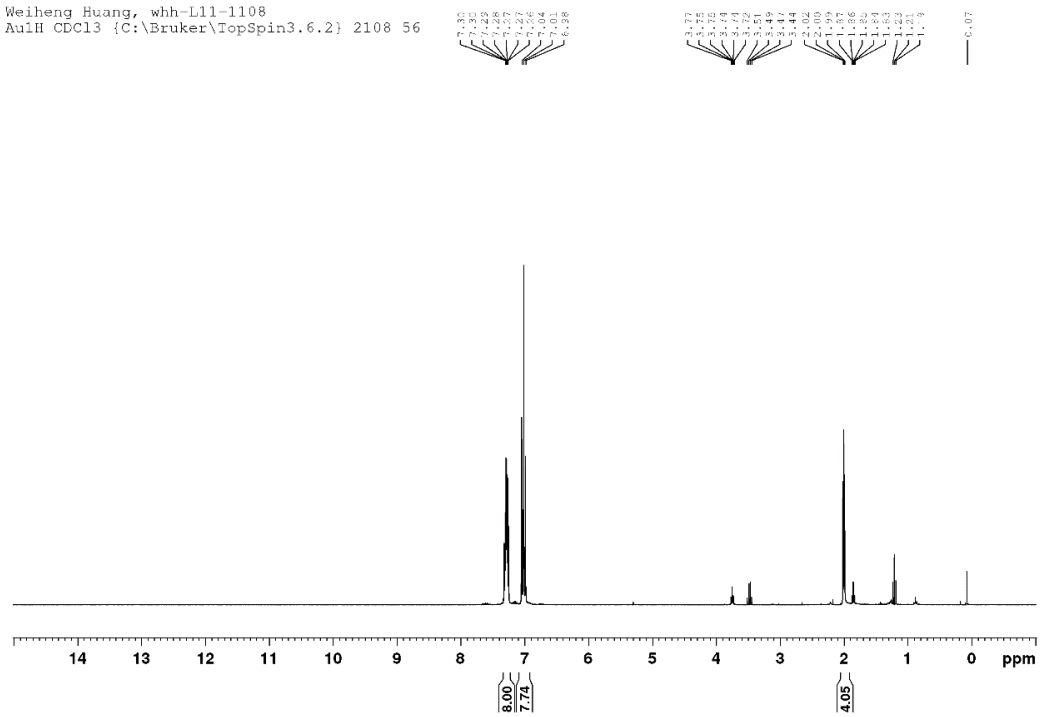

^{19}F NMR (282 MHz, $CDCl_3$) δ/ppm: -111.87.

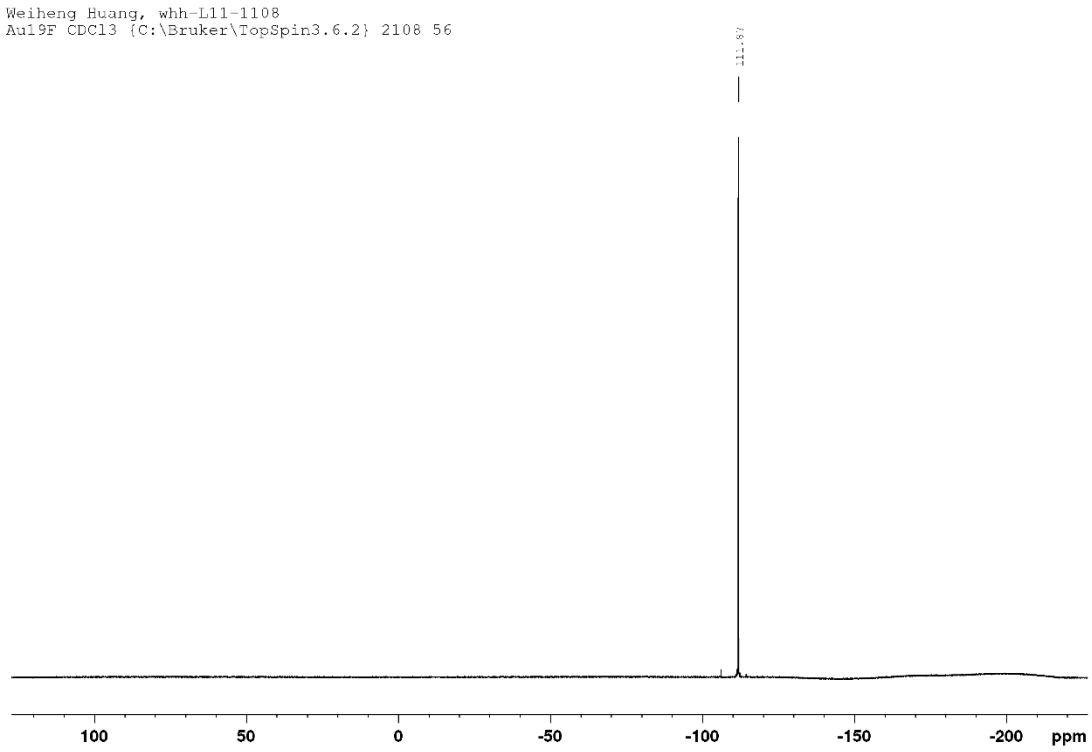

^{31}P NMR (121 MHz, $CDCl_3$) δ/ppm: -15.28.

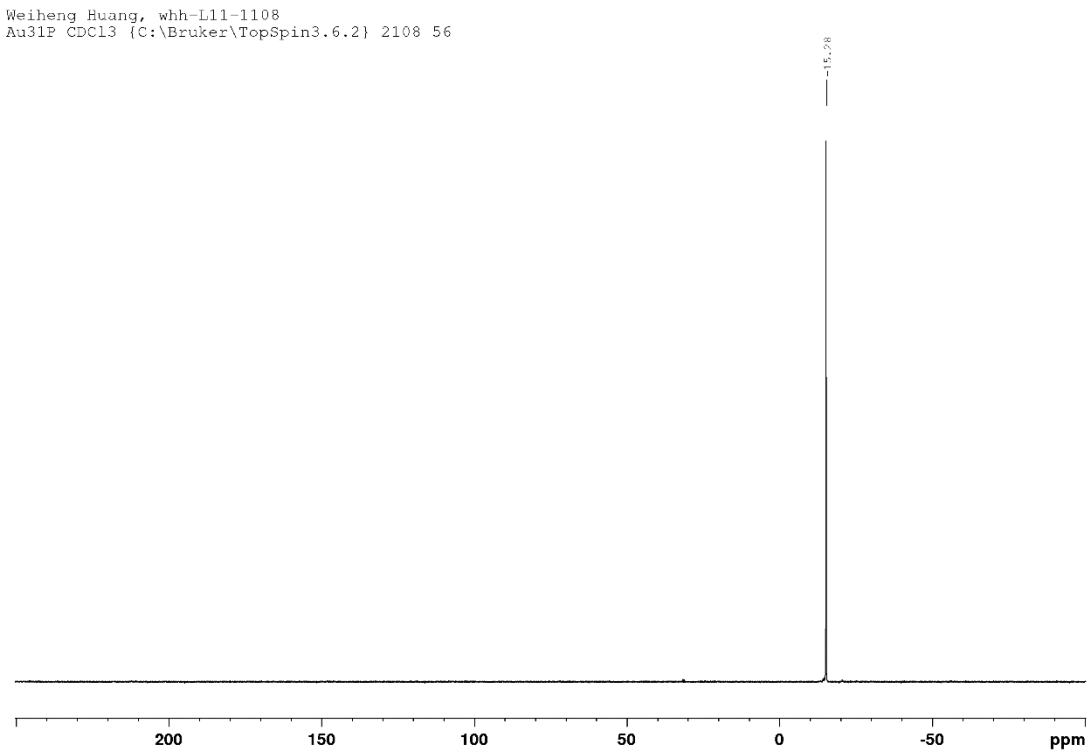

^{13}C NMR (75 MHz, $CDCl_3$) δ/ppm: 161.95, 134.76, 134,65, 166.15, 24.40.

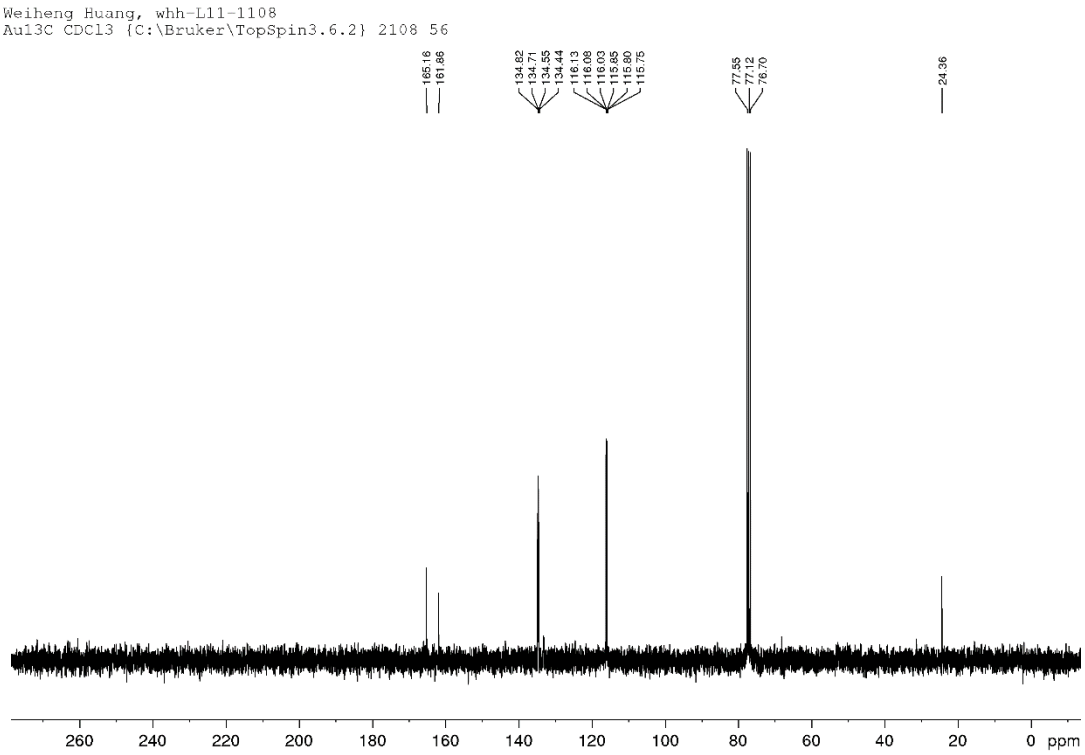

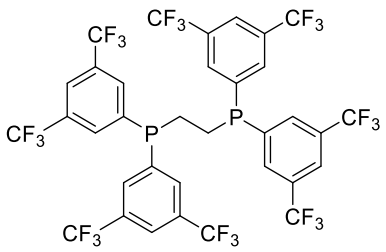

1,2-bis(bis(3,5-bis(trifluoromethyl)phenyl)phosphaneyl)ethane (L12)

^{1}H NMR (300 MHz, $CDCl_3$) δ/ppm: 7.91 (s, 4H), 7.75 (s, 8H), 2.24 (t, *J* = 10.80, 4H). *THF: 3.76, 1.85; *Acetone: 2.17.

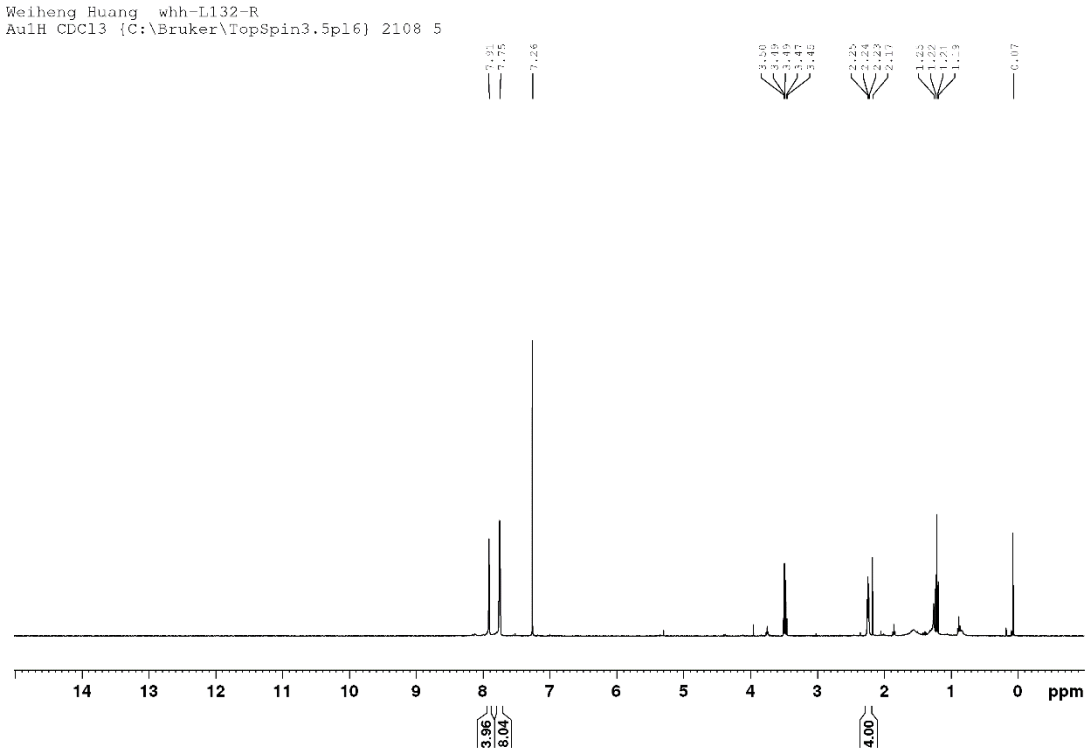

^{19}F NMR (282 MHz, $CDCl_3$) δ/ppm: -63.11.

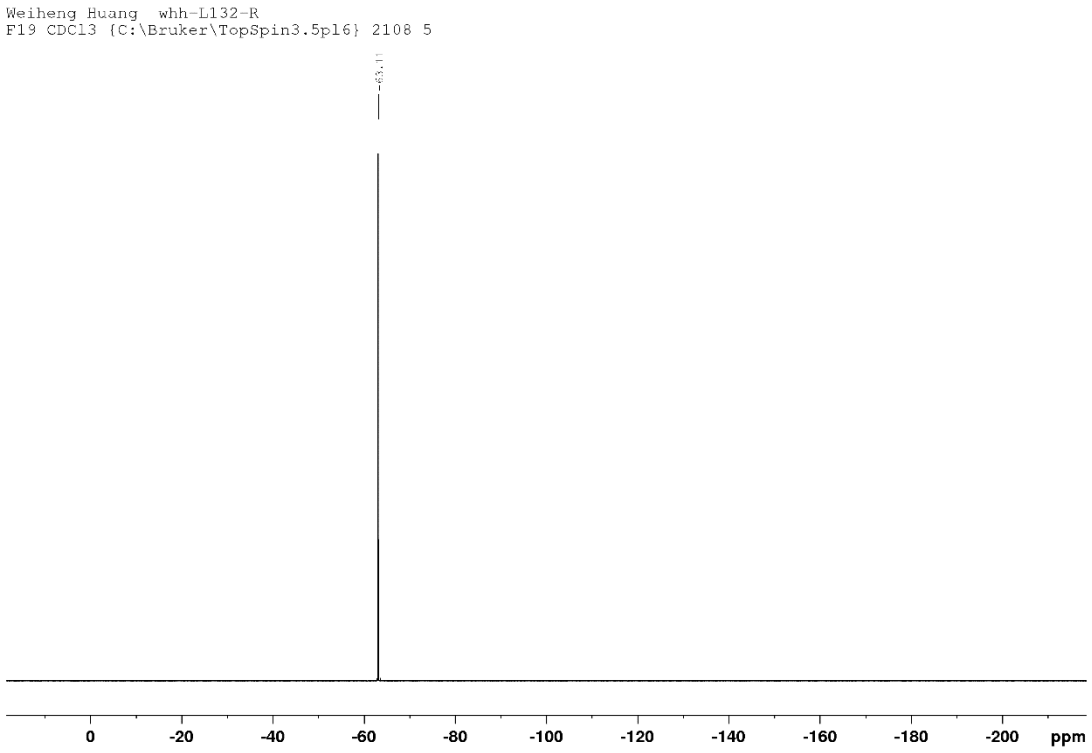

^{31}P NMR (121 MHz, $CDCl_3$) δ/ppm: -12.21.

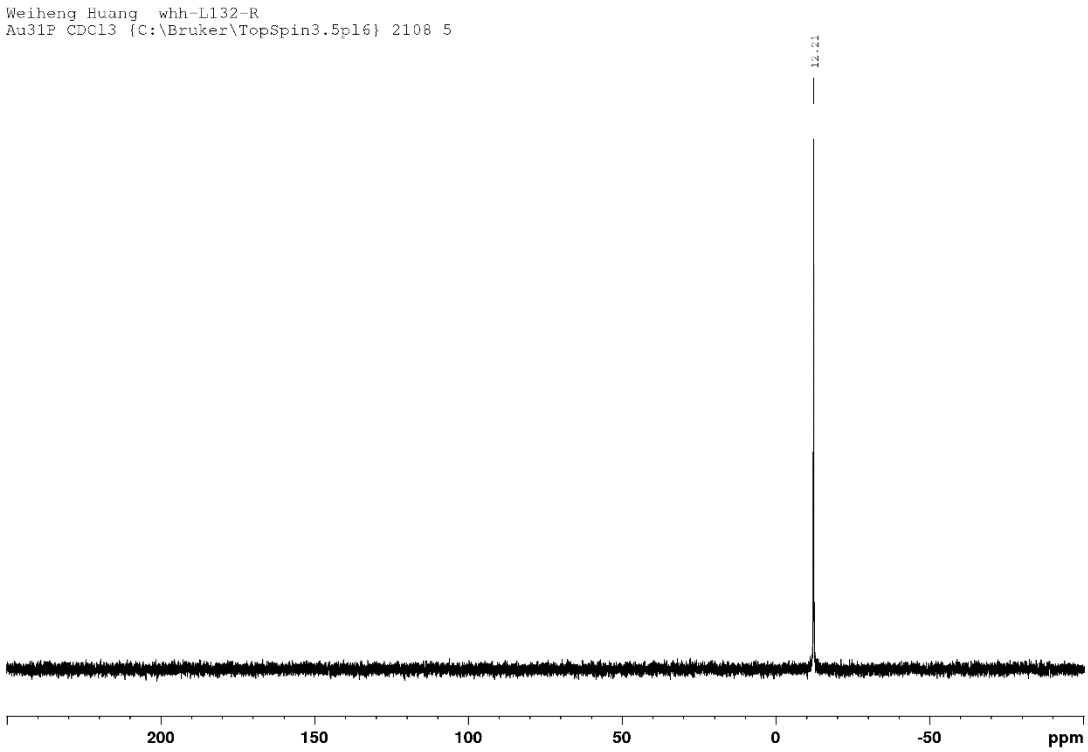

^{13}C NMR (75 MHz, $CDCl_3$) δ/ppm: 139.30, 132.82, 132.52, 124.29, 124.08, 121.57, 24.05.

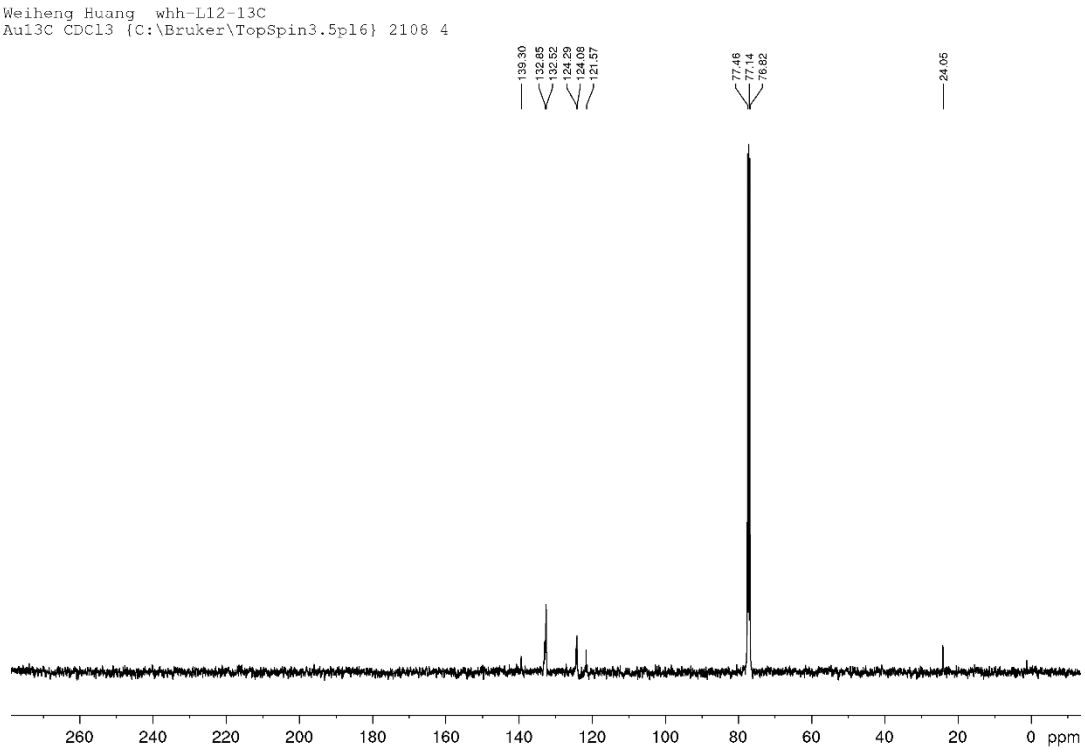

7.Charaterization of the Alcohols

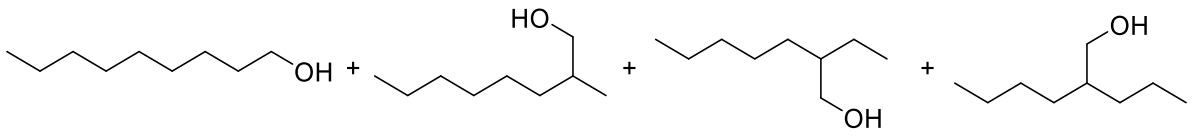

Nonan-1-ol (**2**), 2-methyloctan-1-ol (**2'**), 2-ethylheptan-1-ol (**2''**) and 2-propylhexan-1-ol (**2'''**)

^{1}H NMR shows a n and iso (2:1) mixture.

^{13}C NMR (75 MHz, $CDCl_3$) δ/ppm: 68.46, 65.76, 65.34, 63.10, 42.08, 40.37, 35.85, 33.56, 33.27, 32.88, 32.39, 31.99, 30.72, 30.49, 29.72, 29.69, 29.56, 29.38, 29.20, 27.05, 26.67, 25.86, 24.99, 23.44, 23.21, 22.77, 20.12, 16.68, 14.56, 14,19, 11.18.

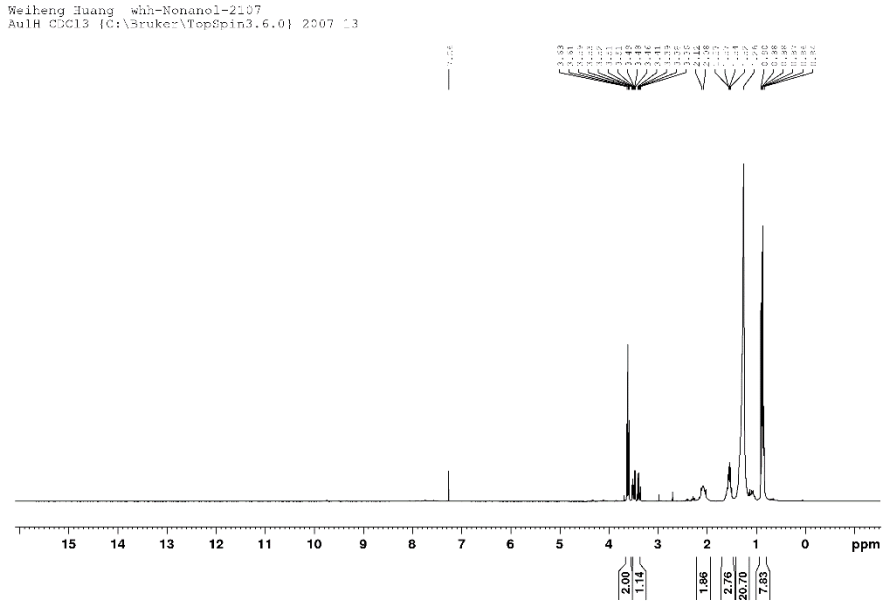

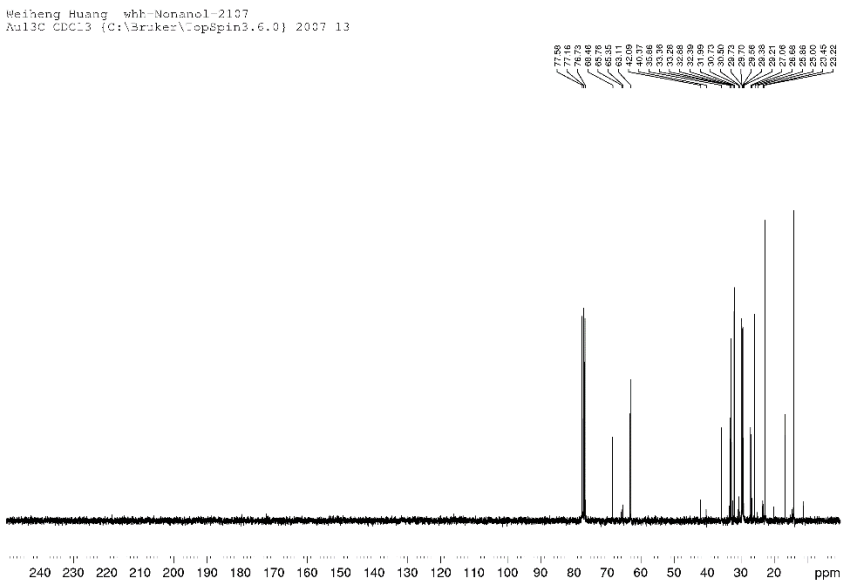

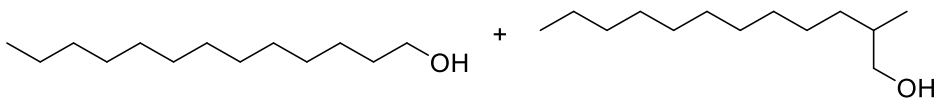

Tridecan-1-ol (**2a**) and 2-methyldodecan-1-ol (**2a'**).

^{1}H NMR shows a n and iso (2:1) mixture.

^{13}C NMR (75 MHz, $CDCl_3$) δ/ppm: 68.48, 63.11, 35.81, 33.20, 32.85, 31.97, 30.00, 29.69, 29.66, 29.49, 29.40, 27.03, 25.79, 22.73, 16.63, 14.15.

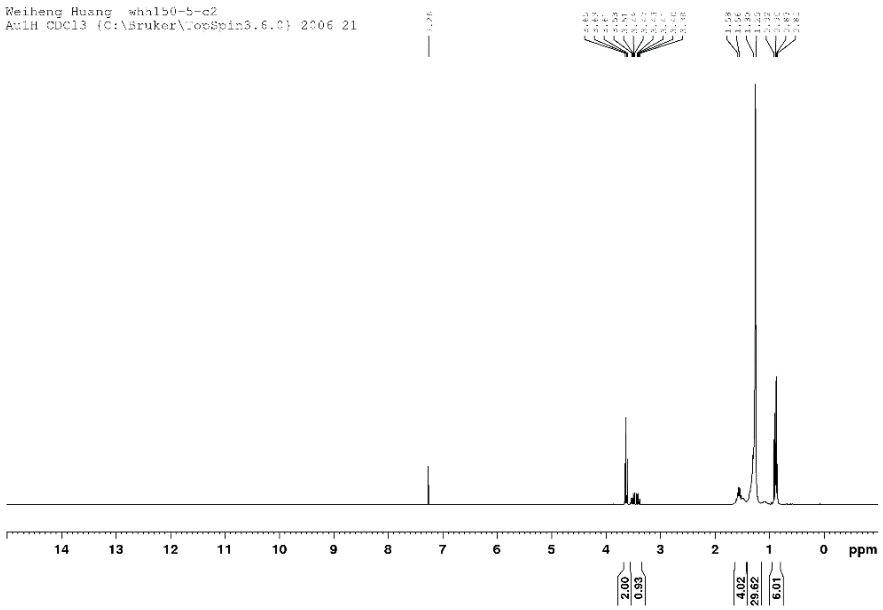

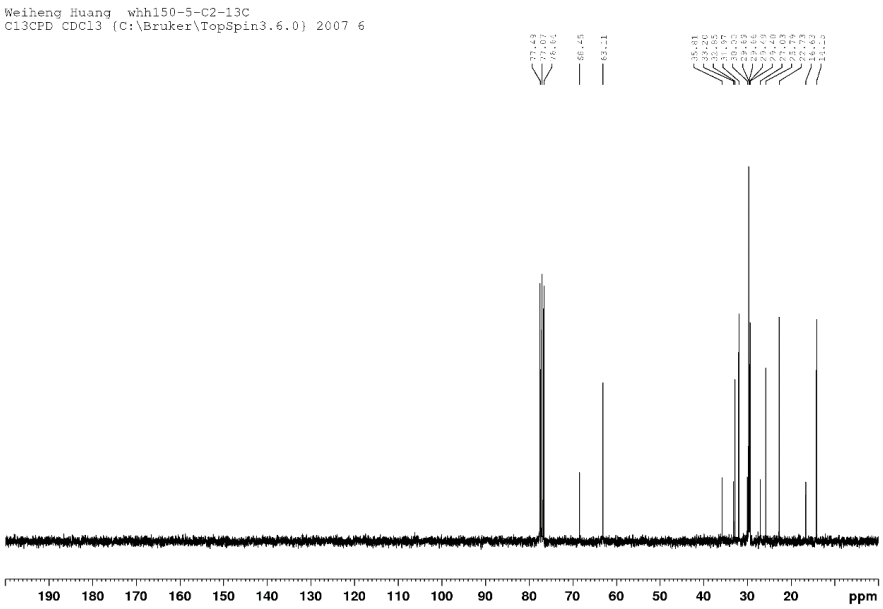

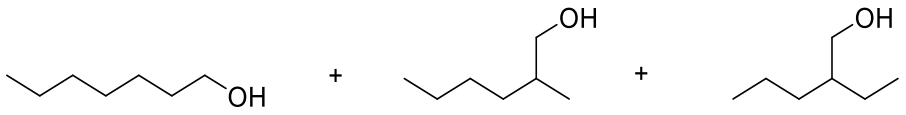

Heptan-1-ol (**2b**), 2-methylhexan-1-ol (**2b'**) and 2-ethylpentan-1-ol (**2b''**).

^{1}H NMR shows a n and iso (2:1) mixture.

^{13}C NMR (75 MHz, $CDCl_3$) δ/ppm: 68.39, 63.02, 35.80, 32.93, 32.84, 31.90, 29.28, 29.19, 25.79, 23.05, 22.68, 16.65, 14.13.

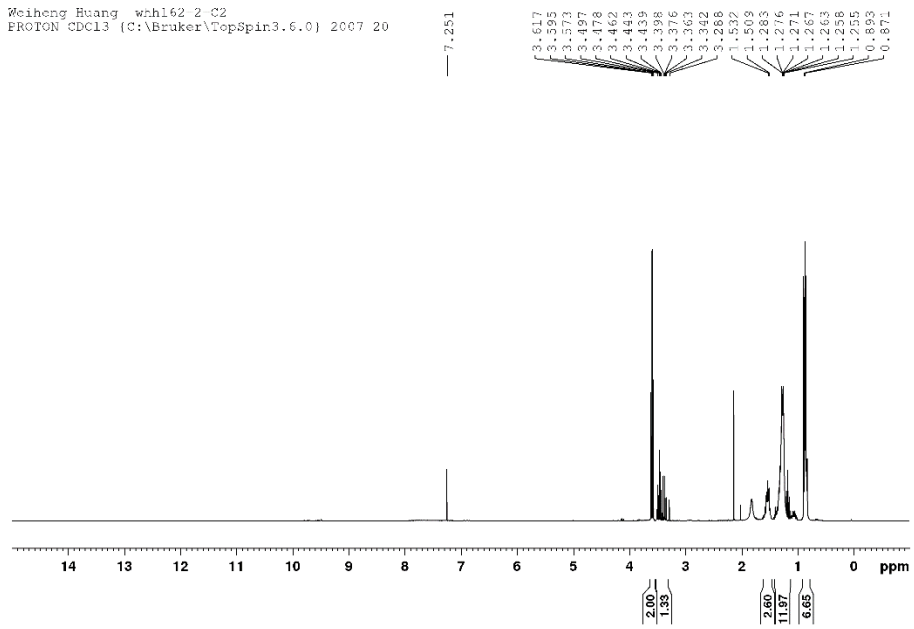

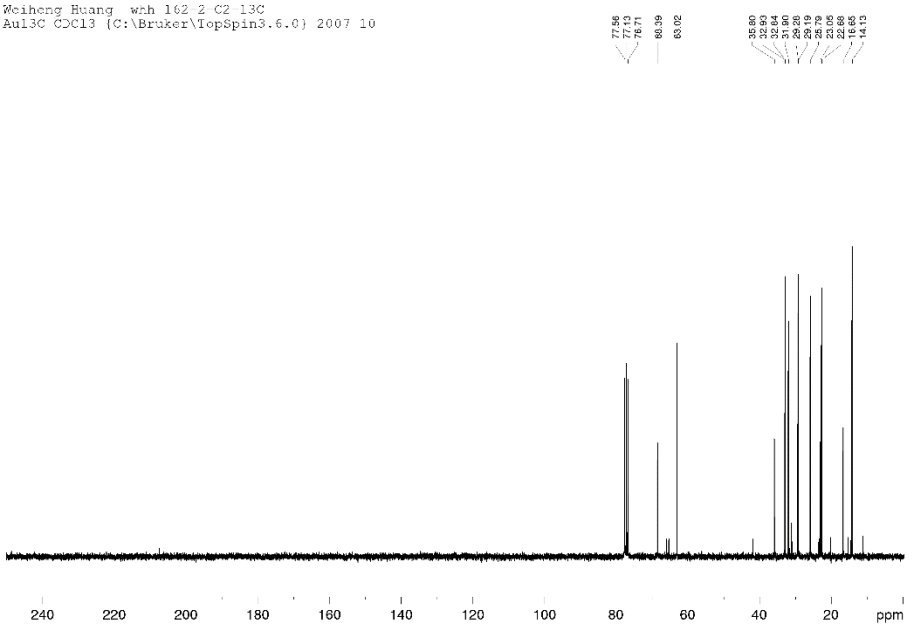

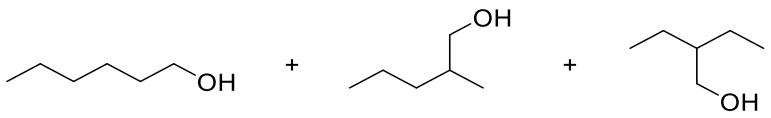

Hexan-1-ol (**2c**), 2-methylpentan-1-ol (**2c'**) and 2-ethylbutan-1-ol (**2c''**)

^{1}H NMR shows a n and iso (1:1) mixture.

^{13}C NMR (75 MHz, $CDCl_3$) δ/ppm: 68.49, 65.97, 63.16, 35.57, 35.50, 33.98, 32.83, 31.74, 31.36, 25.52, 24.58, 22.98, 22.73, 22.42, 20.17, 16.63, 15.34, 14.43, 14.12, 13.99.

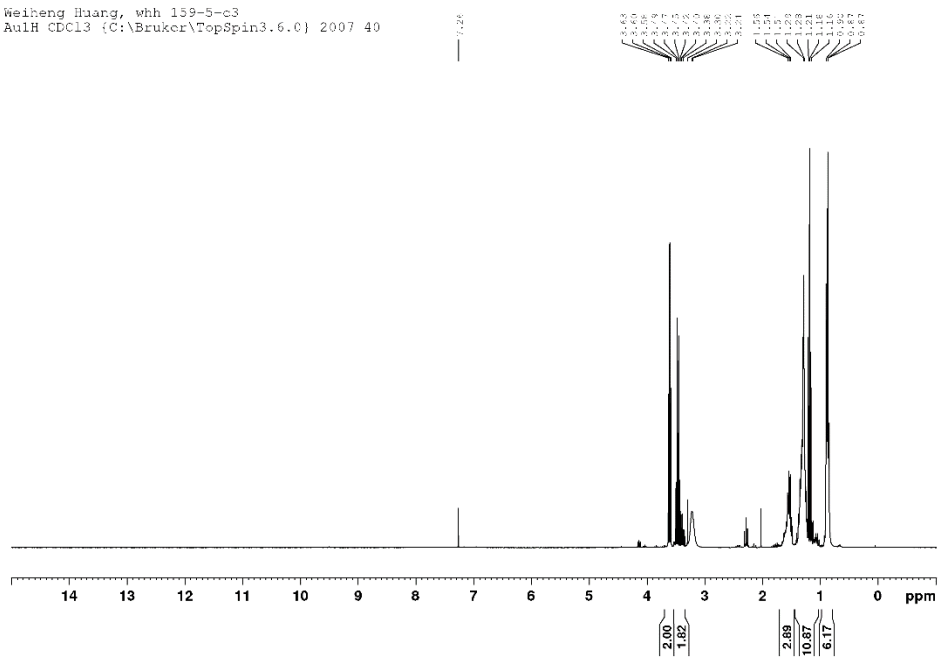

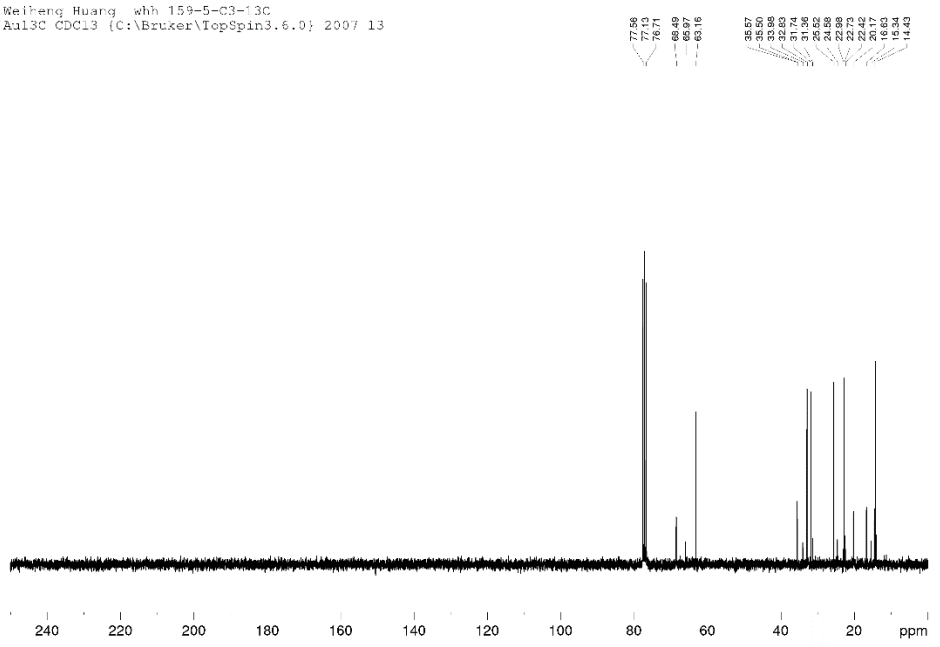

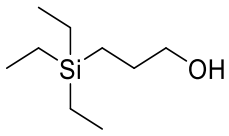

3-(triethylsilyl)propan-1-ol (**2d**)

^{1}H NMR (300 MHz, $CDCl_3$) δ/ppm: 3.59 (t, *J* = 6.8 Hz, 2H), 1.60-1.52 (m, 2H), 0.99-0.90 (m, 9H), 0.63-0.46 (m, 8H).

^{13}C NMR (75 MHz, $CDCl_3$) δ/ppm: 66.15, 27.29, 7.40, 6.65, 3.28.

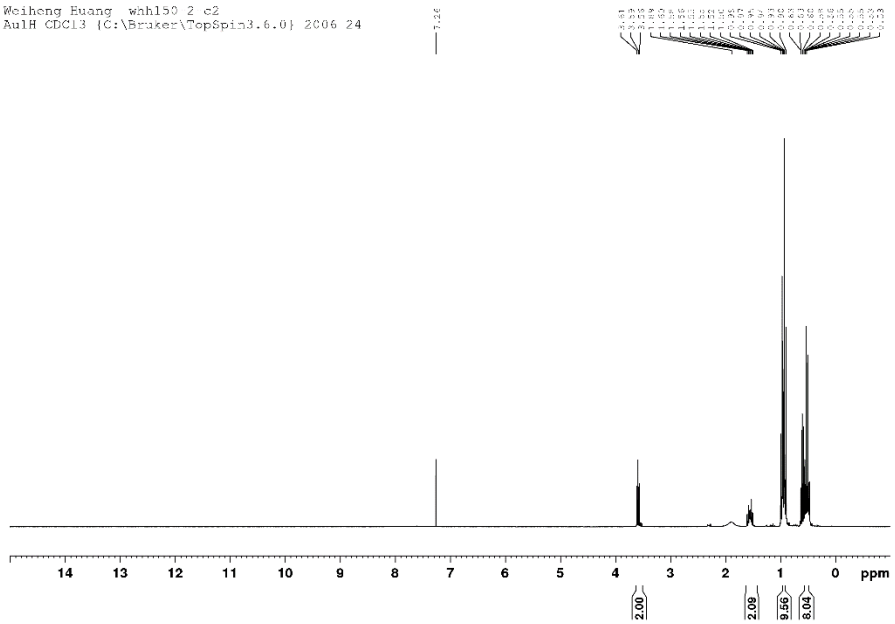

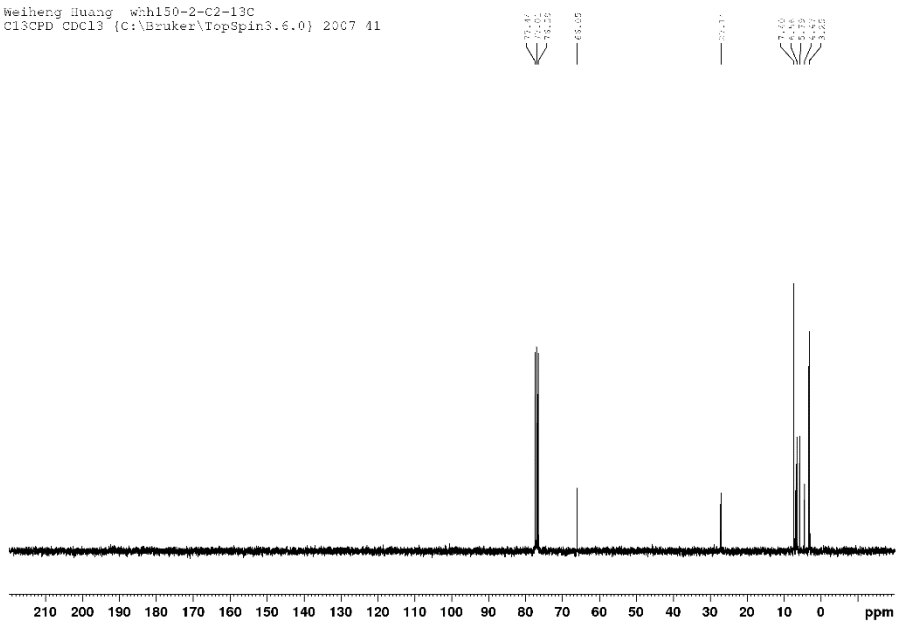

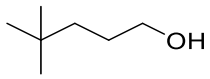

4,4-dimethylpentan-1-ol (**2e**)

^{1}H NMR (300 MHz, $CDCl_3$) δ/ppm: 3.62 (t, *J* = 6.7 Hz, 2H), 1.56-1.50 (m, 2H), 1.23-1.18 (m, 2H), 0.88 (s, 9H).

^{13}C NMR (75 MHz, $CDCl_3$) δ/ppm: 63.98, 39.99, 30.13, 29.39, 28.10.

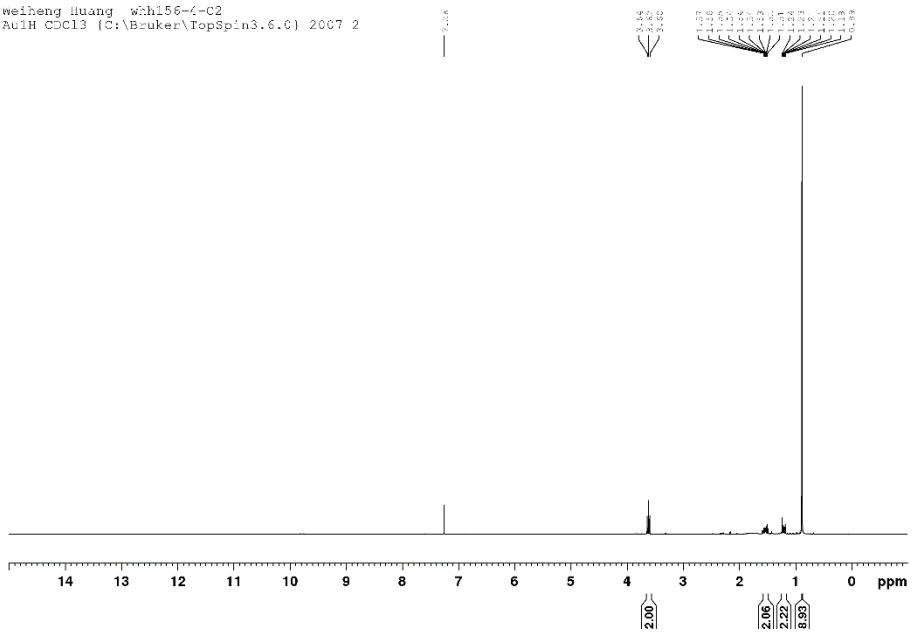

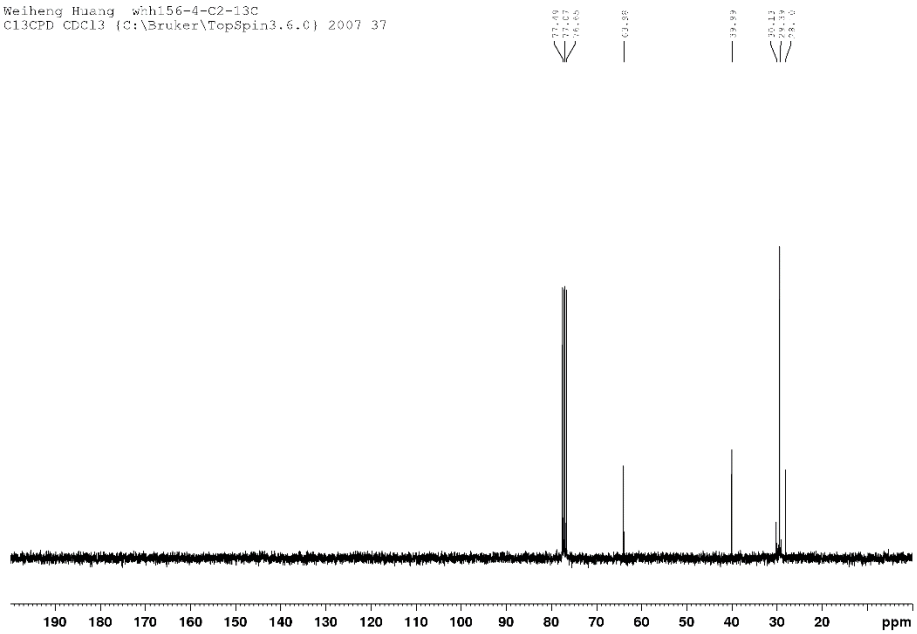

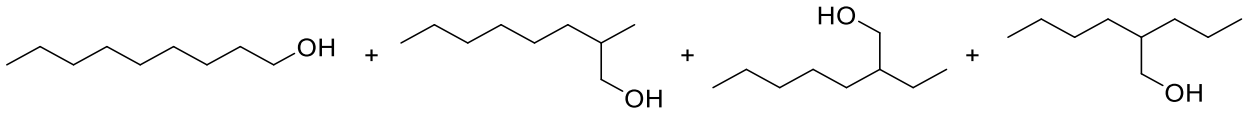

Nonan-1-ol (**2f**), 2-methyloctan-1-ol (**2f'**), 2-ethylheptan-1-ol (**2f''**) and 2-propylhexan-1-ol (**2f'''**)

^{1}H NMR shows a n and iso (1:9) mixture.

^{13}C NMR (75 MHz, $CDCl_3$) δ/ppm: 68.46, 65.76, 65.34, 63.10, 42.08, 40.37, 35.85, 33.56, 33.27, 32.88, 32.39, 31.99, 30.72, 30.49, 29.72, 29.69, 29.56, 29.38, 29.20, 27.05, 26.67, 25.86, 24.99, 23.44, 23.21, 22.77, 20.12, 16.68, 14.56, 14,19, 11.18.

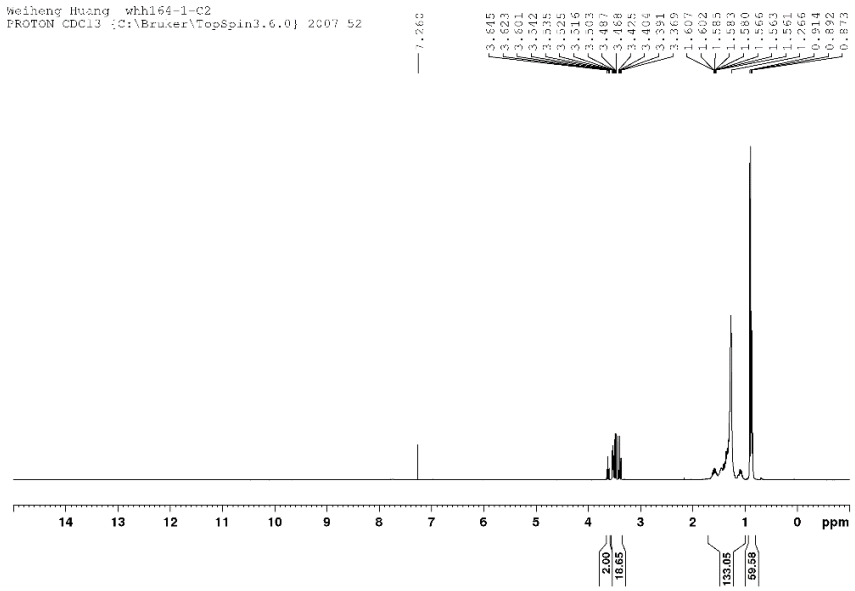

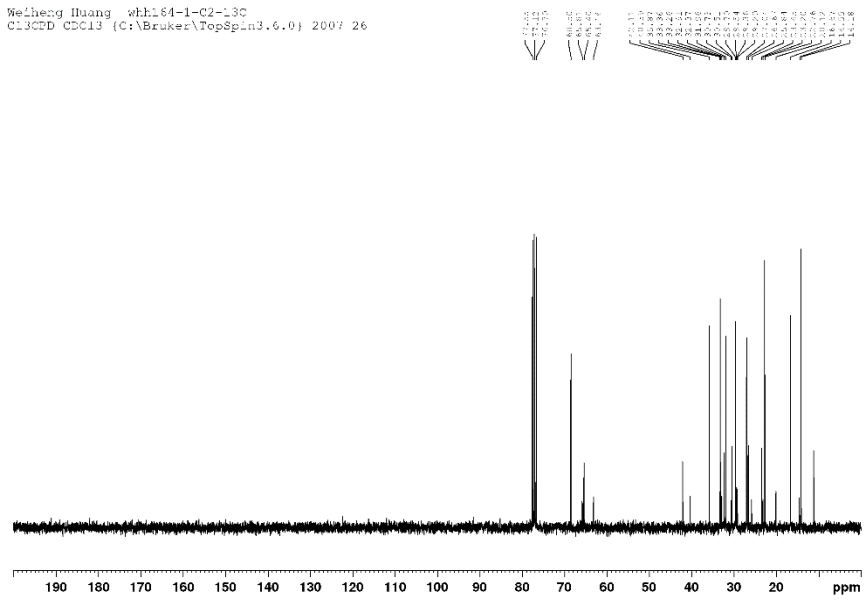

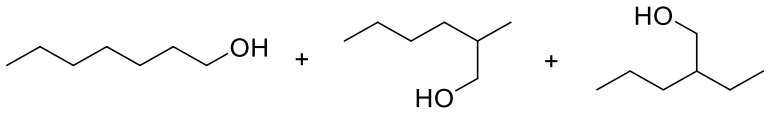

Heptan-1-ol (**2g**), 2-methylhexan-1-ol (**2g'**) and 2-ethylpentan-1-ol (**2g''**)

^{1}H NMR shows a n and iso (1:4) mixture.

^{13}C NMR (75 MHz, $CDCl_3$) δ/ppm: 68.36, 65.25, 62.99, 41.81, 35.80, 32.94, 32.83, 31.90, 29.28, 29.19, 25.79, 23.41, 23.05, 22.67, 20.09, 16.65, 14.51, 14.12, 11,12.

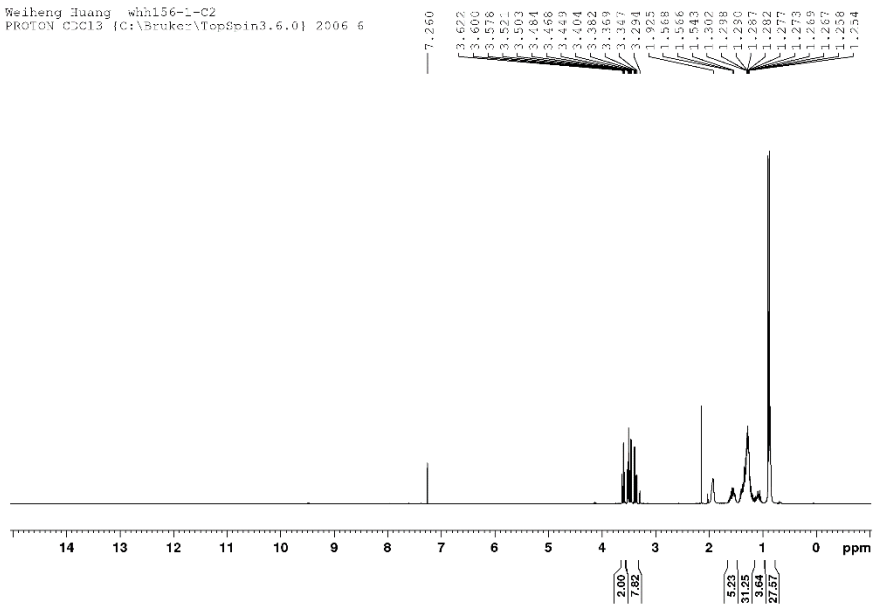

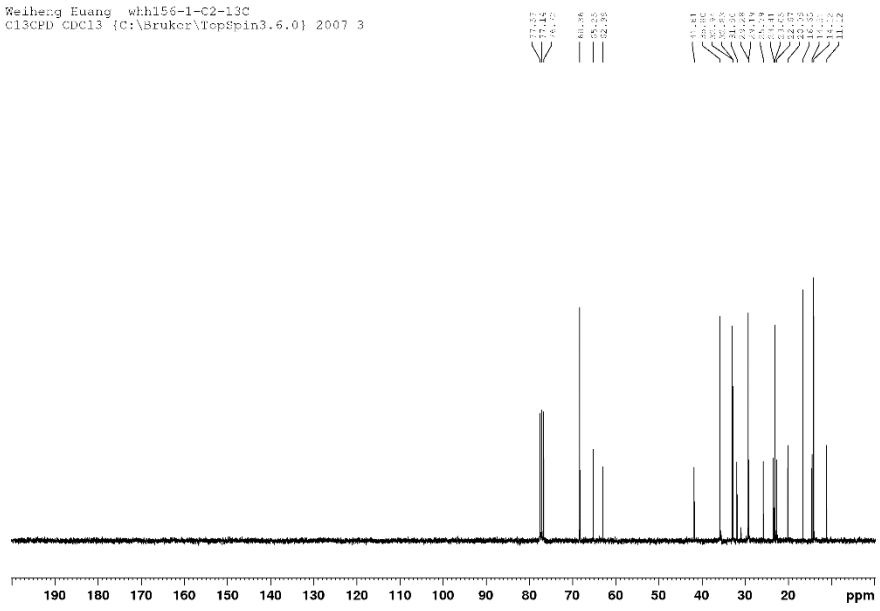

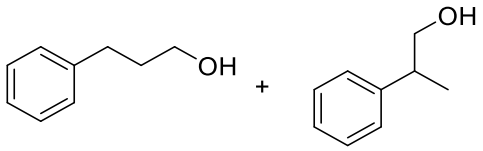

3-phenylpropan-1-ol (**2h**) and 2-phenylpropan-1-ol (**2h'**)

^{1}H NMR shows a n and iso (1:3) mixture.

^{13}C NMR (100 MHz, $CDCl_3$) δ/ppm: 143.75, 141.88, 128.67, 128.47, 128.44, 127.53, 126.70, 125.90, 68.72, 62.25, 42.47, 34.24, 22.11, 17.63.

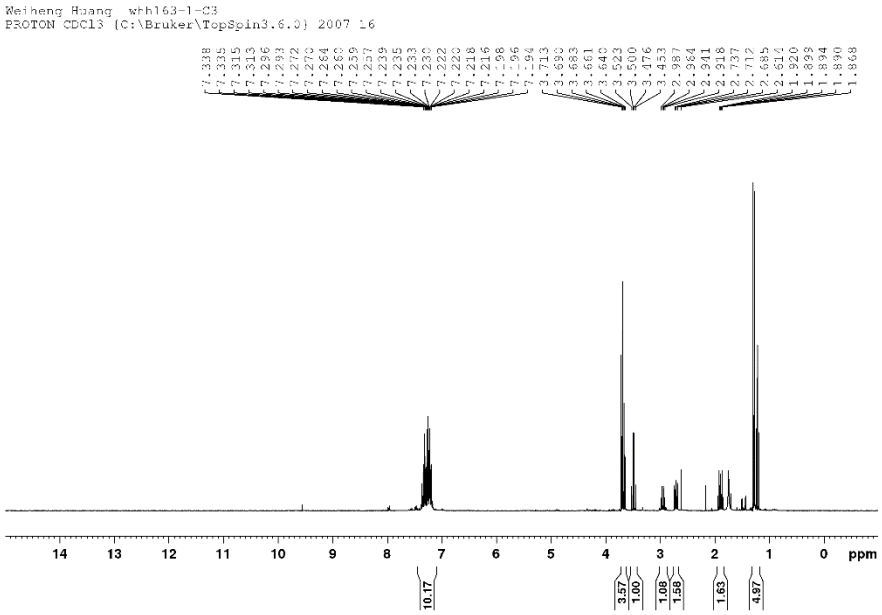

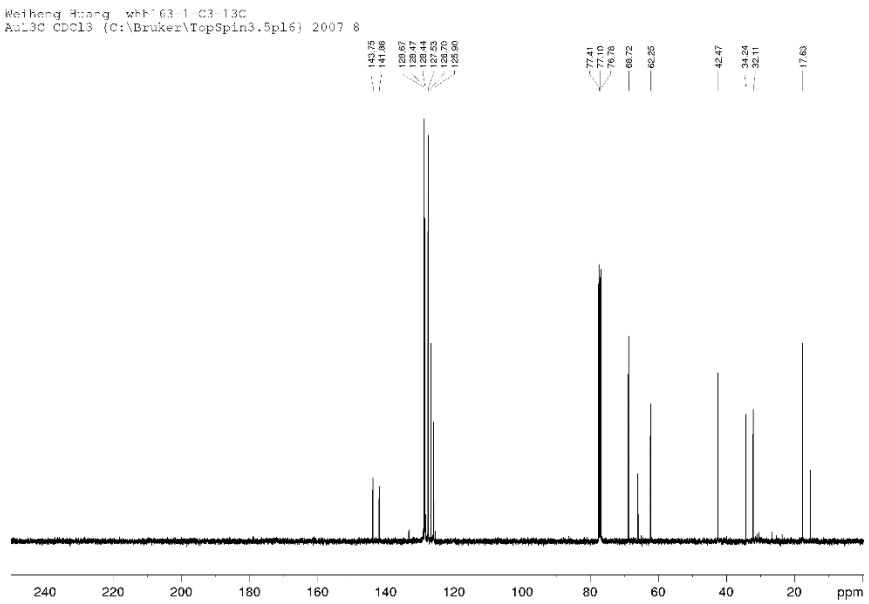

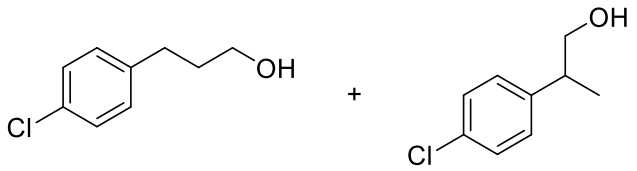

3-(4-chlorophenyl)propan-1-ol (**2i**) and 2-(4-chlorophenyl)propan-1-ol (**2i'**)

^{1}H NMR shows a n and iso (1:4) mixture.

^{13}C NMR (100 MHz, $CDCl_3$) δ/ppm: 142.38, 140.36, 132.39, 131.65, 129.88, 128.94, 128.79, 128.57, 68.55, 62.05, 41.95, 34.14, 31.47, 17.65.

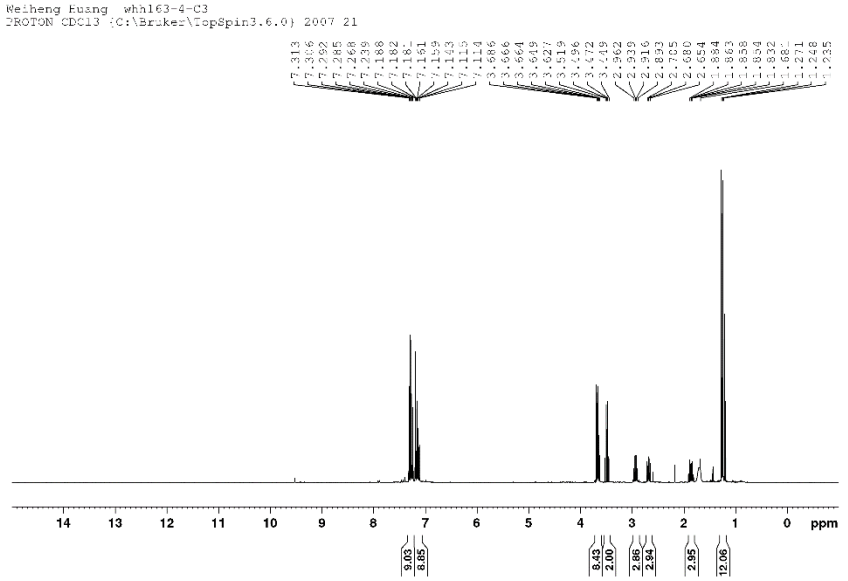

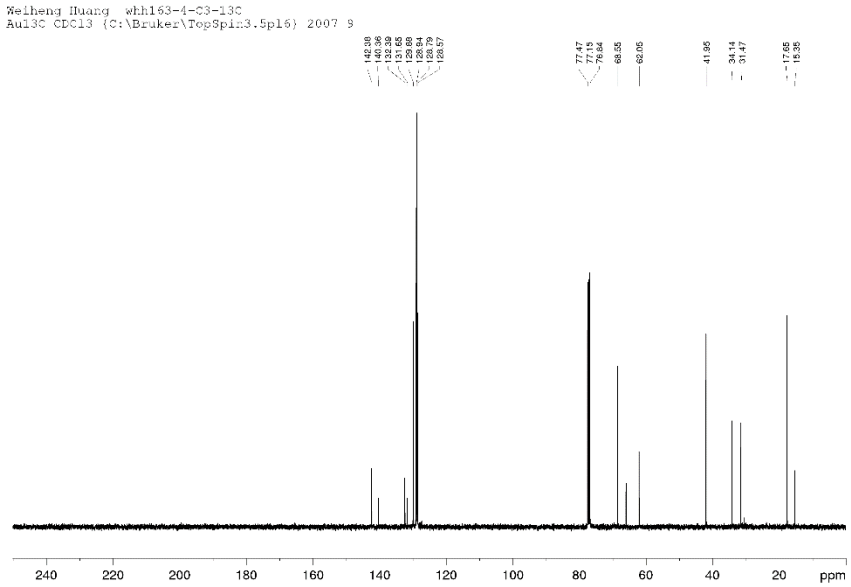

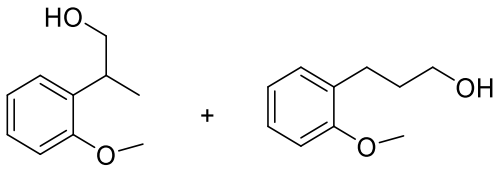

2-(2-methoxyphenyl)propan-1-ol (**2j**) and 3-(2-methoxyphenyl)propan-1-ol (**2j'**)

^{1}H NMR shows a n and iso (1:1) mixture.

^{13}C NMR (75 MHz, $CDCl_3$) δ/ppm:157.45, 157.35, 131.92, 130.14, 130.06, 127.44, 127.39, 127.22, 120.82, 120.74, 110.63, 110.35, 67.79, 61.98, 55.41, 55.38, 35.22, 32.93, 26.02, 16.64.

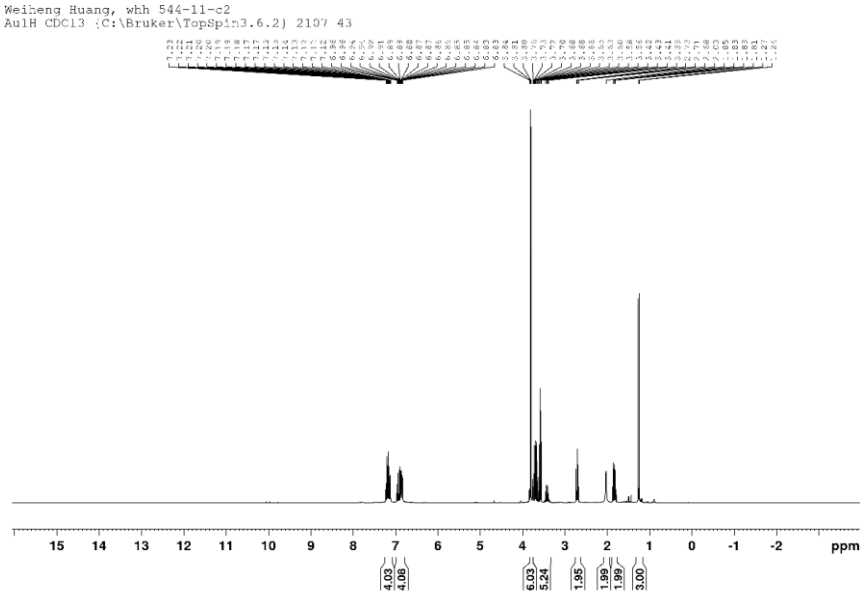

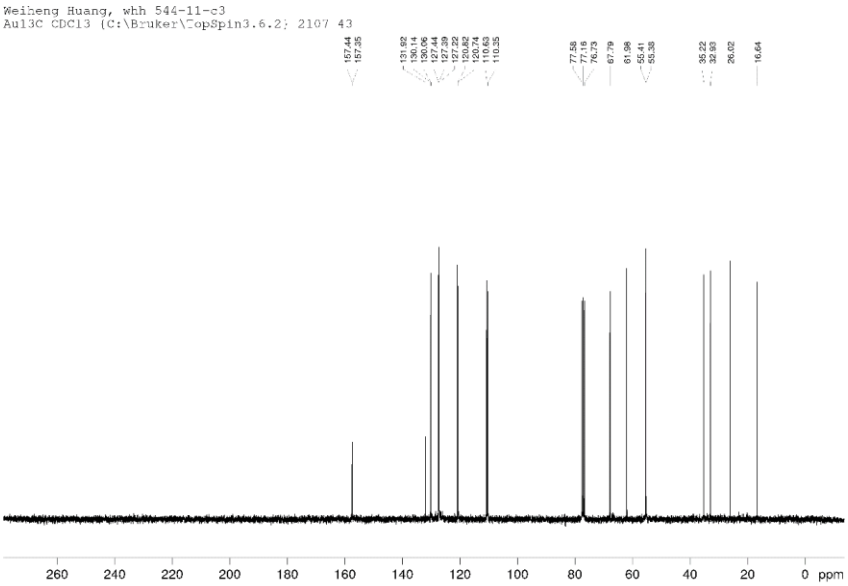

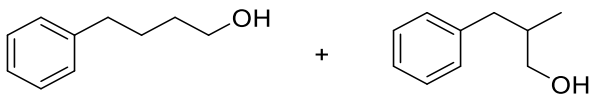

4-phenylbutan-1-ol (**2k**) and 2-methyl-3-phenylpropan-1-ol (**2k'**)

^{1}H NMR shows a n and iso (2:1) mixture.

^{13}C NMR (75 MHz, $CDCl_3$) δ/ppm: 142.40, 140.72, 129.22, 128.47, 128.37, 128.32, 125.81, 67.65, 62.79, 39.76, 37.83, 35.70, 27.61, 16.51.

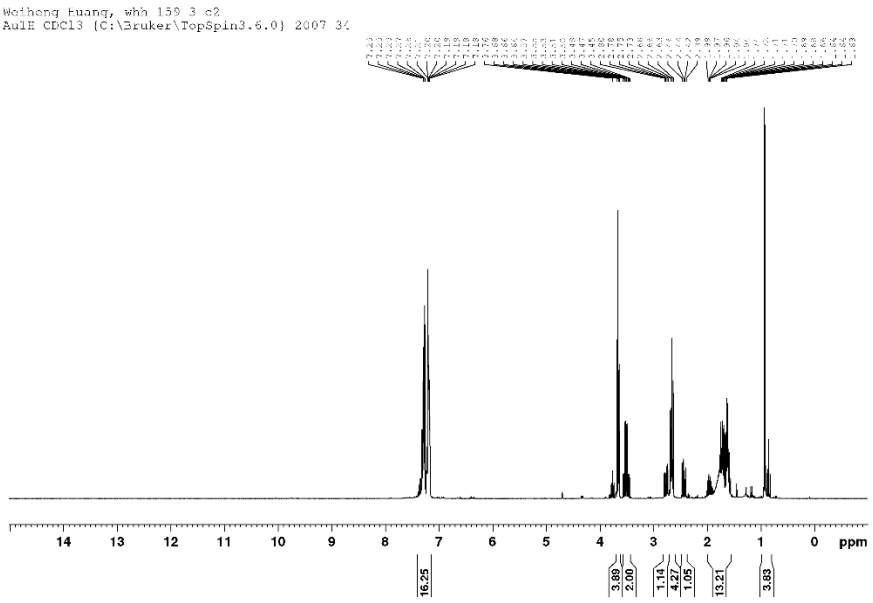

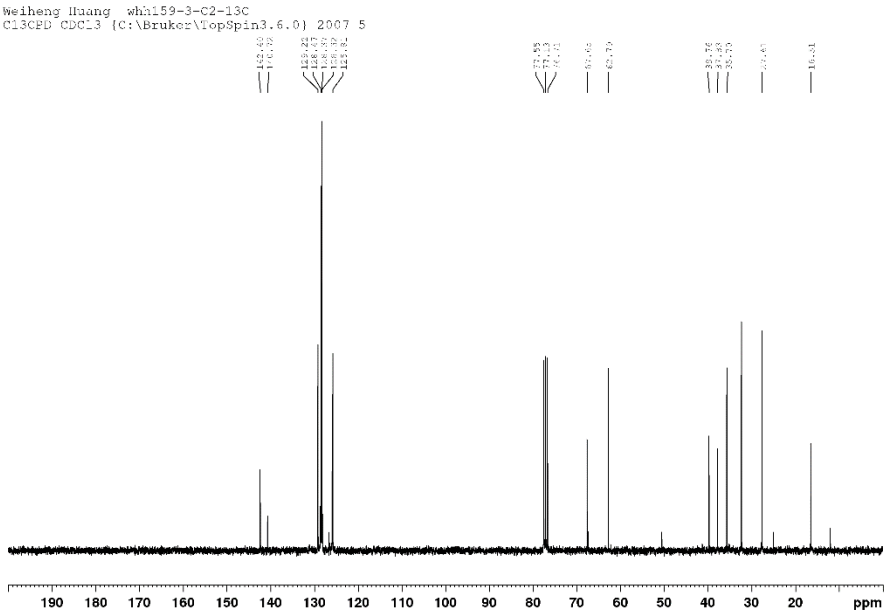

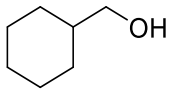

Cyclohexylmethanol (**2l**)

^{1}H NMR (300 MHz, $CDCl_3$) δ/ppm: 3.43 (d, *J* = 6.4, 2H), 1.75-1.69 (m, 5H), 1.47-1.42 (m, 1H), 1.22-1.18 (m, 3H), 0.97-0.89 (m, 2H).

^{13}C NMR (75 MHz, $CDCl_3$) δ/ppm: 68.75, 40.52, 29.62, 26.64, 25.89.

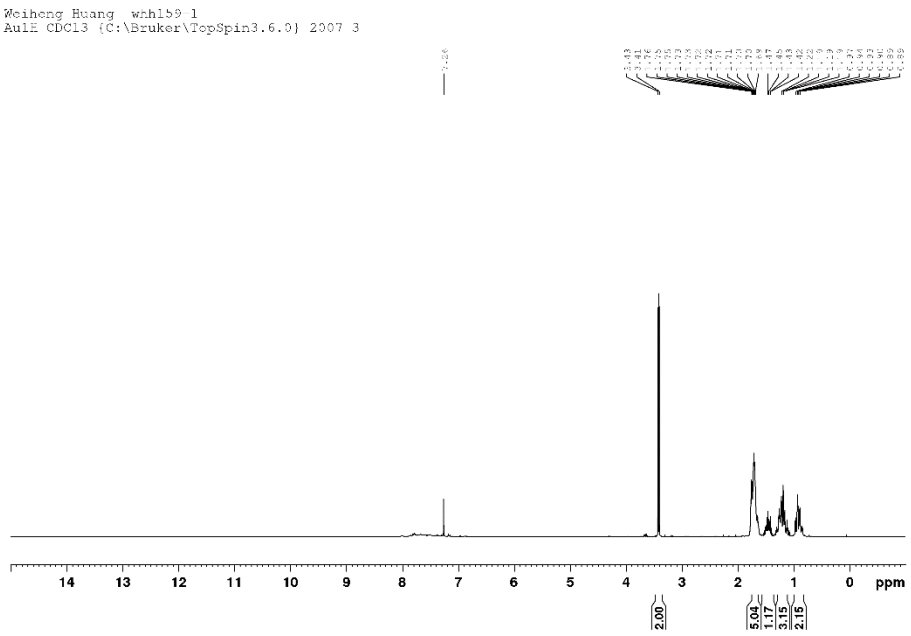

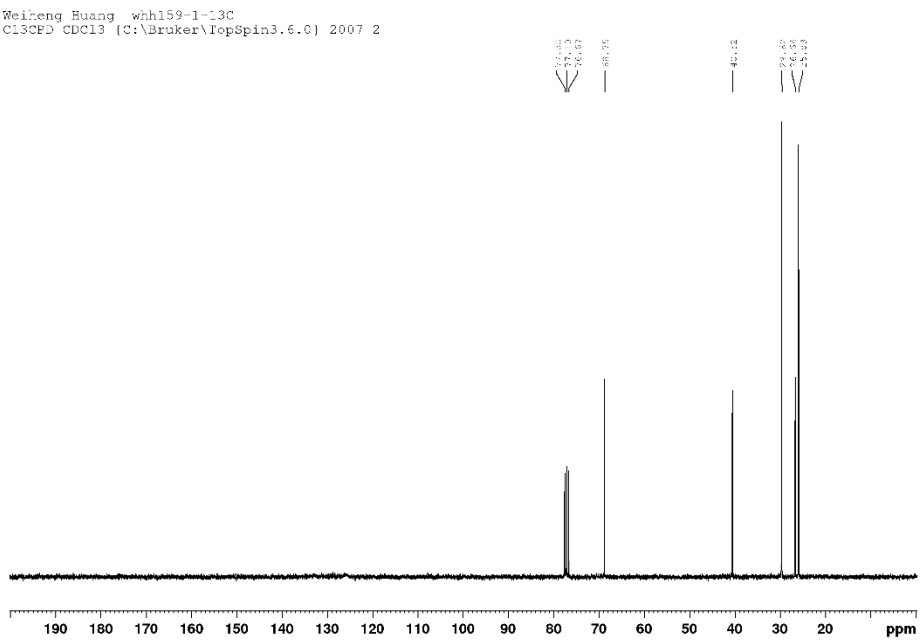

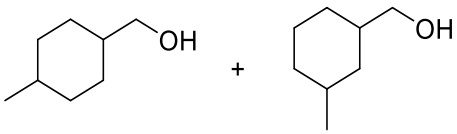

(4-methylcyclohexyl)methanol (**2m**) and (3-methylcyclohexyl)methanol (**2m'**)

^{1}H NMR shows a symmetric and asymmetric (8:2) mixture.

^{13}C NMR (75 MHz, $CDCl_3$) δ/ppm: 68.87, 65.94, 40.68, 40.34, 38.43, 35.39, 34.94, 32.94, 32.36, 29.61, 29.25, 25.89, 22.99, 22.73, 15.32.

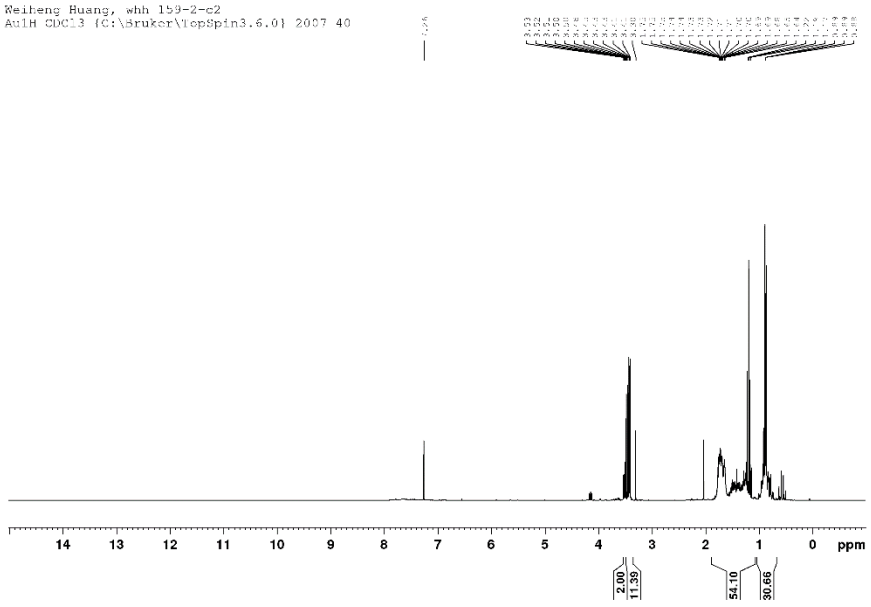

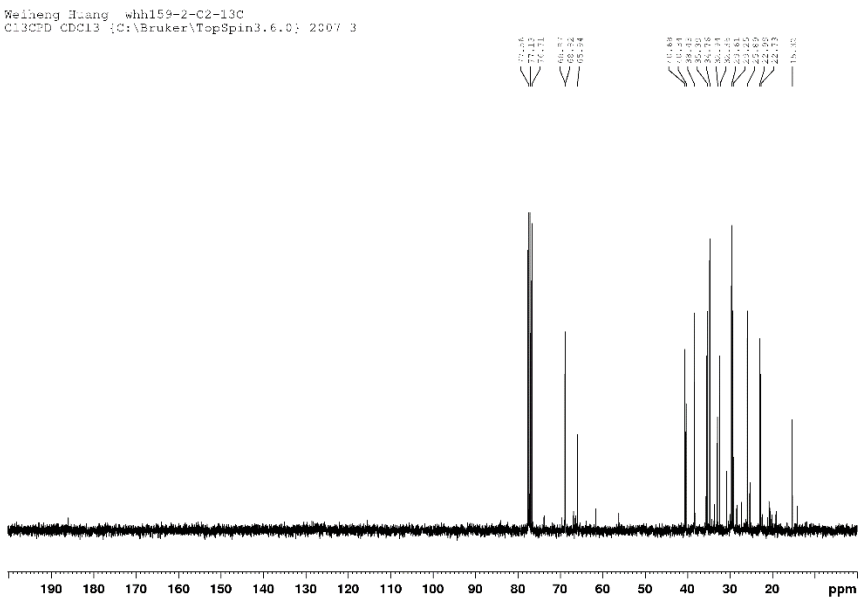

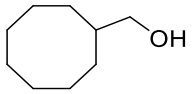

Cyclooctylmethanol (**2n**)

^{1}H NMR (300 MHz, $CDCl_3$) δ/ppm: 3.36 (d, *J* = 4.3, 2H), 1.66-1.19 (m, 15H).

^{13}C NMR (75 MHz, $CDCl_3$) δ/ppm: 69.21, 40.41, 29.41, 27.01, 26.56, 25.66.

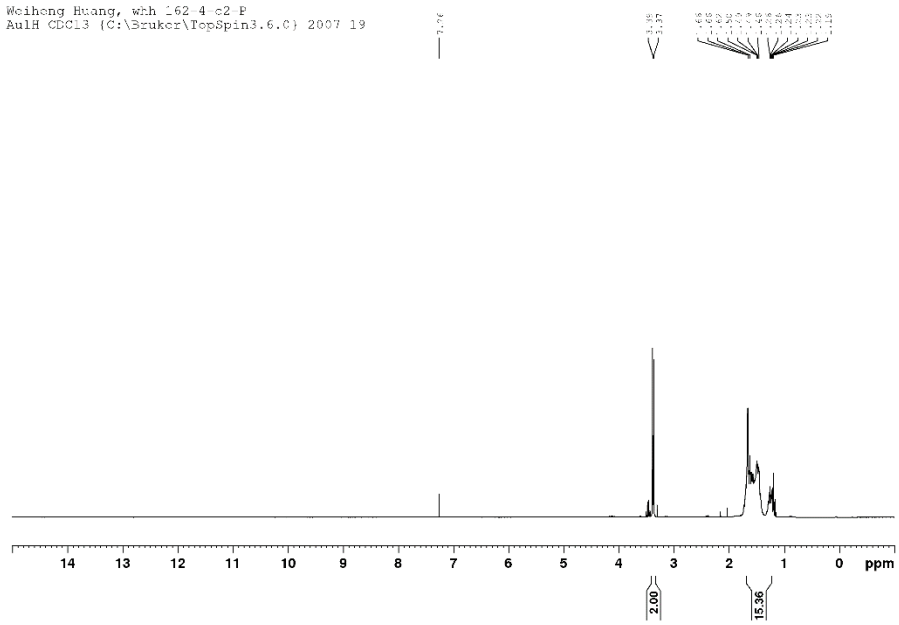

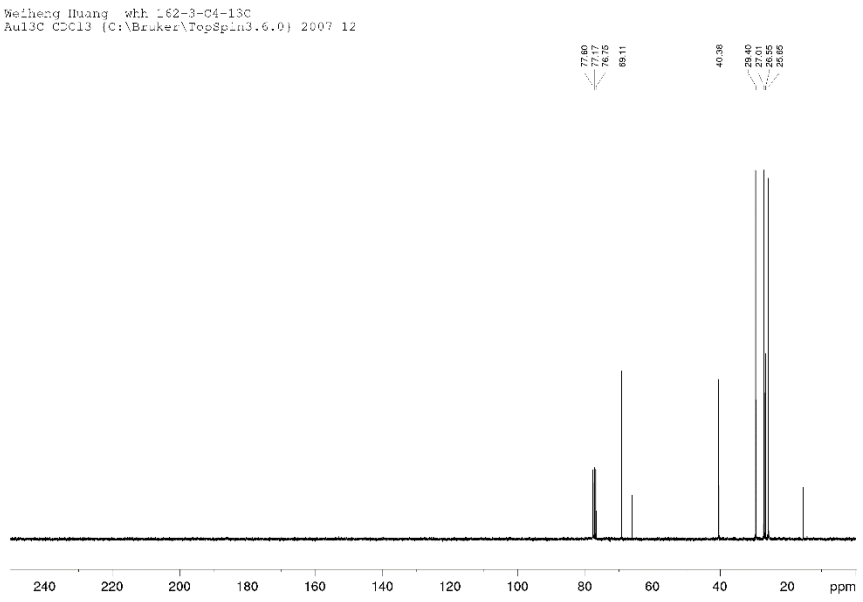

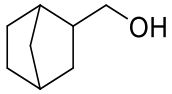

Bicyclo[2.2.1]heptan-2-ylmethanol (**2o**)

^{1}H NMR (300 MHz, $CDCl_3$) δ/ppm: 3.36-3.30 (m, 2H), 2.22 (s, 1H), 2.16 (s, 1H), 1.57-1.11 (m, 9H).

^{13}C NMR (75 MHz, $CDCl_3$) δ/ppm: 67.02, 45.00, 38.20, 36.20, 36.51, 35.25, 34.11, 29.93, 29.04.

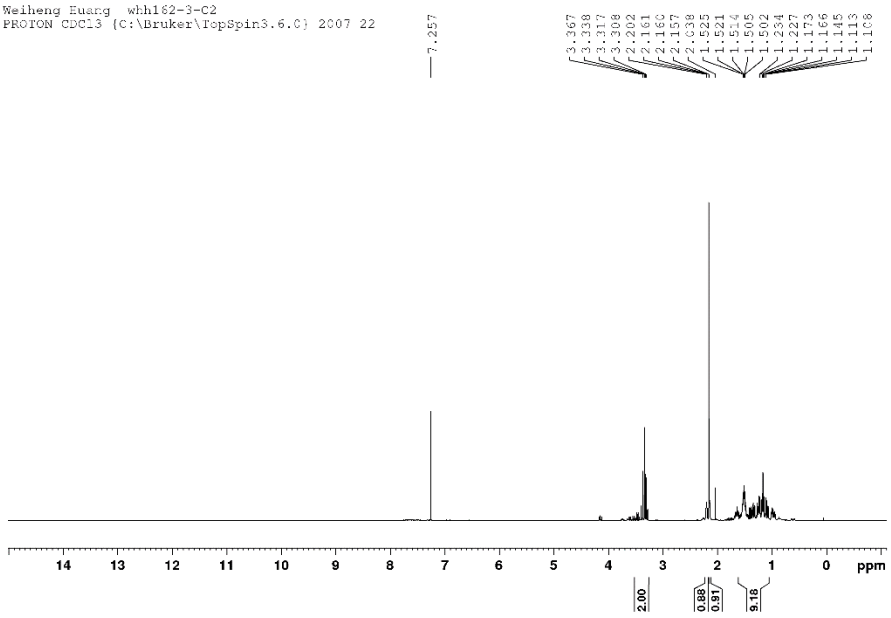

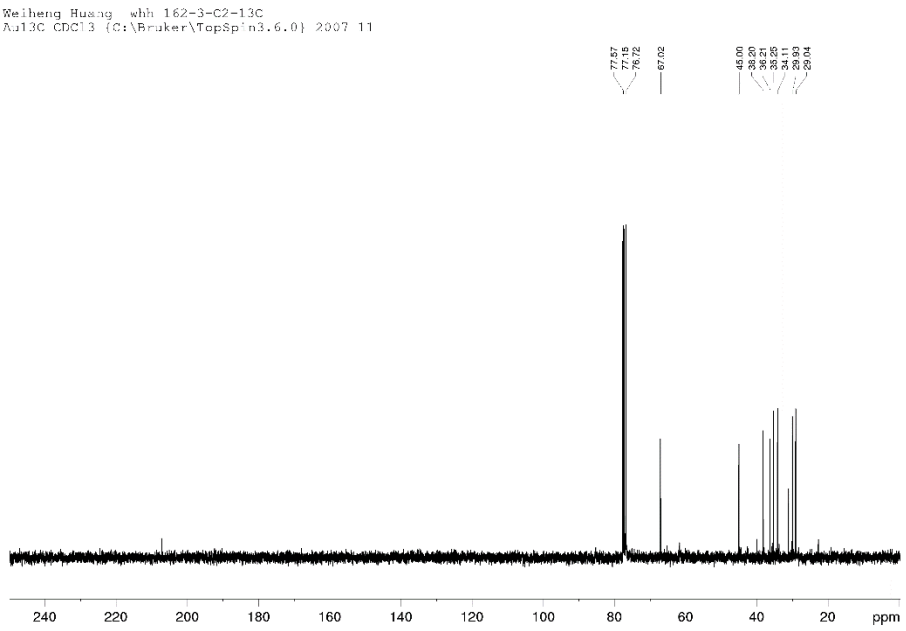

Computational investigations

(1) Models and methods: All calculations were performed with Gaussian 16 program.[4] All structures were optimized firstly in gas phase and characterized either as authentic transition states with only one imaginary frequency or energy minimums with real frequencies by frequency analysis at the M06L[5] level in combination of a mixed basis set (BS: LANL2DZ[6] for iridium and TZVP[7] for other non-metal elements). Single-point energy calculations including solvation effect were then carried out by using the SMD model[8] at the same level on the gas phase optimized geometries (M06L-SMD/BS//M06L/BS), where we used methanol for NMP as solvent, since they have nearly the same dielectric constant (32.6 vs. 32). Considering the importance of dispersion interaction of the real-size ligands involving multiple benzene rings, further single point energy calculations at the M062X[9]-GD3[10] level on the M06L optimized gas phase geometries were performed (M062X-GD3-SMD/BS//M06L/BS). For discussing the reactivity and selectivity, we used Gibbs free energy which includes the thermal correction at 298.15 K and 1 atm. To fit the experimental temperature, thermal correction to Gibbs free energy at 413 K (140 °C) and 1 atm was included (M062X-GD3-SMD-413 K). We compared several sets of computed results (Figure DFT-S1) and found best agreement between experiment and M062X as discussed below.

(2) Benchmark testing: Firstly, the stability of different Iridium hydride complexes was compared using different methods (M06L and M062X) in gas phase at 298 K; in solution at 298 K; in solution at the working temperature 413 K. The substitution Gibbs free energies of CO ligand in $HIr(CO)_4$ by monodentate PPh_3 and/or bidentate DPPE ligands are shown in Figure DFT-S1 and the results for both *p*-OCH_3 modified PPh_3 (**L1**) and *p*-CF_3 modified DPPE (**L10**) are shown in Figure DFT-S2.

As shown in Figure DFT-S1, it is to see that at the M062X-D3-SMD-413K level, the **DPPE-EA** complex, *e,a*-$HIr(CO)_2$(DPPE), with one P center at the axial position and one P center at the equatorial position is most stable (–24.5 kcal/mol), while the positional isomer **DPPE-EE**, *e,e*-$HIr(CO)_2$(DPPE), with two P centers at the equatorial positions is 4.2 kcal/mol less stable. The **DPPE-EA-mono** complex, *a*-$HIr(CO)_3$(DPPE), with only one P center of DPPE at the axial position is much less stable (–10.0 kcal/mol). These results show that DPPE prefers bidentate coordination at the axial and equatorial positions and other configurations are less stable and therefore not competitive thermodynamically.

For PPh_3 substitution, the **1Ph$_3$-A** complex, *a*-$HIr(CO)_3(PPh_3)$, with PPh_3 at the axial position, and the **2Ph$_3$-EA** complex, *e,a*-$HIr(CO)_2(PPh_3)_2$, with one PPh_3 at the axial position and one PPh_3 at the equatorial position, have very close substitution Gibbs free energy (–12.9 vs. –13.2 kcal/mol), while their corresponding isomer, the **1Ph$_3$-E** complex, *e*-$HIr(CO)_3(PPh_3)$, with PPh_3 at the equatorial position, and the **2Ph$_3$-EE** complex, *e,e*-$HIr(CO)_2(PPh_3)_2$, with two PPh_3 both at the equatorial position, are less stable (–8.7 vs. –9.4 kcal/mol). However, the **3Ph$_3$-EEA** complex, *e,e,a*-$HIr(CO)(PPh_3)_3$, with one PPh_3 at the axial position and two PPh_3 at the equatorial positions is much less stable (–0.1 kcal/mol). These results show the preference of the axial over the equatorial coordination for one and two PPH_3 ligands; and mono and bis PPh_3 coordinated complexes have comparative stability and equilibrium under stoichiometric conditions. The **3Ph$_3$-EEA** complex, $HIr(CO)(PPh_3)_3$, which is commercially available (CAS17250-25-8), should be stable under appropriate condition, i.e., with excess PPh_3 and under CO poor atmosphere.

The M062X computed results can be verified by the FTIR and NMR experiments reported by Kubis *et al.*[11] They found equilibrium between $HIr(CO)_3(PPh_3)$ and $HIr(CO)_2(PPh_3)_2$ under varying $[PPh_3]/[Ir]$ ratio of 4, 10 and 20 as well as varying CO pressure. At a given CO pressure, the $HIr(CO)_2(PPh_3)_2$ to $HIr(CO)_3(PPh_3)$ ratio increases with the increase of $[PPh_3]/[Ir]$ ratio, indicating that high $[PPh_3]/[Ir]$ ratio favors the formation of $HIr(CO)_2(PPh_3)_2$. They also found that at a given $[PPh_3]/[Ir]$ ratio, the $HIr(CO)_2(PPh_3)_2$ to $HIr(CO)_3(PPh_3)$ ratio decreases with the increase of CO pressure, indicating that high CO pressure favors the formation of $HIr(CO)_3(PPh_3)$. However, they did not observe the formation of $HIr(CO)(PPh_3)_3$. Furthermore, they observed the formation of trihydride complex $H_3Ir(CO)(PPh_3)_2$ at very high $[H_2]/[CO]$ ratio. In addition, we found that the substitution of one equivalent H_2 in $H_3Ir(CO)(PPh_3)_2$ by one equivalent CO to form $Ir(CO)_2(PPh_3)_2$ from *fac*- and *mer*-configuration [*fac/mer*-$H_3Ir(CO)(PPh_3)_2 + CO = HIr(CO)_2(PPh_3)_2 + H_2$] is exothermic by 7.7 and 12.7 kcal/mol, respectively, and therefore favored thermodynamically. This shows that $H_3Ir(CO)(PPh_3)_2$ is not stable in CO containing environment.

The above results show that the potential pre- or active catalysts in PPh_3-Ir system depend on CO pressure as well as $[PPh_3]/[Ir]$ ratio. Since only CO gas and H_2O were used in our experiment, and H_2 comes from water-gas shift reaction ($CO + H_2O = CO_2 + H_2$), our reaction environment has very high CO concentration (13-40 bar) and very limited H_2 concentration or extremely high $[CO]/[H_2]$ ratio. One can easily exclude the formation *fac/mer*-$H_3Ir(CO)(PPh_3)_2$ and therefore we did not pay further attention to corresponding reactions.

Furthermore, the disproportionation reaction from two equivalent $HIr(CO)_3(PPh_3)$ into $HIr(CO)_2(PPh_3)_2$ and $HIr(CO)_4$ is endothermic by 12.6 kcal/mol. It indicates that the reverse reaction is much favored thermodynamically. We can deduce that for $[PPh_3]/[Ir] \geq 1$, the parent $HIr(CO)_4$ does not exist, while $HIr(CO)_3(PPh_3)$ and $HIr(CO)_2(PPh_3)_2$ co-exist in equilibrium. This is just the case in our experiment which normally have $[PPh_3]/[Ir] = 1.1$.

It is also to note that the mixed **DPPE-EA-1Ph$_3$-E** complex, $HIr(CO)(DPPE)(PPh_3)$, with bidentate DPPE at the axial and equatorial positions and PPh_3 at the equatorial position also has close substitution Gibbs free energy (–23.0 kcal/mol) with respect of the **DPPE-EA** complex, *e,a*-$HIr(CO)_2(DPPE)$ (–24.5 kcal/mol). This shows that under high ligand to metal ratio, the mixed **DPPE-EA-1Ph$_3$-E** complex can be formed. However, this is not possible under our reaction conditions with extremely high CO pressure and fixed ligand to metal ratio (Figure DFT-S3). The other positional isomers of the mixed $HIr(CO)(DPPE)(PPh_3)$ complex are much less stable (–17.2, –16.4, –14.2 kcal/mol).

Differently from M062X, M06L shows the stability order of **DPPE-EA** > **DPPE-EE** ≈ **1Ph$_3$-A** > other complexes. The formation of multiple PPh_3 coordinated complex as well as the PPh_3 and DPPE mixed coordination are endothermic when solvation effect was included. The energy difference between **1Ph$_3$-A** and **2Ph$_3$-EA** is 7.3 kcal/mol at 298 K and 9.9 kcal/mol at 413K. Such large free energy difference suggests the only formation of $HIr(CO)(PPh_3)_3$ even at high PPh_3 concentration; and this does not agree with the reported experimental results. Therefore, only M062X-GD3 can give reliable energies.

Since the complexes of *p*-OCH_3 modified PPh_3 (**L1**) and *p*-CF_3 modified DPPE (**L10**) ligands have been found to have better catalytic performance in our experiment, the stability of the **L1**/**L10** coordinated Iridium hydride complexes was computed (Figure DFT-S2). It shows that the two isomers of **L10** coordinated bidentate complexes, **L10-EA** and **L10-EE**, are much

more stable than the two isomers of **L1** coordinated monodentate complexes **L1-E** and **L1-A** under M062X-GD3-SMD level (–23.8 vs. –14.4 and –20.2 vs. –10.6 kcal/mol). It can be found that both **L1** and **L10** coordinated isomers at the axial positions (**L1-A** and **L10-EA**) are more stable than those at only equatorial positions (**L1-E** and **L10-EE**). Furthermore, two **L10** coordinated complex **2L10** has lower substitution Gibbs free energy than the **L10-EA** by 2.3 kcal/mol. This shows that the two **L10** coordinated complex can only be formed under very high ligand to metal ratio, and once the **2L10** complex formed, the catalyst would be deactivated due to the lack of vacancy for substrate coordination. However, this is not possible under our reaction conditions with extremely high CO pressure and fixed ligand to metal ratio (Figure DFT-S3). Surprisingly, the **L1** and **L10** mix-coordinated complex **L10-EA-L1-E** (–25.2 kcal/mol) is more stable than the complexes with only one kind of ligand by 1.4 and 10.8 kcal/mol, respectively. It demonstrates that in the system with both **L1** and **L10** ligands, **L10-EA** and **L1-A** could be found for [**L1**+**L10**]/[Ir] ≤ 1, while **L10-EA-L1-E** could be found for [**L1**+**L10**]/[Ir] > 1. Therefore, the system containing two kinds of ligand will become much more complicated. Under our reaction conditions with extremely high CO pressure and fixed ligand to metal ratio, however, the formation of **L10-EA-L1-E** should be less likely (Figure DFT-S3) and the much low concentration even if the **L10-EA-L1-E** is formed should not determine and control the reaction activity. Therefore, no further reaction activity for **L10-EA-L1-E** complex was considered.

(3) Activity and selectivity: To understand the whole reaction mechanism, we systematically calculated the reaction pathways for the formation of linear aldehyde, alkane and alcohol in the hydroformylation with 1-butene as substrate for terminal olefine catalyzed by the parent $HIr(CO)_4$ (Scheme S1). Benchmark testing was done once again to find a reliable method for describing the reactivity of $HIr(CO)_4$ reasonably. Single-point energies using B3PW91[12], B3PW91-GD3, M062X, M062X-GD3, MN15[13] methods were done based on the M06L optimized gas phase geometries. The obtained apparent barriers for the formation of aldehyde, alkane and alcohol with respect to the $HIr(CO)_4$ are listed in Table DFT-S1. It is found that all methods give similar results and the same trend. Considering the most reliable results of M062X-GD3-SMD in estimating the stability on the basis of the ligand exchange Gibbs free energy (Figure DFT-S1), the results of M062X-GD3-SMD at 413 K were used in following discussion and the results of M06L were also listed for comparison.

Based on the results mentioned above, the whole reaction processes of one/two PPh_3 and one DPPE coordinated complexes with 1-butene as substrate for terminal olefine were studied. Considering their very similar coordination skeletons between PPh_3 and **L1** as well as between DPPE and **L10** ligands, it is reasonably to suppose that **L1/L10** have similar potential energy surfaces (PES) with those of PPh_3/DPPE in the whole hydroformylation and hydrogenation process, and only the possible rate-determining transition states of **L1**/**L10** coordinated Iridium hydride complexes were considered. The obtained minimum apparent barriers of the formation of aldehyde, alkane, and alcohol using different catalysts with respect to their pre-catalysts are listed in Table DFT-S2, and the full PES of different catalysts are shown in Figure DFT-S4-S6. It should be mentioned that the real catalytic cycle starts with the formation of the coordinatively unsaturated active catalysts up on CO dissociation from the pre-catalysts, and this is the so-called initiation step in general. The coordinatively unsaturated active catalytic species in the whole reaction is donated as **IM1**. The corresponding mechanism is shown in Scheme S2. Based on this initiation mechanism, the effective barriers are obtained (Table DFT-

S3). It is noted that the **DPPE-EE** and **L10-EE** isomers, which need considerably higher energy (33.6/31.3 kcal/mol) in the initiation step towards CO dissociation than the **EA** isomers, should have rather low reaction possibility along the **EE** pathway. Therefore, we only kept the results of the two **EA** isomers in Table DFT-S3, and the following discussion of **DPPE** and **L10** ligands refers only to the **EA** isomers.

In our experiments we tested different pre-catalysts under varying reaction conditions, for example, different solvents, varying CO pressure and temperature, H_2O content, acid, LiCl additive, ligand to metal ratio, as well as one system with two ligands in different ratios, using either water-gas shift reaction for producing H_2 ($CO + H_2O = CO_2 + H_2$) or synthesis ($CO + H_2$) gas. Computationally, our reaction can be considered as stoichiometric under ideal condition with synthesis gas. Therefore, the computed reaction activity and product selectivity should be used as a reference for experiment, and comparison between computation and experiment should be made under as close condition as possible. It is noted that we computed only the linear reaction paths and did not consider the isomerization and the corresponding *iso* reaction paths. In addition, we did not consider the side reactions of aldehyde and alcohol condensation, which might affect the yield and selectivity.

(3a) Activity and selectivity of $HIr(CO)_4$: For the parent complex $HIr(CO)_4$ (Table DFT-S2), the apparent barrier of aldehyde and alkane formation is 21.6, 25.1 kcal/mol, respectively. At low temperature (M062X-D3-SMD-298 K), the barrier of aldehyde and alkane formation is even lower (20.9/21.5 kcal/mol). Apparently, aldehyde has higher kinetic selectivity than alkane. Indeed, this computed result agrees with our experimental finding under synthesis gas condition (Table S1), i.e., the selectivity of aldehyde is higher than that of alkane at low temperature, indicating the lower kinetic barrier of aldehyde formation than that of alkane formation. However, it is noted that alkane formation is more favored thermodynamically than aldehyde formation (–18.7 vs. –13.8 kcal/mol). Based on the rather low apparent barriers, it is to expect that the selectivity of aldehyde vs. alkane can be switched simply by increasing temperature, since high temperature affects reaction with higher barrier more strongly than that with lower barrier according to Eyring–Polanyi equation, and the selectivity changes from kinetic to thermodynamic controlled. This trend is found in our experiment (Table S1).

In a reaction using 0.2 mol% [Ir(cod)acac], 10.2 mmol 1-octene (10.2 mmol) in THF (6 ml) solution at 100 °C under synthesis gas condition (CO/H_2 =2:1, 20 bar) without acid and additive for 16 hours, Piras *et al.*,[14] found the formation of both aldehyde (30%) and alkane (65%), and this agrees with our computed results. In a reaction using 0.05 mmol of $Ir_4(CO)_{12}$, 22 mL of 25% aqueous trimethylamine, 78 mL of THF, 350 psi of CO, and 150 psi of propylene at 125 °C in an autoclave, a ratio of aldehyde to alcohol of 300 after 10 hours was found, however, alkane from propylene hydrogenation was not observed.[15] This is different from reaction under acidic or neutral conditions.

Next, one might expect the formation of alcohol from the corresponding hydrogenation of the formed aldehyde. However, the rather higher barrier of alcohol formation (45.3 kcal/mol) suppresses aldehyde hydrogenation to alcohol. This is also true for reaction at higher temperature using synthesis gas (Table S1) and water-gas shift reaction (Table S2).

(3b) Activity and selectivity of $HIr(CO)_3(PPh_3)$: For reactions catalyzed by $HIr(CO)_3(PPh_3)$, the apparent barrier of aldehyde and alkane formation is 31.7 and 32.6 kcal/mol, respectively (Table DFT-S2), the initiation step needs to overcome 6.0 and 6.6 kcal/mol, respectively. The

lowest effective barrier of aldehyde and alkane formation is 25.7 and 26.0 kcal/mol, respectively (Table DFT-S3). Obviously, aldehyde has higher selectivity than alkane, and this agrees with our current results by using synthesis gas (CO/H_2 = 1/1, 40 bar) resulting aldehyde (81%) and alkane (19%) (Table 1, entry 1). The higher selectivity of aldehyde over alkane is also confirmed by a previously reported experiment using the well-defined catalyst $[Ir_2(CO)_6(PPh_3)_2]$ producing aldehyde/alkane ratio of 46% to 41% (solvent THF, 100 °C).[11]

Next, the barrier of alcohol formation of 47.3 kcal/mol is considerably high and the effective barrier is 40.7 kcal/mol. Therefore, alcohol formation is kinetically unlikely or has very low selectivity in this system. These results are confirmed by a previously reported experimental study using 3,3-dimethyl-1-butene as substrate under the given reaction conditions ([Ir] = 5.0 mM, $[PPh_3]$ = 20 mM, [olefin] = 0.9 M, 100 °C, $p(CO)$ = 1 MPa, $p(H_2)$ = 1 MPa, toluene),[8] and aldehyde has higher selectivity than alkane (83.9 vs. 15.5%) and the yield of alcohol is rather low (0.6%).

(3c) Activity and selectivity of $HIr(CO)_2(PPh_3)_2$: As discussed in the relative stability of the pre-catalysts (Figure DFT-S1), $HIr(CO)_3(PPh_3)$ and $HIr(CO)_2(PPh_3)_2$ have close stability and equilibrium under stoichiometric condition as well as high $[PPh_3]/[Ir]$ ratio increases the percentage content $HIr(CO)_2(PPh_3)_2$ under equilibrium, we computed the corresponding reactions catalyzed by $HIr(CO)_2(PPh_3)_2$. At first, it is found that the apparent barrier of $HIr(CO)_2(PPh_3)_2$ is higher than that of $HIr(CO)_3(PPh_3)$ by 4.2 kacl/mol for aldehyde formation, and this shows that under the same temperature, reaction catalyzed by $HIr(CO)_2(PPh_3)_2$ should be slower than that catalyzed by of $HIr(CO)_3(PPh_3)$ and long reaction time is needed to get high conversion and yield. Indeed, with the increase of $[PPh_3]/Ir$ ratio, which should increase the content of $HIr(CO)_2(PPh_3)_2$, the reaction did not have full conversion after 20 h; and higher conversion was only found by extending the reaction time from 20h to 48 h (Table 1, entry 3). This relation was also reported in a previous study, i.e., at $[PPh_3]/Ir$ =4/1, the conversion became lower that that at $[PPh_3]/Ir$ =1/1 (74% vs. 87%), and higher conversion was achieved only after longer reaction time (20 vs. 16h). This shows that the computed activity is verified by the experiment.

Apart from the activity, we also computed the selectivity. It is found that the formation of aldehyde and alkane has equal barrier (26.5 kcal/mol), and it does not show any selectivity. Therefore, one can conclude that the selectivity of aldehyde and alkane is mainly $HIr(CO)_3(PPh_3)$ controlled.

To our surprise, the $HIr(CO)_2(PPh_3)_2$ catalyzed alcohol formation has low effective barrier (31.3 kcal/mol) and it is to believe that at certain concentration of $HIr(CO)_2(PPh_3)_2$ in the system, the formed aldehyde should be hydrogenated to alcohol. This phenomenon is indeed reported by Kubis et al in their experimental work,[8] where they found 0.6% selectivity of alcohol for $[PPh_3]/[Ir]$ =4 under syngas condition at 100 °C. Since the $[PPh_3]/[Ir]$ is normally 1.1:1 in our work with very high CO concentration (pressure), the mainly catalyst should be one PPh_3 coordinated complexes $HIr(CO)_3(PPh_3)$, we therefore only discussed the results of **$1Ph_3$-A/$1Ph_3$-E** catalyzed reactions.

(3c) Activity and selectivity of $HIr(CO)_2(DPPE)$: For $HIr(CO)_2$(DPPE) catalyzed reactions (Table DFT-S3), the effective barrier of the formation of aldehyde and alkane is 23.8, 26.8 kcal/mol, respectively, aldehyde should be the predominant product over alkane. Since the effective barrier 36.3 kcal/mol) of alcohol formation is lower than that using $HIr(CO)_3(PPh_3)$

(40.7 kcal/mol) (Table DFT-S3), it should be possible to hydrogenate aldehyde to alcohol under the same reaction condition. Indeed, the experimentally observed yield ratio of (alcohol+aldehyde)/alkane is (15+35)/25 along with 20% internal olefine (Table S4, entry 2). Next, we considered the formation of internal olefine, and this step is actually the internal β-hydride elimination from the previously formed terminal alkyl complex from Ir-H insertion; and this barrier (28.9 kcal/mol) is close to that of alkane formation (28.9 vs. 26.8 kcal/mol), which gives higher ratio of alkane over internal olefine, in agreement with the experiment (25% to 20%).

(3d) Activity and selectivity of $HIr(CO)_3$(L1): For $HIr(CO)_3$(**L1**) catalyzed reactions, the effective barrier for the formation of aldehyde, alkane and alcohol is 23.8, 25.6, 40.6 kcal/mol, respectively, and they are slightly lower than those catalyzed by $HIr(CO)_3(PPh_3)$ (25.7, 26.0, 40.7 kcal/mol, respectively). The larger barrier difference in forming aldehyde and alkane using $HIr(CO)_3$(**L1**) than using $HIr(CO)_3(PPh_3)$ (1.8 vs. 0.3 kcal/mol) should give higher aldehyde to alkane ratio for the former than for the latter. This relation is actually found in our experiment, i.e., the selectivity ratio of aldehyde/alkane is 90/10, very close to the experimental result (96:2, Table 1, Entry 5), and higher than that (81:19, Table 1, Entry 1) for using $HIr(CO)_3(PPh_3)$. In addition, one can see that the barrier of aldehyde hydrogenation to alcohol is still too high under reaction conditions and this is probably why alcohol was not detected (Table 1, Entry 5).

(3e) Activity and selectivity of $HIr(CO)_2$(L10): For $HIr(CO)_2$(**L10**) catalyzed reactions, the effective barrier for the formation of aldehyde, alkane and alcohol is 24.8, 30.2, 38.4 kcal/mol, respectively, higher than those (23.8, 26.8, 36.3 kcal/mol, respectively) catalyzed by $HIr(CO)_2$(DPPE). It shows that aldehyde should be the principal product. The larger difference in effective barrier for the formation of aldehyde and alkane of $HIr(CO)_2$(**L10**) compared to that of $HIr(CO)_2$(DPPE) (5.4 vs. 3.0 kcal/mol) indicates a higher aldehyde selectivity; and this trend is verified experimentally (Table 1, entry 14 and 15), the ratio of (aldehyde+alcohol)/alkane is (1+47)/36 for $HIr(CO)_2$(DPPE), while (26+47)/18 for $HIr(CO)_2$(**L10**). The different *n/iso* ratio in aldehyde and alcohol reveals the participation of internal olefines as intermediate from terminal olefine isomerization on one hand, and the corresponding reaction of internal olefines to aldehydes and alcohols on the other hand. Comparing the activity and selectivity of **L1** and **L10** ligand coordinated complex, $HIr(CO)_3$(**L1**) has lower effective barriers for the formation of aldehyde (23.8 vs 24.8 kcal/mol) and alkane (25.6 vs 30.2 kcal/mol) than $HIr(CO)_2$(**L10**), while $HIr(CO)_2$(**L10**) has lower effective barrier for alcohol formation (38.4 vs 40.6 kcal/mol) (Table DFT-S3). Qualitatively, one can conclude that when reaction system containing both $HIr(CO)_3$(**L1**) and $HIr(CO)_2$(**L10**), $HIr(CO)_3$(**L1**) will be more dominant for aldehyde and alkane formation, while $HIr(CO)_2$(**L10**) should be more dominant for alcohol formation. The mixed system should probably produce alcohol from such one-pot domino reaction more efficient than the solo system.

The Cartesian coordinates (xyz files) of all used structures optimized at M06L level and their corresponding thermal correction to Gibbs free energy, single point energy calculated at M062X-D3 level are afforded.

Table DFT-S1. The minimum barriers of aldehyde, alkane and alcohol formation on the potential energy surface (PES) of pure carbonyl Iridium catalyst considering the solvation effect (methanol) at 413K under different methods.

kcal/mol	Aldehyde	Alkane	Alcohol
B3PW91	28.8	32.5	56.8
B3PW91-D3	23.4	27.1	52.7
M062X	21.9	25.5	45.6
M062X-D3	21.6	25.1	45.3
MN15	24.3	28.4	51.8
M06L	27.4	31.3	52.7

Table DFT-S2. The minimum barriers of aldehyde, alkane and alcohol formation on the PES of different catalysts at M06L and M062X-D3 level with respect to the catalysts.

Unit	M06L-gas-298K			M06L-sol-298K		
kcal/mol	Aldehyde	Alkane	Alcohol	Aldehyde	Alkane	Alcohol
CO	27.2	27.2	48.8	26.6	27.5	48.9
$1Ph_3$-A	34.9	34.9	46.9	36.5	36.5	49.5
$1Ph_3$-E	34.6	34.6	50.1	37.4	37.4	49.5
$2Ph_3$-EA	40.9	40.9	43.5	45.8	45.8	48.4
$2Ph_3$-EE	36.7	36.7	47.0	42.2	42.2	51.0
DPPE-EA	36.4	36.4	45.4	41.0	41.0	48.2
DPPE-EE	43.0	43.0	47.4	42.5	42.5	50.9
L1-A	34.9	34.9	45.8	36.4	36.4	49.3
L1-E	32.7	32.7	45.8	35.8	35.8	49.3
L10-EA	35.2	35.2	44.8	40.0	40.0	48.5
L10-EE	41.3	41.3	44.8	40.1	40.1	48.5
Unit	M06L-sol-413K			M062X-D3-sol-413K		
kcal/mol	Aldehyde	Alkane	Alcohol	Aldehyde	Alkane	Alcohol
CO	27.4	31.3	52.7	21.6	25.1	45.3
$1Ph_3$-A	38.6	39.7	54.2	31.7	33.5	47.3
$1Ph_3$-E	39.2	39.2	54.2	32.6	32.6	47.3
$2Ph_3$-EA	47.1	47.1	52.1	39.0	39.0	43.8
$2Ph_3$-EE	43.8	43.8	52.7	35.9	35.9	45.0
DPPE-EA	42.3	42.6	52.5	33.8	36.8	46.3
DPPE-EE	41.0	41.0	52.5	33.6	33.6	46.3
L1-A	38.4	38.7	53.6	31.5	32.4	46.6
L1-E	37.2	37.9	53.6	29.8	31.6	46.6
L10-EA	41.4	43.9	53.2	33.1	38.5	46.7
L10-EE	39.2	39.2	53.2	31.3	31.3	46.7

Table DFT-S3. The effective barriers of aldehyde, alkane and alcohol formation on the PES of different catalysts at M06L and M062X-D3 level with respect to the real active species.

Unit	M06L-gas-298K			M06L-sol-298K		
kcal/mol	Aldehyde	Alkane	Alcohol	Aldehyde	Alkane	Alcohol
CO	18.0	18.0	39.6	19.3	20.2	41.6
$1Ph_3$-A	18.4	18.4	30.4	22.7	22.7	35.7
$1Ph_3$-E	21.2	21.2	36.7	23.5	23.5	35.6
$2Ph_3$-EA	31.1	31.1	33.7	25.4	25.4	28.0
$2Ph_3$-EE	19.9	19.9	30.2	24.1	24.1	32.9
DPPE-EA	19.5	19.5	28.5	22.3	22.3	29.5
L1-A	18.9	18.9	29.8	23.0	23.0	35.9
L1-E	20.2	20.2	33.3	22.3	22.3	35.8
L10-EA	19.8	19.8	29.4	22.8	22.8	31.3
Unit	M06L-sol-413K			M062X-D3-sol-413K		
kcal/mol	Aldehyde	Alkane	Alcohol	Aldehyde	Alkane	Alcohol
CO	24.4	28.3	49.7	22.4	25.9	46.1
$1Ph_3$-A	28.7	29.8	44.3	25.7	27.5	41.3
$1Ph_3$-E	29.1	29.1	44.1	26.0	26.0	40.7
$2Ph_3$-EA	30.1	30.1	35.1	26.5	26.5	31.3
$2Ph_3$-EE	30.6	30.6	39.5	26.8	26.8	35.9
DPPE-EA	28.0	28.3	38.2	23.8	26.8	36.3
L1-A	29.1	29.4	44.3	26.2	27.1	41.3
L1-E	27.7	28.4	44.1	23.8	25.6	40.6
L10-EA	29.1	31.6	40.9	24.8	30.2	38.4

$HIr(CO)_4 + nL = HIr(CO)_{4-n}L_n + nCO$

M06L-gas-298K

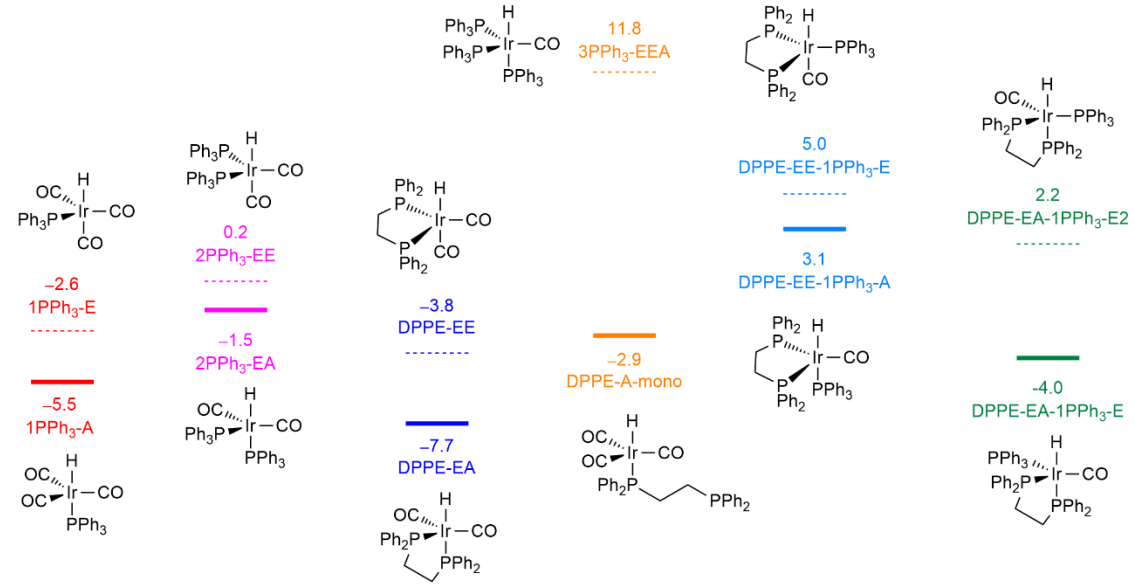

M06L-sol-298K

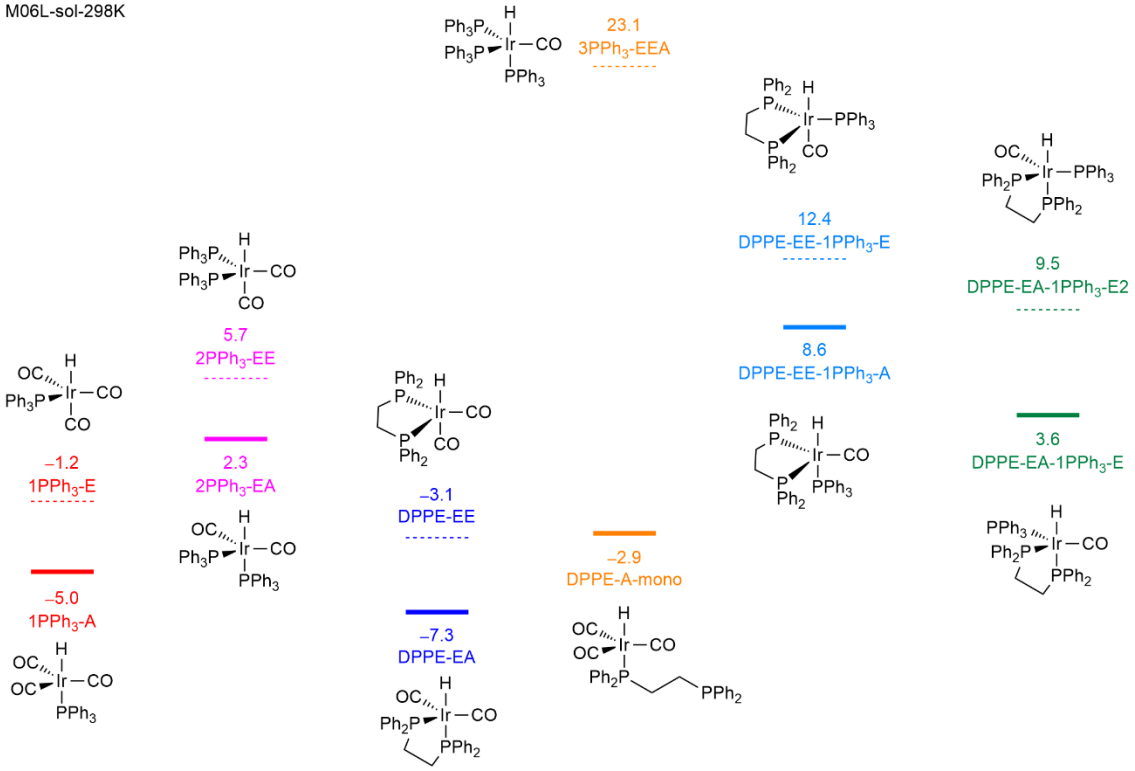

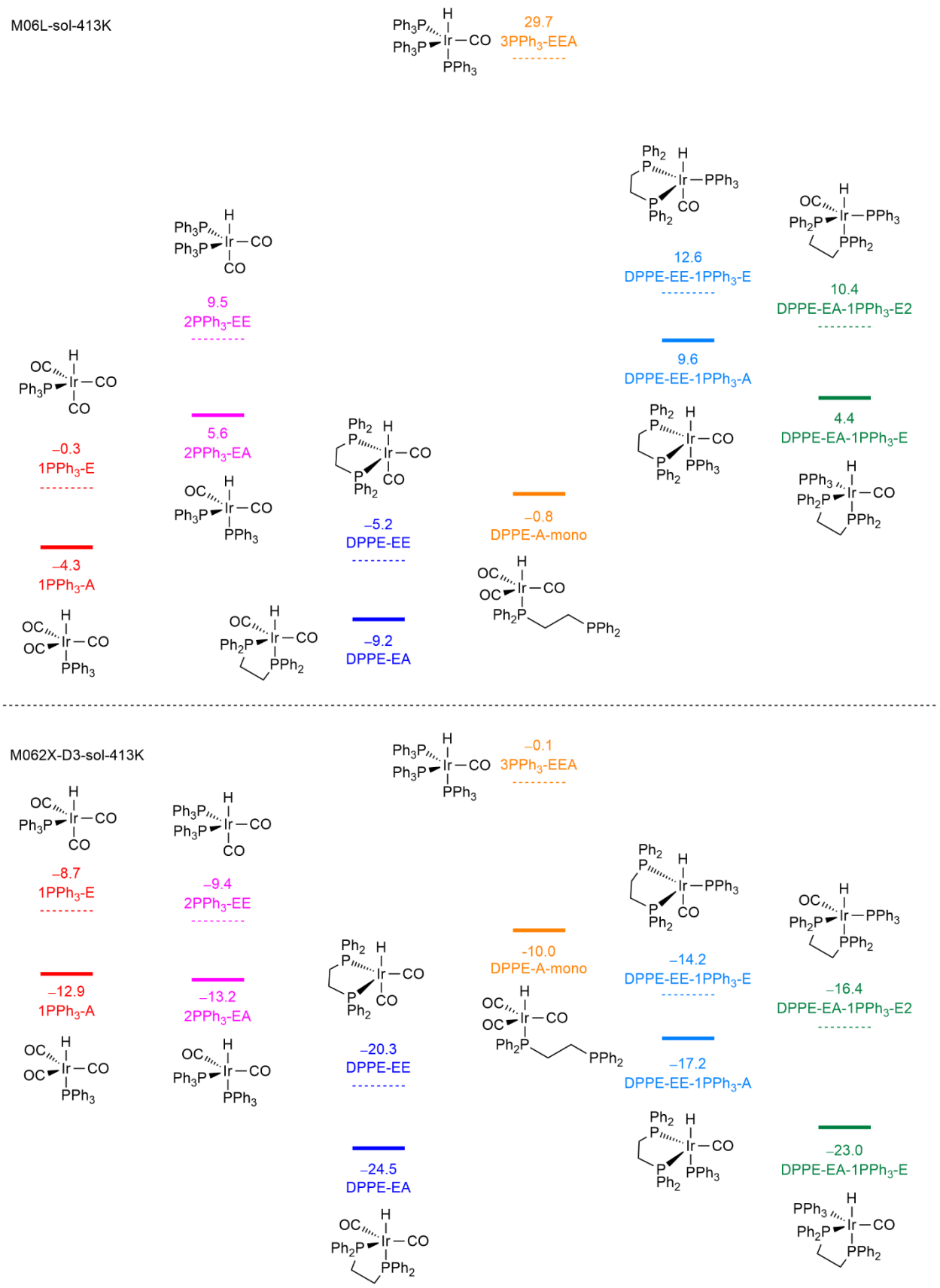

Figure DFT-S1. Ligand substitution free energy profile of different Iridium complex.

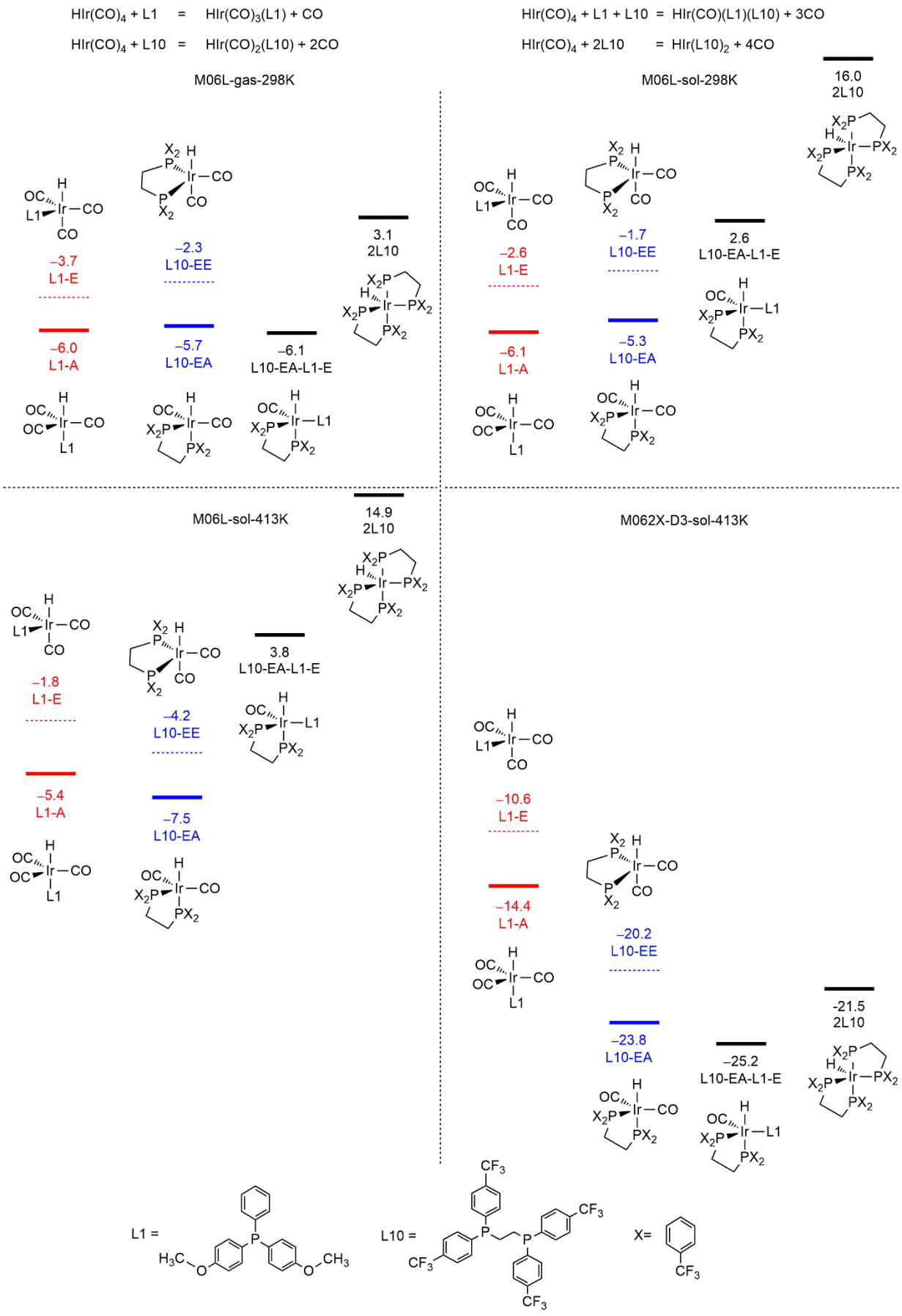

Figure DFT-S2. Ligand Substitution free energy profile of **L1** and **L10** with $HIr(CO)_4$.

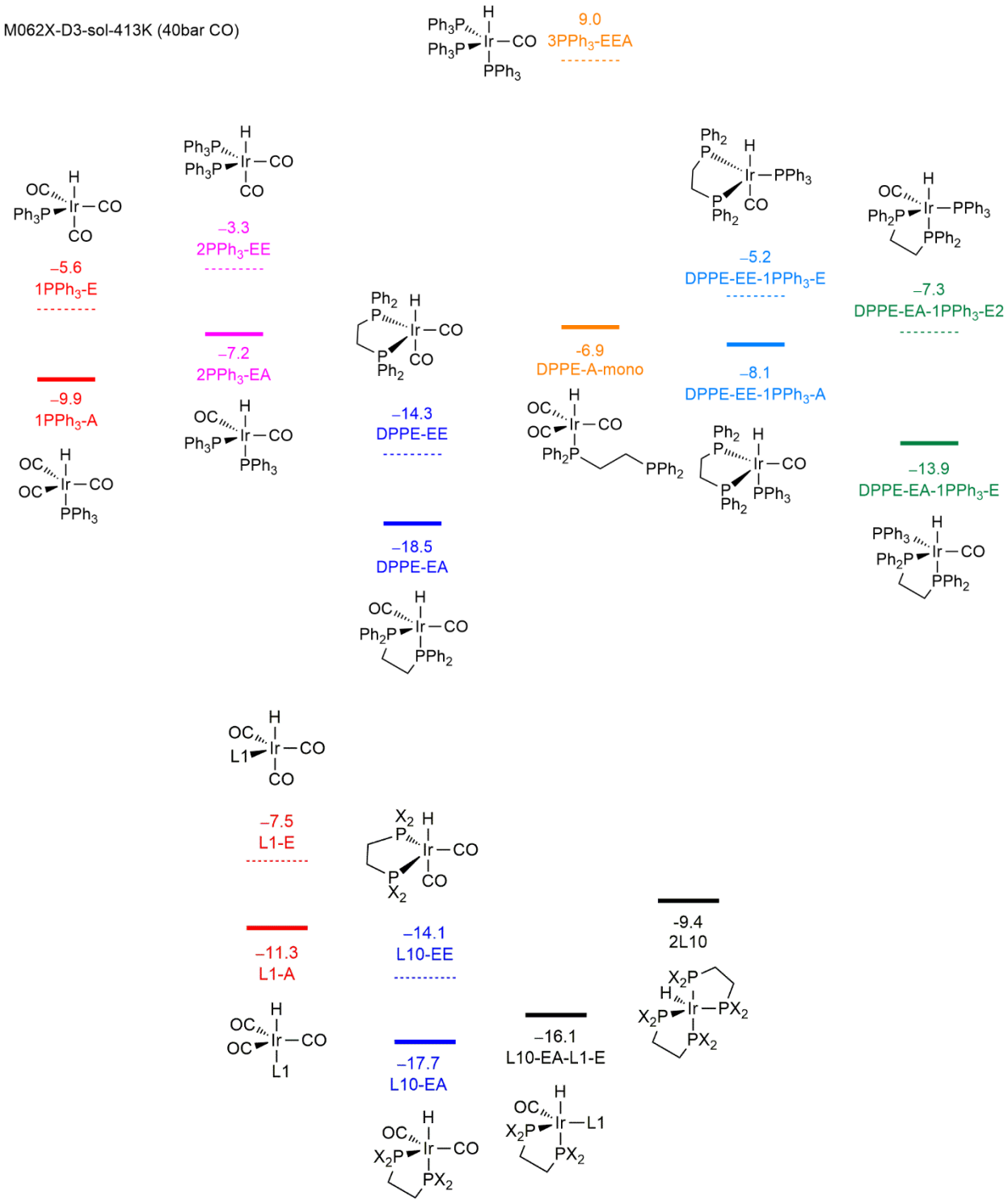

Figure DFT-S3. Ligand Substitution free energy profile of different ligand with $HIr(CO)_4$ at 40 bar CO.

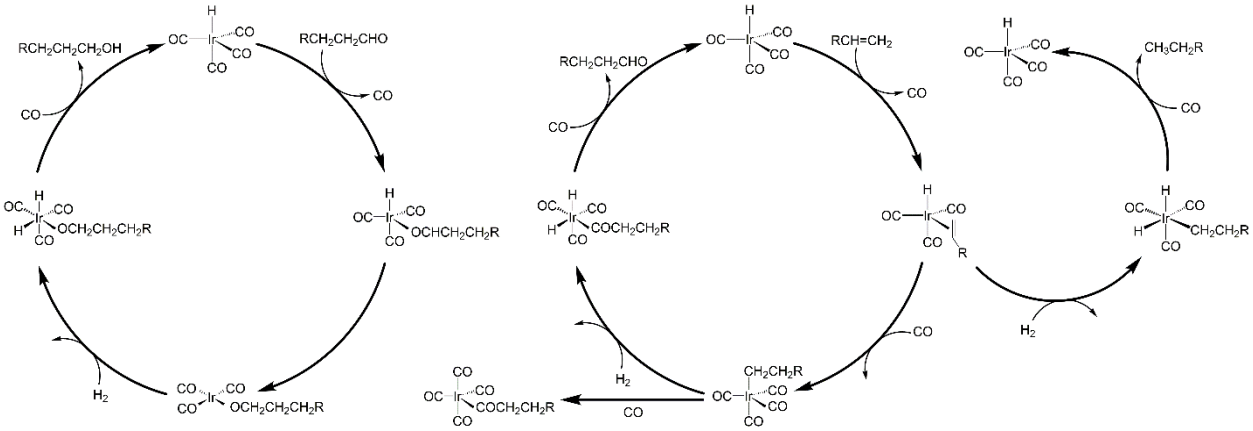

Scheme S1. Catalytic cycle for the hydroformylation (middle part)/hydrogenation (right part)/further reduction (left part) of alkene catalyzed by $HIr(CO)_4$.

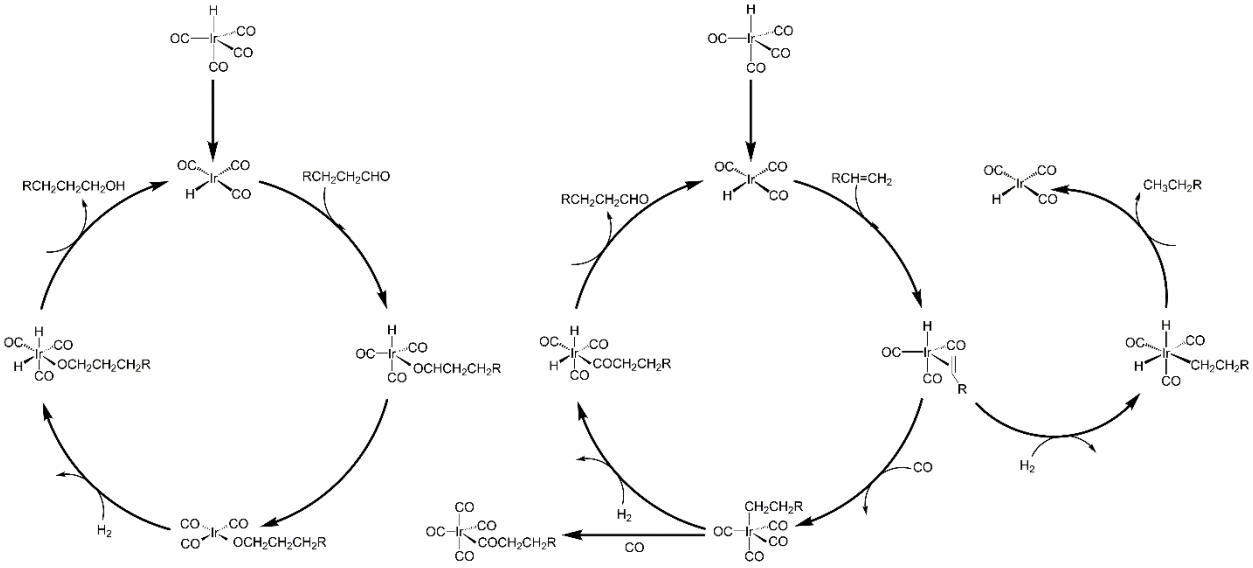

Scheme S2. Initiation mechanism catalytic cycle for the hydroformylation (middle part)/hydrogenation (right part)/further reduction (left part) of alkene catalyzed by $HIr(CO)_4$.

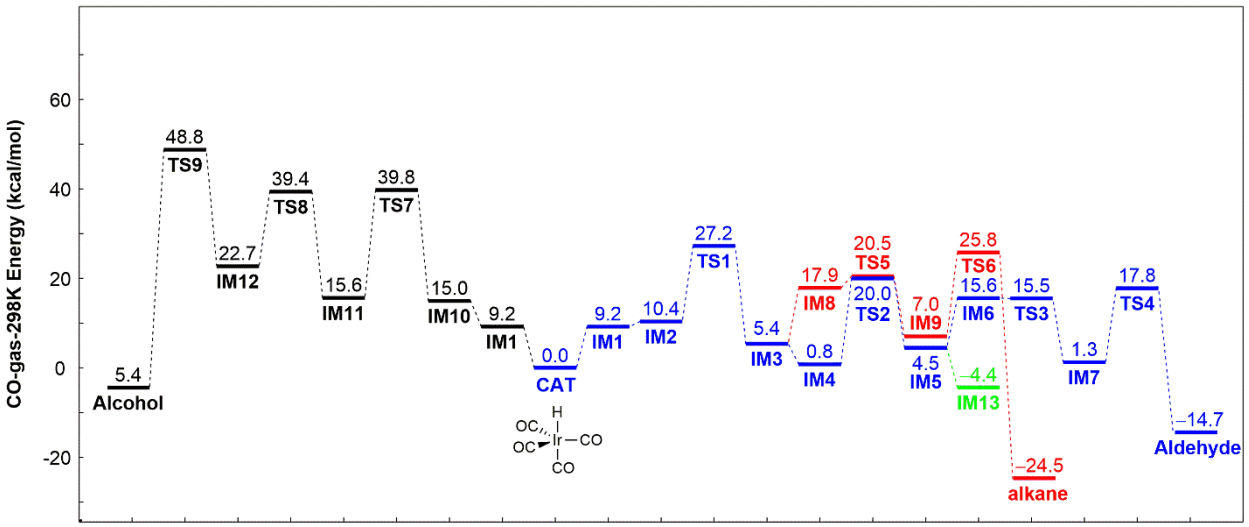
CO-gas-298K Energy (kcal/mol)
60
40
20
0
-20
5.4
Alcohol
48.8
TS9
22.7
IM12
39.4
TS8
15.6
IM11
39.8
TS7
15.0
IM10
9.2
IM1
0.0
CAT
9.2
IM1
10.4
IM2
27.2
TS1
5.4
IM3
17.9
IM8
0.8
IM4
20.5
TS5
20.0
TS2
7.0
IM9
4.5
IM5
25.8
TS6
15.6
IM6
-4.4
IM13
15.5
TS3
1.3
IM7
17.8
TS4
-14.7
Aldehyde
-24.5
alkane

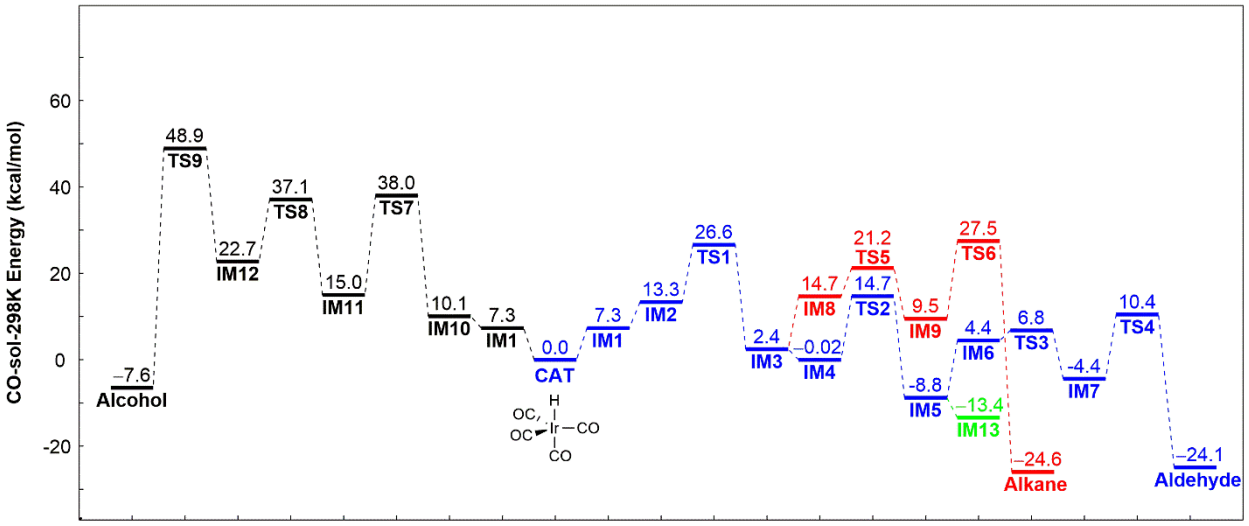
CO-sol-298K Energy (kcal/mol)
60
40
20
0
-20
-7.6
Alcohol
48.9
TS9
22.7
IM12
37.1
TS8
15.0
IM11
38.0
TS7
10.1
IM10
7.3
IM1
0.0
CAT
7.3
IM1
13.3
IM2
26.6
TS1
2.4
IM3
14.7
IM8
-0.02
IM4
21.2
TS5
14.7
TS2
9.5
IM9
-8.8
IM5
27.5
TS6
4.4
IM6
-13.4
IM13
6.8
TS3
-4.4
IM7
10.4
TS4
-24.1
Aldehyde
-24.6
Alkane

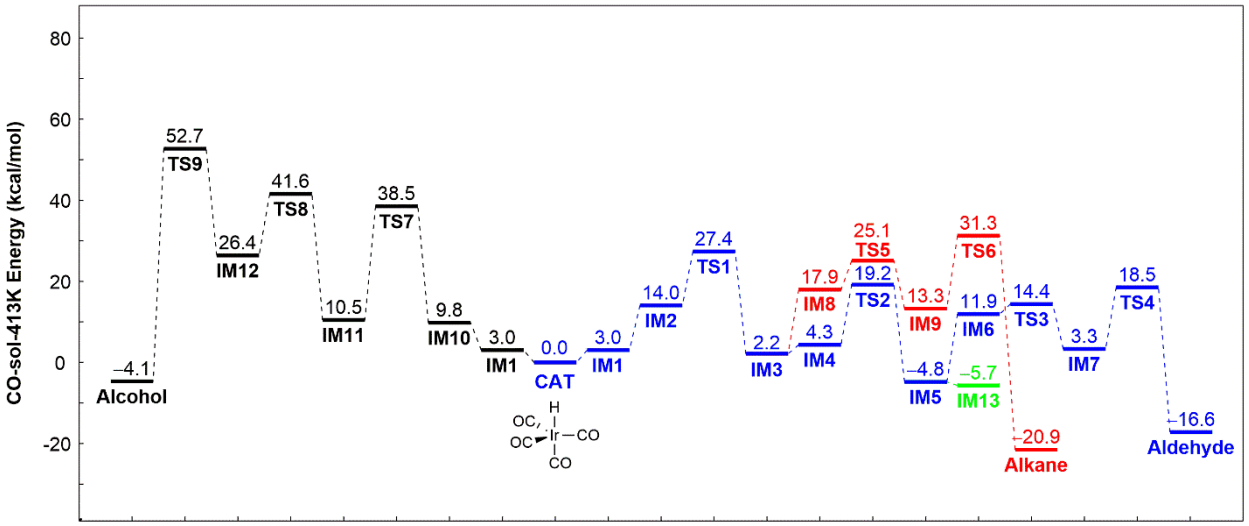
CO-sol-413K Energy (kcal/mol)
80
60
40
20
0
-20
-4.1
Alcohol
52.7
TS9
26.4
IM12
41.6
TS8
10.5
IM11
38.5
TS7
9.8
IM10
3.0
IM1
0.0
CAT
3.0
IM1
14.0
IM2
27.4
TS1
2.2
IM3
17.9
IM8
4.3
IM4
25.1
TS5
19.2
TS2
13.3
IM9
-4.8
IM5
31.3
TS6
11.9
IM6
-5.7
IM13
14.4
TS3
3.3
IM7
18.5
TS4
-16.6
Aldehyde
-20.9
Alkane

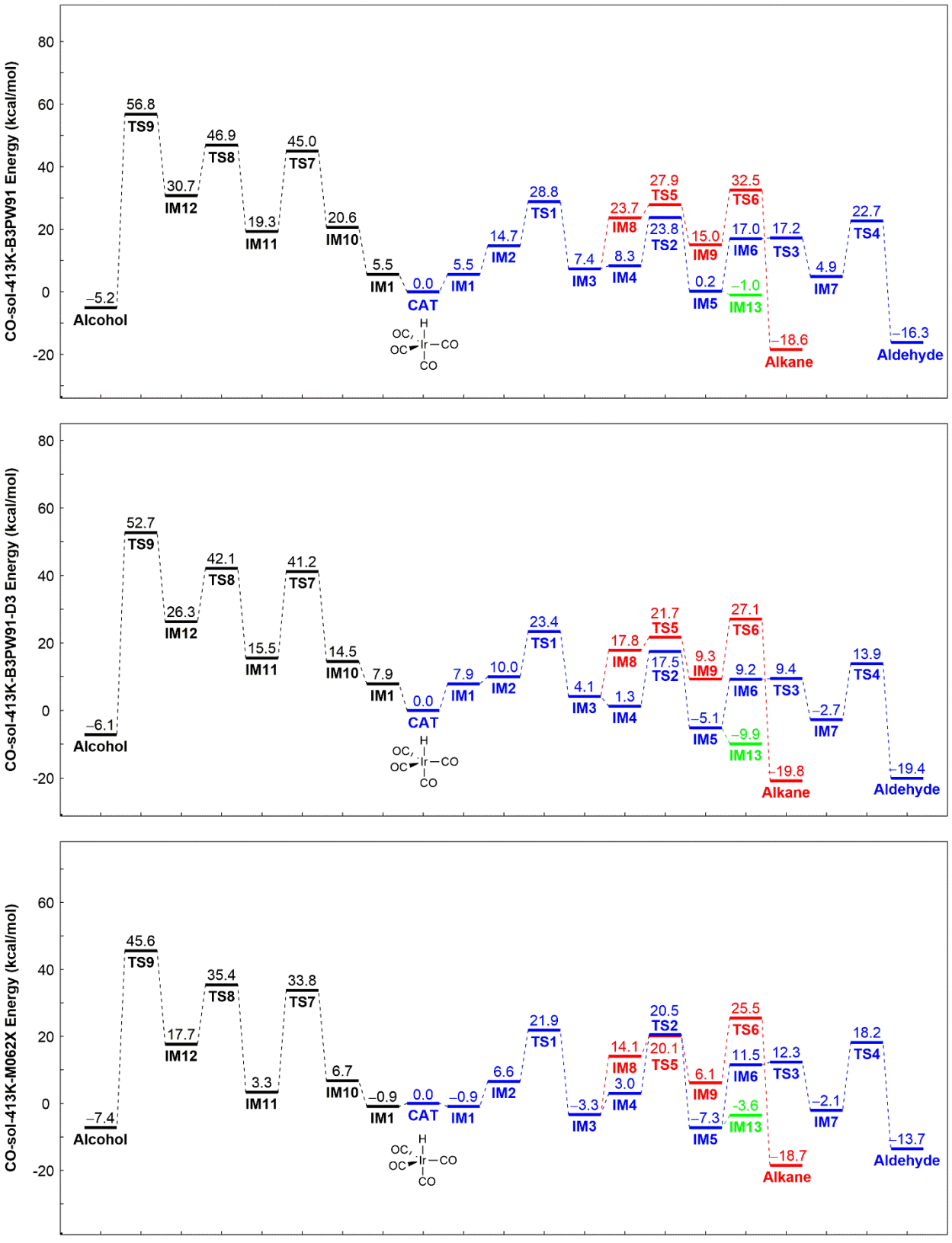
CO-sol-413K-B3PW91 Energy (kcal/mol)
80
60
40
20
0
-20
−5.2
Alcohol
56.8
TS9
30.7
IM12
46.9
TS8
19.3
IM11
45.0
TS7
20.6
IM10
5.5
IM1
0.0
CAT
5.5
IM1
14.7
IM2
28.8
TS1
7.4
IM3
23.7
IM8
8.3
IM4
27.9
TS5
23.8
TS2
15.0
IM9
0.2
IM5
32.5
TS6
17.0
IM6
−1.0
IM13
17.2
TS3
−18.6
Alkane
4.9
IM7
22.7
TS4
−16.3
Aldehyde
CO-sol-413K-B3PW91-D3 Energy (kcal/mol)
80
60
40
20
0
-20
−6.1
Alcohol
52.7
TS9
26.3
IM12
42.1
TS8
15.5
IM11
41.2
TS7
14.5
IM10
7.9
IM1
0.0
CAT
7.9
IM1
10.0
IM2
23.4
TS1
4.1
IM3
17.8
IM8
1.3
IM4
21.7
TS5
17.5
TS2
9.3
IM9
−5.1
IM5
27.1
TS6
9.2
IM6
−9.9
IM13
9.4
TS3
−19.8
Alkane
−2.7
IM7
13.9
TS4
−19.4
Aldehyde
CO-sol-413K-M062X Energy (kcal/mol)
60
40
20
0
-20
−7.4
Alcohol
45.6
TS9
17.7
IM12
35.4
TS8
3.3
IM11
33.8
TS7
6.7
IM10
−0.9
IM1
0.0
CAT
−0.9
IM1
6.6
IM2
21.9
TS1
−3.3
IM3
14.1
IM8
3.0
IM4
20.5
TS2
20.1
TS5
6.1
IM9
−7.3
IM5
25.5
TS6
11.5
IM6
-3.6
IM13
12.3
TS3
−18.7
Alkane
−2.1
IM7
18.2
TS4
−13.7
Aldehyde

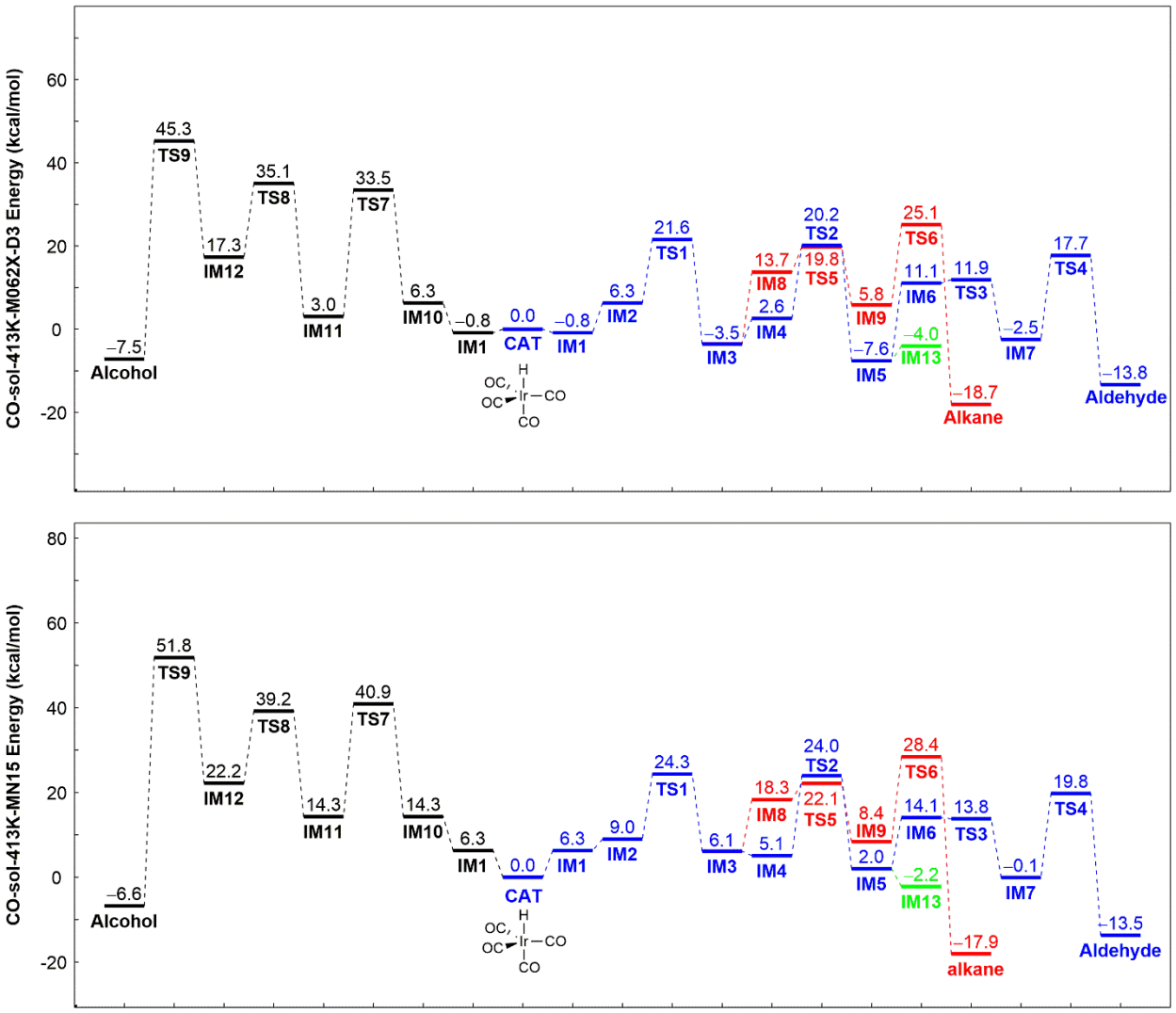

Figure DFT-S4. Free energy profile of the catalytic cycle shown in Scheme S1 catalyzed by $HIr(CO)_4$. (**gas** and **sol** represent considering without or with the methanol solvation effect. M06L method was used when there is no special explanation. **CAT** represents the corresponding catalyst, **IM** represents the intermediate during the reaction, and **TS** represents the transition state. The bule, red and black line indicating the pathway of hydroformylation to aldehyde, hydrogenation to alkane form olefine, and reduction to alcohol from aldehyde, respectively. The green line represents the resting state.)

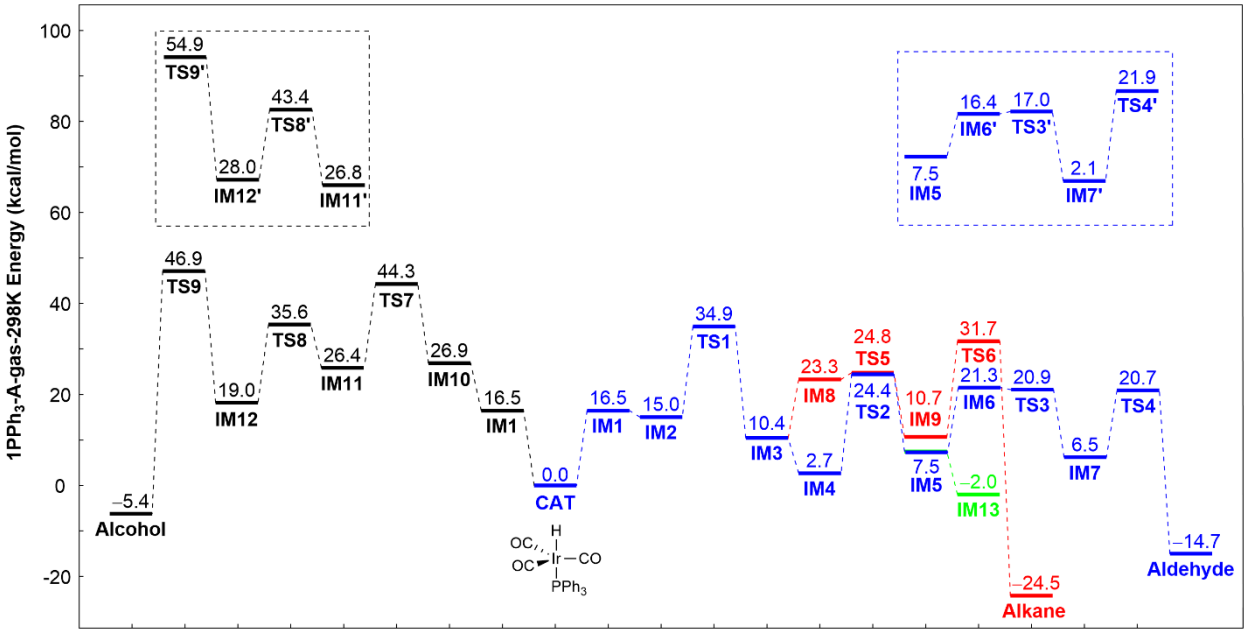
1PPh3-A-gas-298K Energy (kcal/mol)
100
80
60
40
20
0
-20
54.9
TS9'
28.0
IM12'
43.4
TS8'
26.8
IM11'
7.5
IM5
16.4
IM6'
17.0
TS3'
2.1
IM7'
21.9
TS4'
-5.4
Alcohol
46.9
TS9
19.0
IM12
35.6
TS8
26.4
IM11
44.3
TS7
26.9
IM10
16.5
IM1
0.0
CAT
16.5
IM1
15.0
IM2
34.9
TS1
10.4
IM3
23.3
IM8
2.7
IM4
24.8
TS5
24.4
TS2
10.7
IM9
7.5
IM5
31.7
TS6
21.3
IM6
-2.0
IM13
20.9
TS3
6.5
IM7
20.7
TS4
-14.7
Aldehyde
-24.5
Alkane

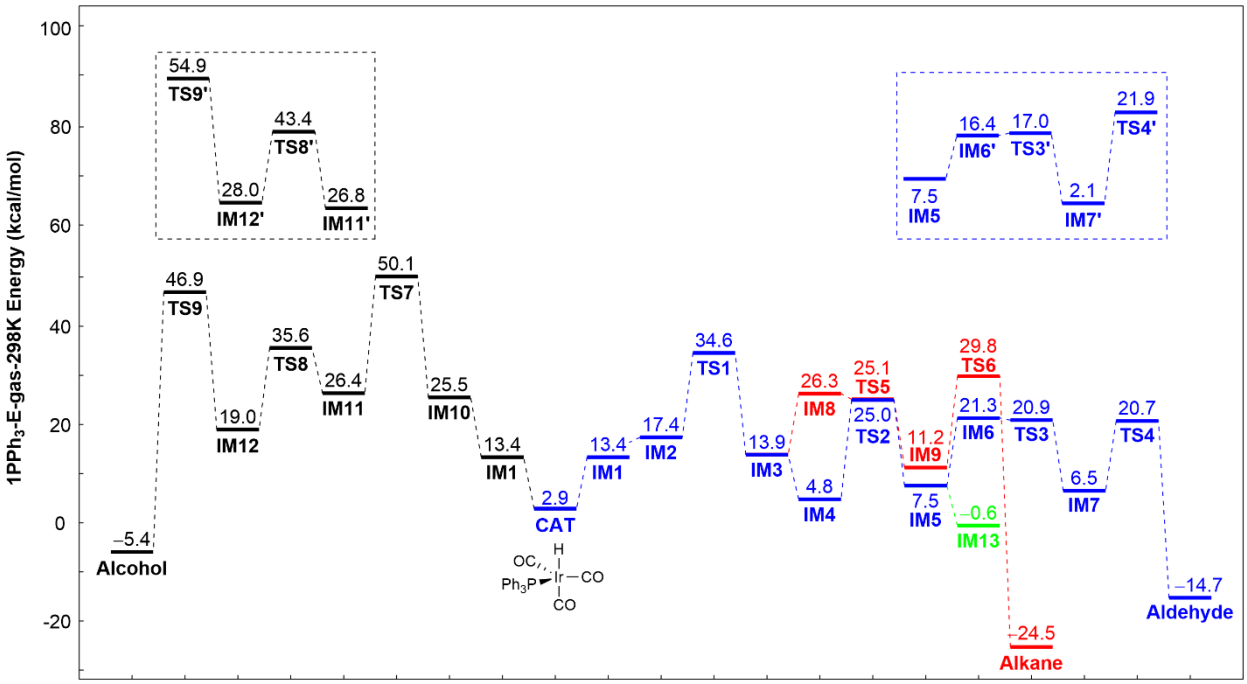
1PPh3-E-gas-298K Energy (kcal/mol)
100
80
60
40
20
0
-20
54.9
TS9'
28.0
IM12'
43.4
TS8'
26.8
IM11'
7.5
IM5
16.4
IM6'
17.0
TS3'
2.1
IM7'
21.9
TS4'
-5.4
Alcohol
46.9
TS9
19.0
IM12
35.6
TS8
26.4
IM11
50.1
TS7
25.5
IM10
13.4
IM1
2.9
CAT
13.4
IM1
17.4
IM2
34.6
TS1
13.9
IM3
26.3
IM8
4.8
IM4
25.1
TS5
25.0
TS2
11.2
IM9
7.5
IM5
29.8
TS6
21.3
IM6
-0.6
IM13
20.9
TS3
6.5
IM7
20.7
TS4
-14.7
Aldehyde
-24.5
Alkane

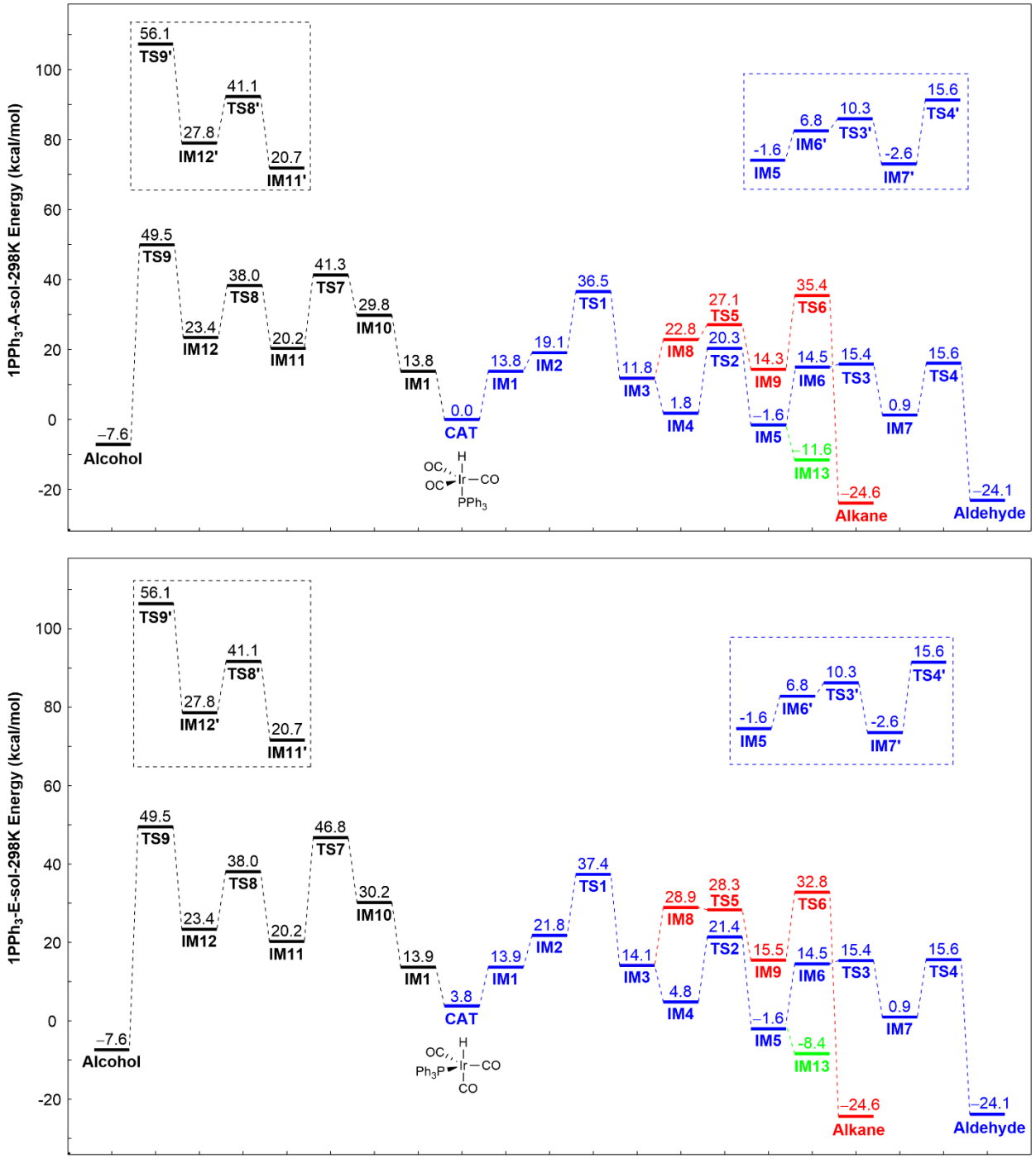
1PPh3-A-sol-298K Energy (kcal/mol)
100
80
60
40
20
0
-20
56.1
TS9'
27.8
IM12'
41.1
TS8'
20.7
IM11'
-1.6
IM5
6.8
IM6'
10.3
TS3'
-2.6
IM7'
15.6
TS4'
49.5
TS9
-7.6
Alcohol
23.4
IM12
38.0
TS8
20.2
IM11
41.3
TS7
29.8
IM10
13.8
IM1
0.0
CAT
13.8
IM1
19.1
IM2
36.5
TS1
11.8
IM3
22.8
IM8
1.8
IM4
27.1
TS5
20.3
TS2
14.3
IM9
-1.6
IM5
35.4
TS6
14.5
IM6
-11.6
IM13
15.4
TS3
0.9
IM7
15.6
TS4
-24.6
Alkane
-24.1
Aldehyde
H
OC
OC
Ir
CO
PPh3
1PPh3-E-sol-298K Energy (kcal/mol)
100
80
60
40
20
0
-20
56.1
TS9'
27.8
IM12'
41.1
TS8'
20.7
IM11'
-1.6
IM5
6.8
IM6'
10.3
TS3'
-2.6
IM7'
15.6
TS4'
49.5
TS9
-7.6
Alcohol
23.4
IM12
38.0
TS8
20.2
IM11
46.8
TS7
30.2
IM10
13.9
IM1
3.8
CAT
13.9
IM1
21.8
IM2
37.4
TS1
14.1
IM3
28.9
IM8
4.8
IM4
28.3
TS5
21.4
TS2
15.5
IM9
-1.6
IM5
32.8
TS6
14.5
IM6
-8.4
IM13
15.4
TS3
0.9
IM7
15.6
TS4
-24.6
Alkane
-24.1
Aldehyde
H
OC
Ph3P
Ir
CO
CO

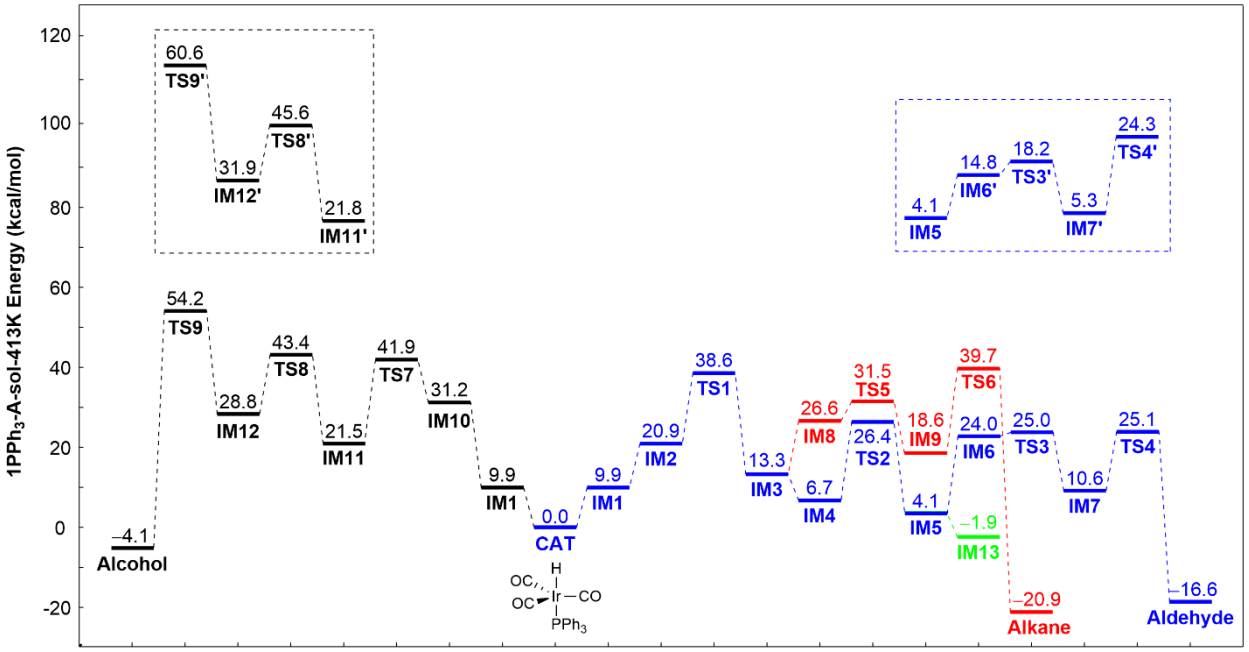
1PPh3-A-sol-413K Energy (kcal/mol)
120
100
80
60
40
20
0
-20
60.6
TS9'
31.9
IM12'
45.6
TS8'
21.8
IM11'
4.1
IM5
14.8
IM6'
18.2
TS3'
5.3
IM7'
24.3
TS4'
-4.1
Alcohol
54.2
TS9
28.8
IM12
43.4
TS8
21.5
IM11
41.9
TS7
31.2
IM10
9.9
IM1
0.0
CAT
9.9
IM1
20.9
IM2
38.6
TS1
13.3
IM3
26.6
IM8
6.7
IM4
31.5
TS5
26.4
TS2
18.6
IM9
4.1
IM5
39.7
TS6
24.0
IM6
-1.9
IM13
25.0
TS3
10.6
IM7
25.1
TS4
-20.9
Alkane
-16.6
Aldehyde

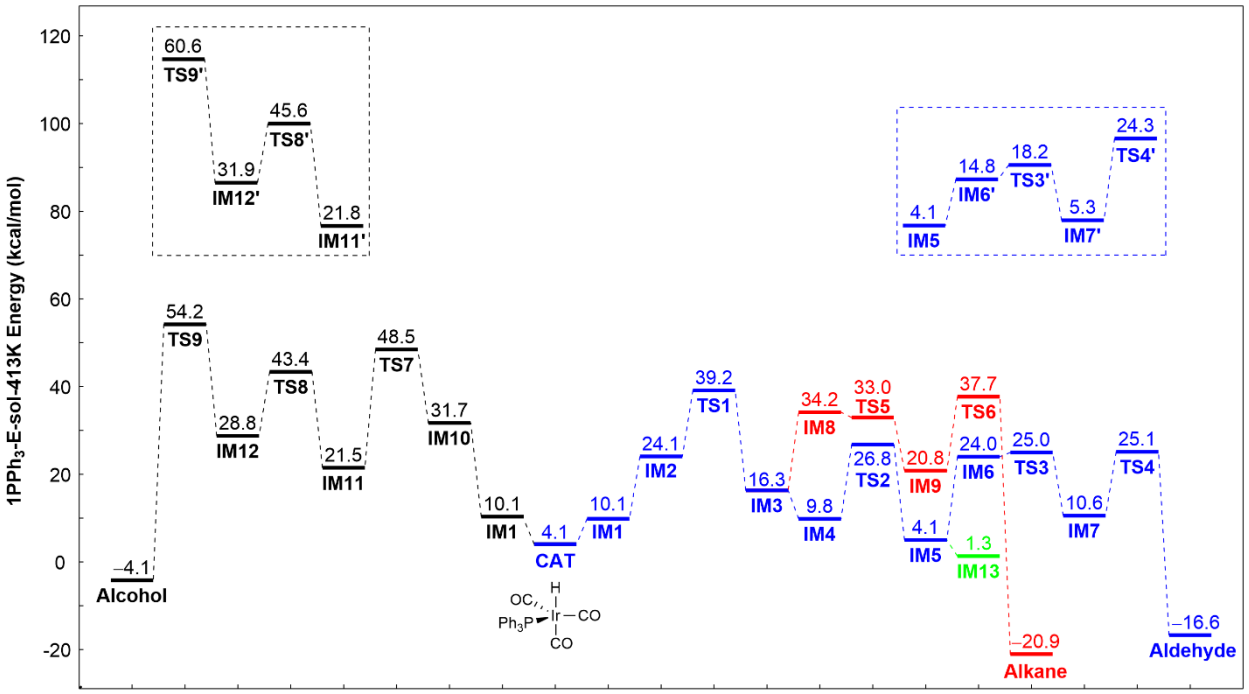
1PPh3-E-sol-413K Energy (kcal/mol)
120
100
80
60
40
20
0
-20
60.6
TS9'
31.9
IM12'
45.6
TS8'
21.8
IM11'
4.1
IM5
14.8
IM6'
18.2
TS3'
5.3
IM7'
24.3
TS4'
-4.1
Alcohol
54.2
TS9
28.8
IM12
43.4
TS8
21.5
IM11
48.5
TS7
31.7
IM10
10.1
IM1
4.1
CAT
10.1
IM1
24.1
IM2
39.2
TS1
16.3
IM3
34.2
IM8
9.8
IM4
33.0
TS5
26.8
TS2
20.8
IM9
4.1
IM5
37.7
TS6
24.0
IM6
1.3
IM13
25.0
TS3
10.6
IM7
25.1
TS4
-20.9
Alkane
-16.6
Aldehyde

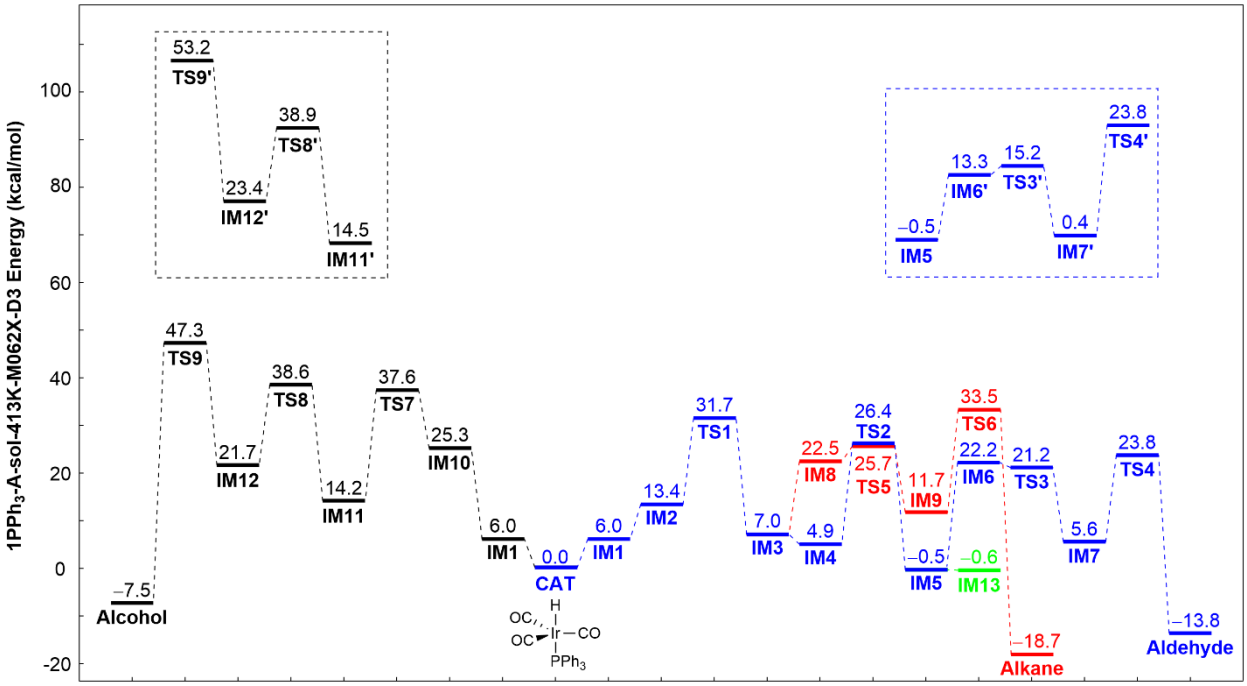
1PPh3-A-sol-413K-M062X-D3 Energy (kcal/mol)
100
80
60
40
20
0
-20
53.2
TS9'
23.4
IM12'
38.9
TS8'
14.5
IM11'
47.3
TS9
21.7
IM12
38.6
TS8
14.2
IM11
37.6
TS7
25.3
IM10
6.0
IM1
0.0
CAT
6.0
IM1
13.4
IM2
31.7
TS1
7.0
IM3
22.5
IM8
4.9
IM4
26.4
TS2
25.7
TS5
11.7
IM9
–0.5
IM5
33.5
TS6
22.2
IM6
–0.6
IM13
–18.7
Alkane
21.2
TS3
5.6
IM7
23.8
TS4
–13.8
Aldehyde
–7.5
Alcohol
–0.5
IM5
13.3
IM6'
15.2
TS3'
0.4
IM7'
23.8
TS4'
H
OC
OC
Ir—CO
PPh3

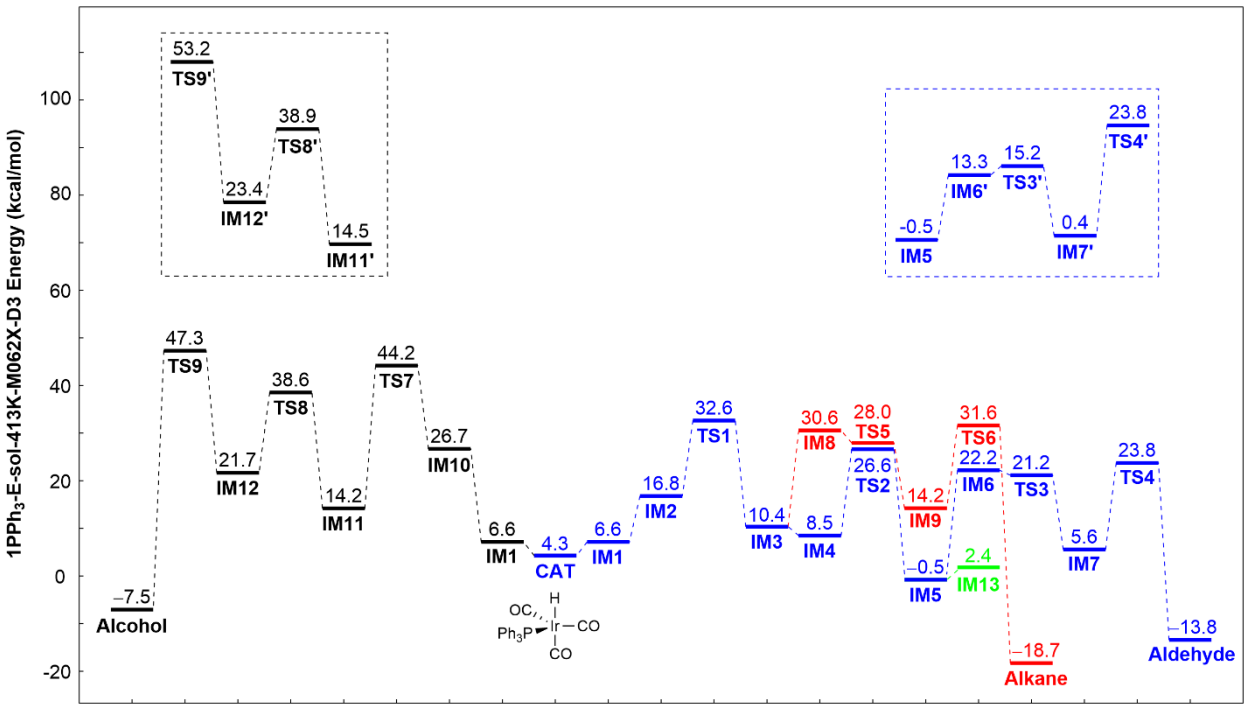
1PPh3-E-sol-413K-M062X-D3 Energy (kcal/mol)
100
80
60
40
20
0
-20
53.2
TS9'
23.4
IM12'
38.9
TS8'
14.5
IM11'
47.3
TS9
21.7
IM12
38.6
TS8
14.2
IM11
44.2
TS7
26.7
IM10
6.6
IM1
4.3
CAT
6.6
IM1
16.8
IM2
32.6
TS1
10.4
IM3
30.6
IM8
8.5
IM4
28.0
TS5
26.6
TS2
14.2
IM9
–0.5
IM5
31.6
TS6
22.2
IM6
2.4
IM13
–18.7
Alkane
21.2
TS3
5.6
IM7
23.8
TS4
–13.8
Aldehyde
–7.5
Alcohol
-0.5
IM5
13.3
IM6'
15.2
TS3'
0.4
IM7'
23.8
TS4'
H
Ph3P
OC
Ir—CO
CO

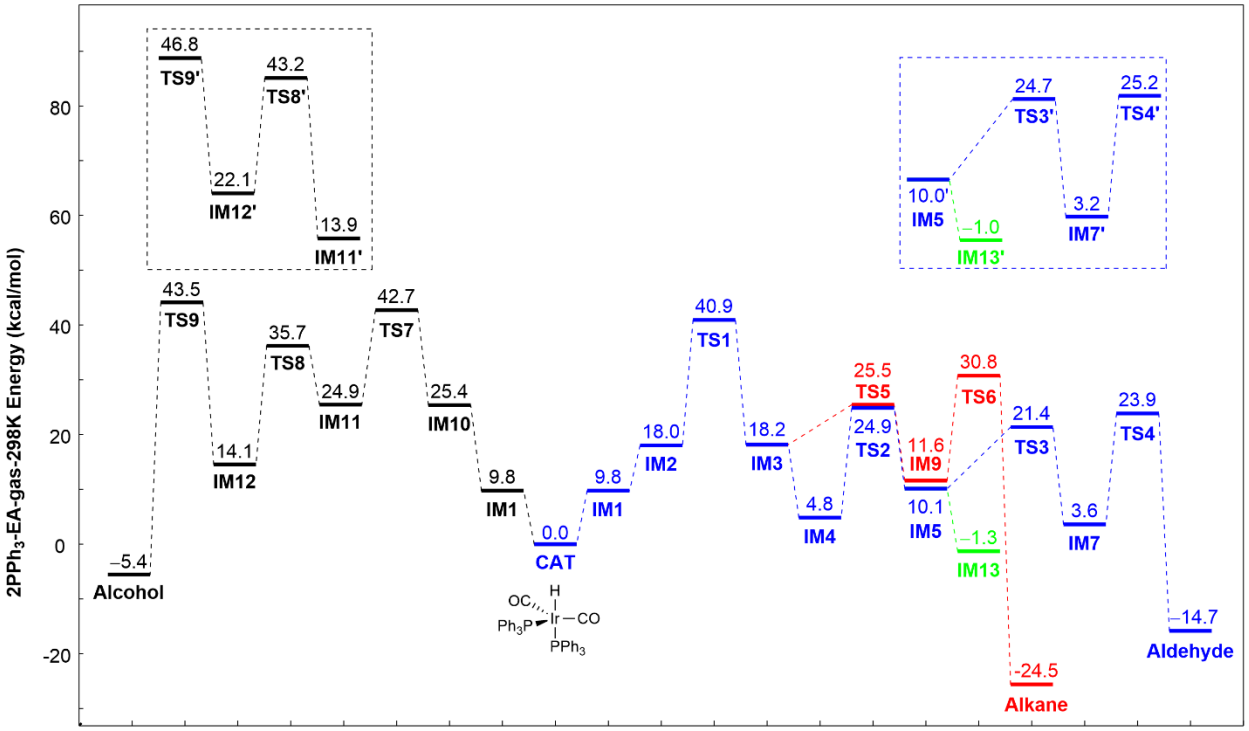
2PPh3-EA-gas-298K Energy (kcal/mol)
80
60
40
20
0
-20
46.8
TS9'
43.2
TS8'
22.1
IM12'
13.9
IM11'
24.7
TS3'
25.2
TS4'
10.0
IM5
-1.0
IM13'
3.2
IM7'
43.5
TS9
35.7
TS8
42.7
TS7
14.1
IM12
24.9
IM11
25.4
IM10
40.9
TS1
25.5
TS5
30.8
TS6
18.0
IM2
18.2
IM3
24.9
TS2
11.6
IM9
21.4
TS3
23.9
TS4
9.8
IM1
4.8
IM4
10.1
IM5
3.6
IM7
-5.4
Alcohol
9.8
IM1
0.0
CAT
-1.3
IM13
-14.7
Aldehyde
-24.5
Alkane

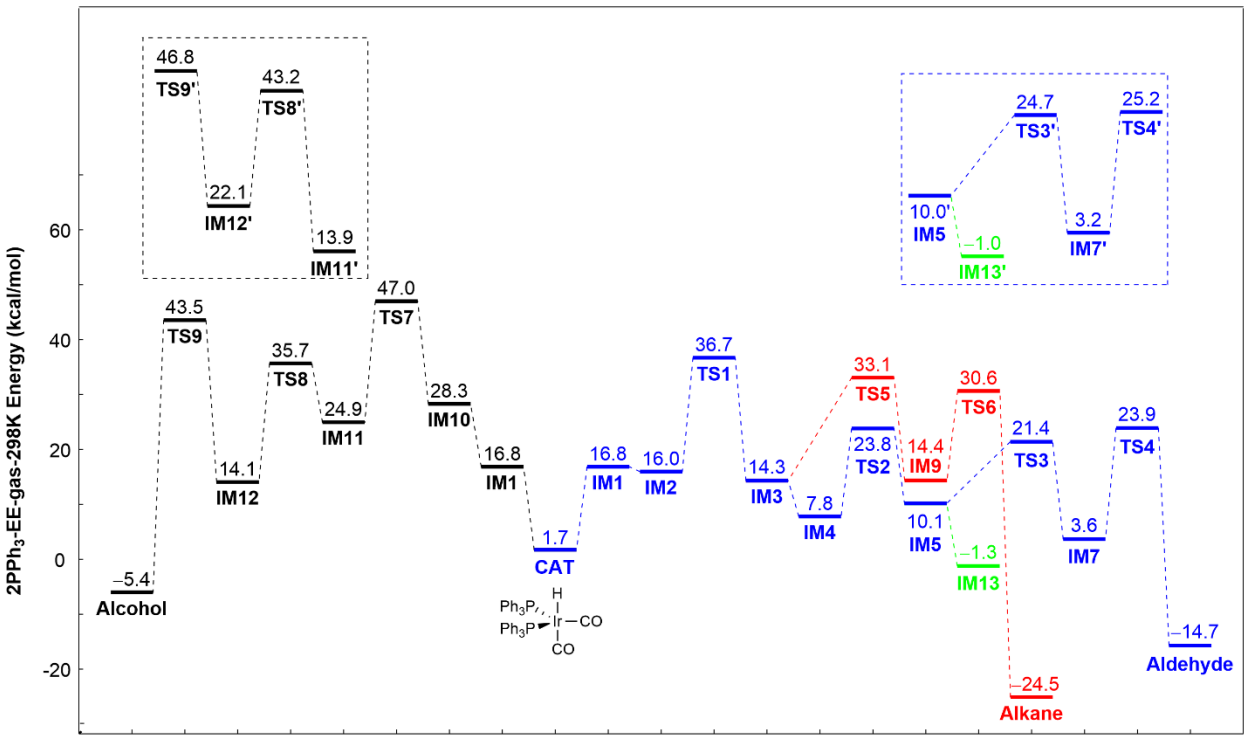
2PPh3-EE-gas-298K Energy (kcal/mol)
60
40
20
0
-20
46.8
TS9'
43.2
TS8'
22.1
IM12'
13.9
IM11'
24.7
TS3'
25.2
TS4'
10.0
IM5
-1.0
IM13'
3.2
IM7'
43.5
TS9
35.7
TS8
47.0
TS7
14.1
IM12
24.9
IM11
28.3
IM10
36.7
TS1
33.1
TS5
30.6
TS6
16.8
IM1
16.0
IM2
14.3
IM3
23.8
TS2
14.4
IM9
21.4
TS3
23.9
TS4
7.8
IM4
10.1
IM5
3.6
IM7
-5.4
Alcohol
16.8
IM1
1.7
CAT
-1.3
IM13
-14.7
Aldehyde
-24.5
Alkane

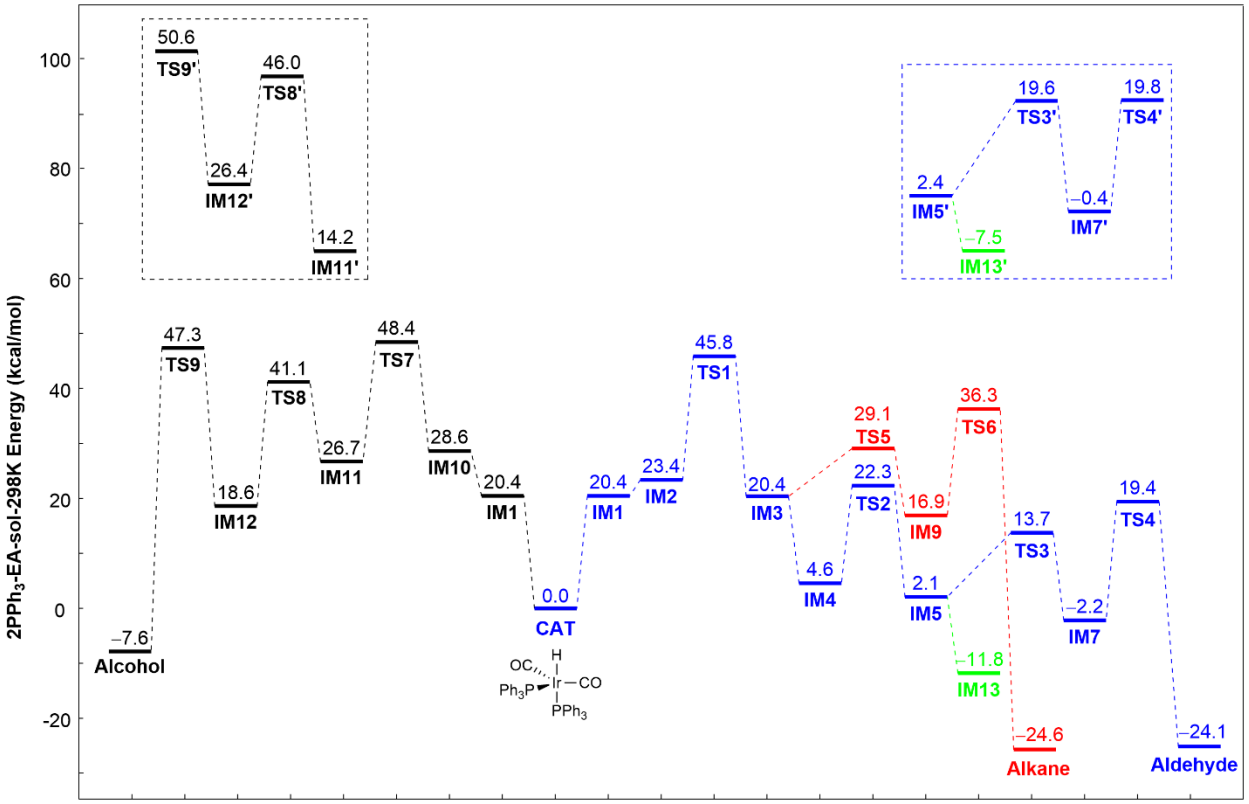
2PPh3-EA-sol-298K Energy (kcal/mol)
100
80
60
40
20
0
-20
50.6
TS9'
46.0
TS8'
26.4
IM12'
14.2
IM11'
19.6
TS3'
19.8
TS4'
2.4
IM5'
-0.4
IM7'
-7.5
IM13'
47.3
TS9
41.1
TS8
48.4
TS7
45.8
TS1
29.1
TS5
36.3
TS6
18.6
IM12
26.7
IM11
28.6
IM10
20.4
IM1
20.4
IM1
23.4
IM2
20.4
IM3
22.3
TS2
16.9
IM9
13.7
TS3
19.4
TS4
-7.6
Alcohol
0.0
CAT
4.6
IM4
2.1
IM5
-2.2
IM7
-11.8
IM13
-24.6
Alkane
-24.1
Aldehyde

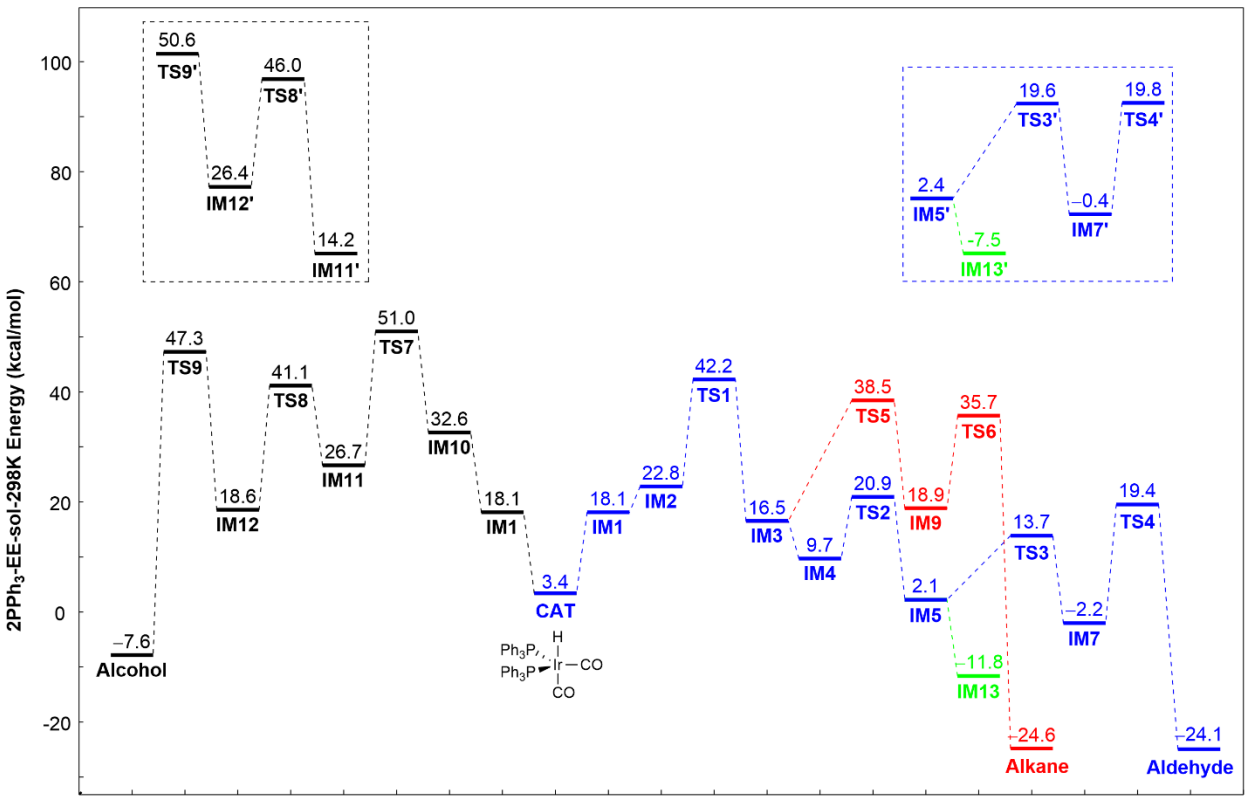
2PPh3-EE-sol-298K Energy (kcal/mol)
100
80
60
40
20
0
-20
50.6
TS9'
46.0
TS8'
26.4
IM12'
14.2
IM11'
19.6
TS3'
19.8
TS4'
2.4
IM5'
-0.4
IM7'
-7.5
IM13'
47.3
TS9
41.1
TS8
51.0
TS7
42.2
TS1
38.5
TS5
35.7
TS6
18.6
IM12
26.7
IM11
32.6
IM10
18.1
IM1
18.1
IM1
22.8
IM2
16.5
IM3
20.9
TS2
18.9
IM9
13.7
TS3
19.4
TS4
-7.6
Alcohol
3.4
CAT
9.7
IM4
2.1
IM5
-2.2
IM7
-11.8
IM13
-24.6
Alkane
-24.1
Aldehyde

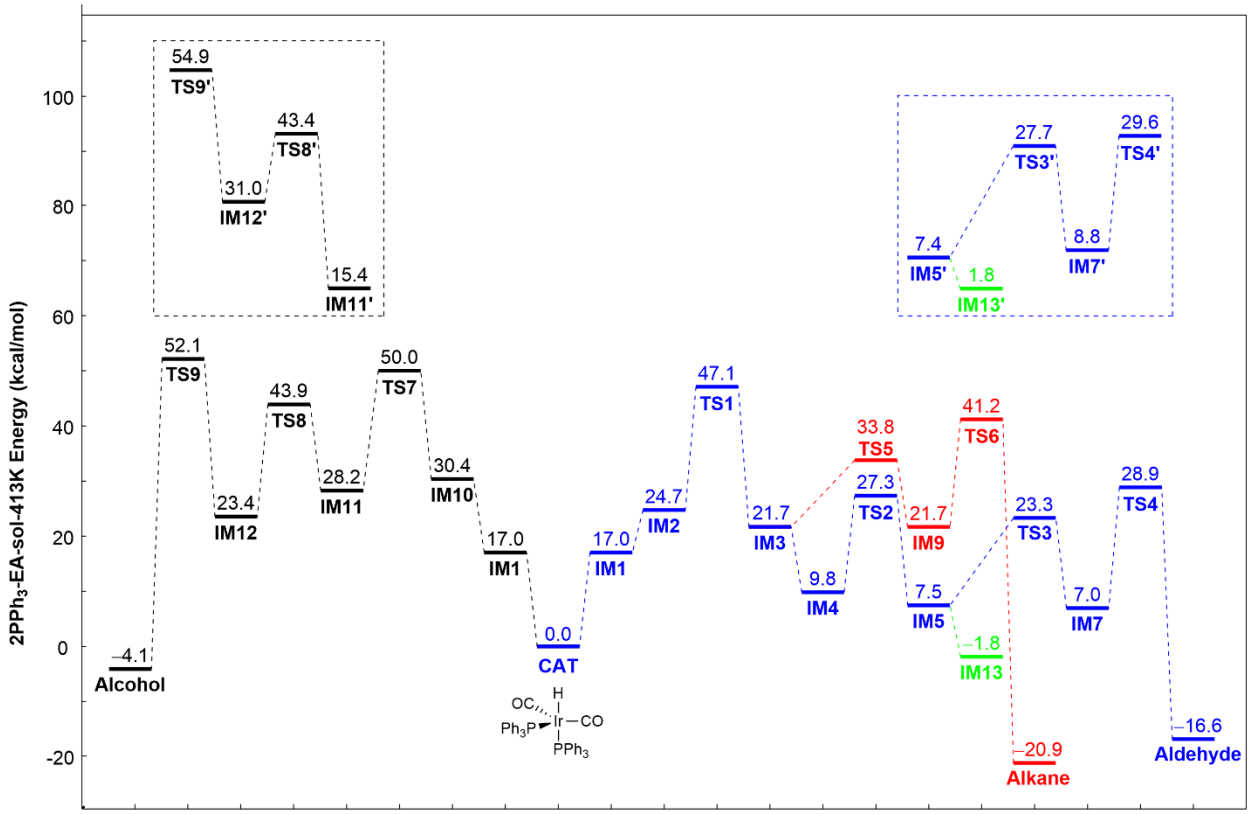
2PPh3-EA-sol-413K Energy (kcal/mol)
100
80
60
40
20
0
-20
54.9
TS9'
31.0
IM12'
43.4
TS8'
15.4
IM11'
7.4
IM5'
27.7
TS3'
1.8
IM13'
8.8
IM7'
29.6
TS4'
52.1
TS9
23.4
IM12
43.9
TS8
28.2
IM11
50.0
TS7
30.4
IM10
17.0
IM1
0.0
CAT
17.0
IM1
24.7
IM2
47.1
TS1
21.7
IM3
9.8
IM4
33.8
TS5
27.3
TS2
21.7
IM9
41.2
TS6
7.5
IM5
-1.8
IM13
23.3
TS3
7.0
IM7
28.9
TS4
-4.1
Alcohol
-20.9
Alkane
-16.6
Aldehyde

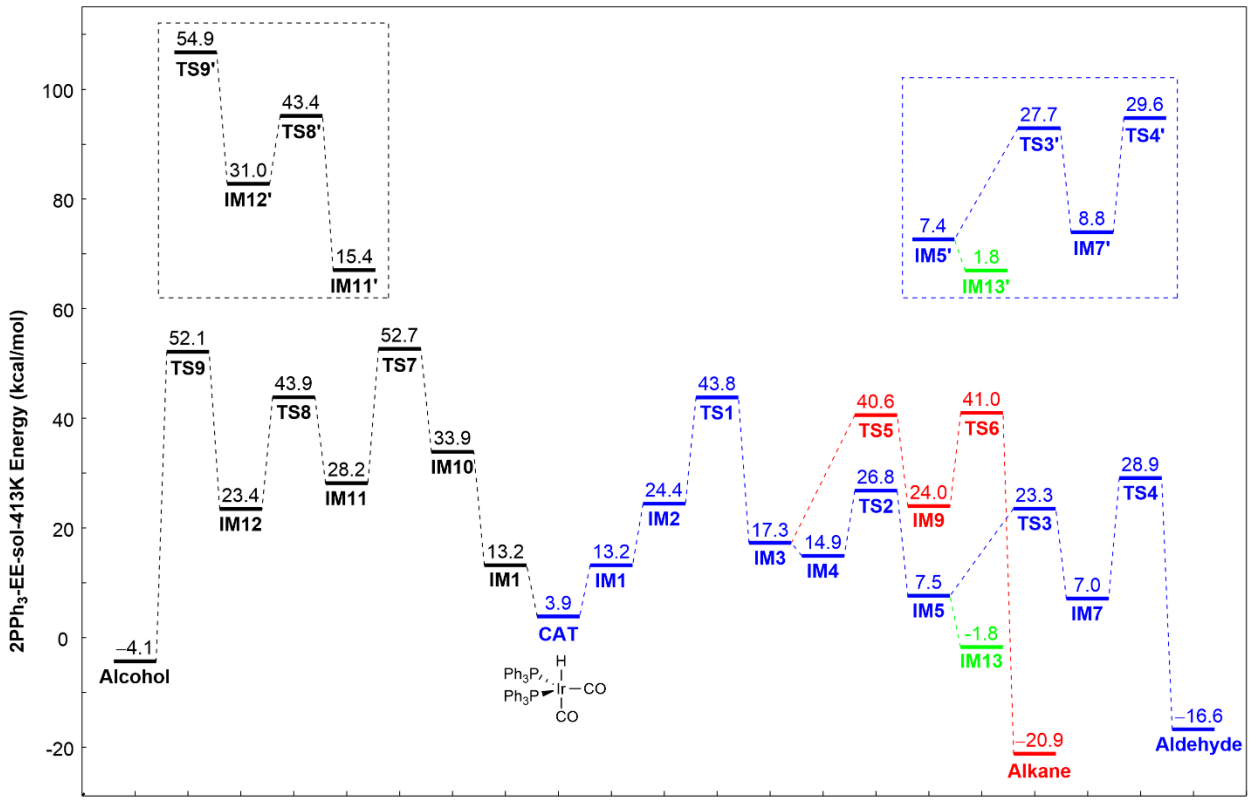
2PPh3-EE-sol-413K Energy (kcal/mol)
100
80
60
40
20
0
-20
54.9
TS9'
31.0
IM12'
43.4
TS8'
15.4
IM11'
7.4
IM5'
27.7
TS3'
1.8
IM13'
8.8
IM7'
29.6
TS4'
52.1
TS9
23.4
IM12
43.9
TS8
28.2
IM11
52.7
TS7
33.9
IM10
13.2
IM1
3.9
CAT
13.2
IM1
24.4
IM2
43.8
TS1
17.3
IM3
14.9
IM4
40.6
TS5
26.8
TS2
24.0
IM9
41.0
TS6
7.5
IM5
-1.8
IM13
23.3
TS3
7.0
IM7
28.9
TS4
-4.1
Alcohol
-20.9
Alkane
-16.6
Aldehyde

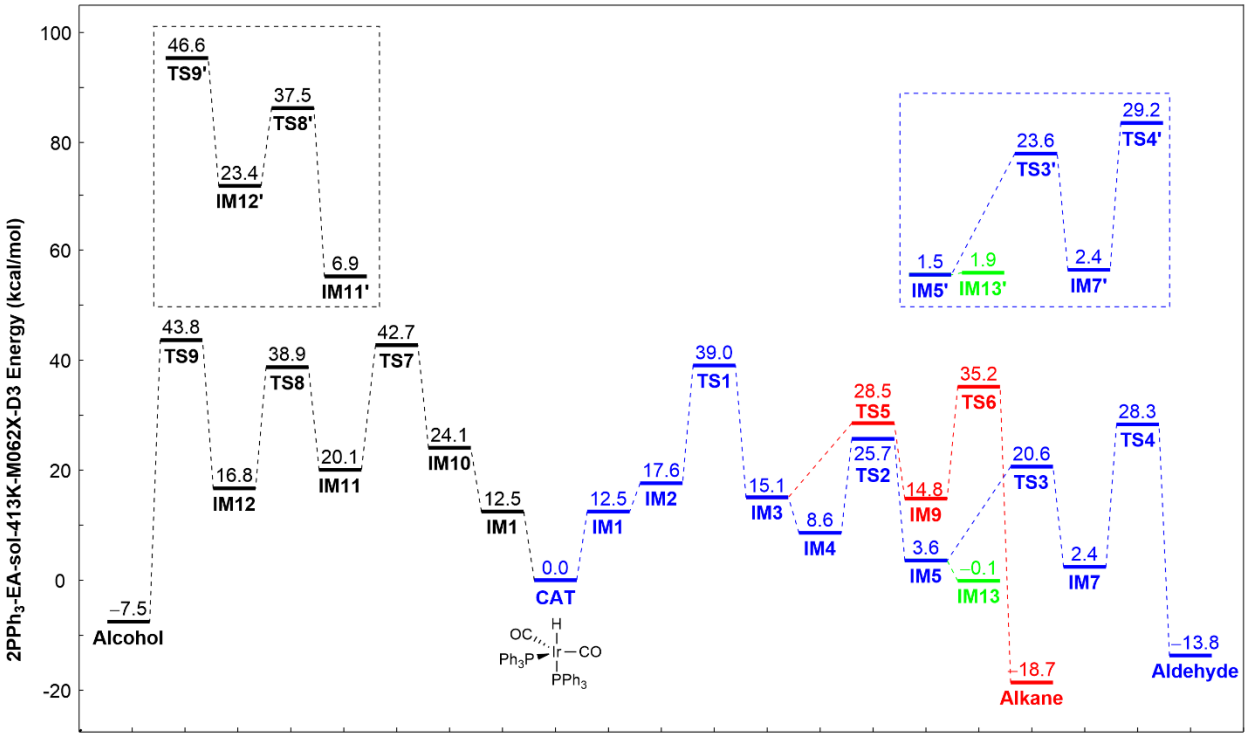
2PPh3-EA-sol-413K-M062X-D3 Energy (kcal/mol)
100
80
60
40
20
0
-20
46.6
TS9'
23.4
IM12'
37.5
TS8'
6.9
IM11'
1.5
IM5'
1.9
IM13'
23.6
TS3'
2.4
IM7'
29.2
TS4'
43.8
TS9
16.8
IM12
38.9
TS8
20.1
IM11
42.7
TS7
24.1
IM10
12.5
IM1
0.0
CAT
12.5
IM1
17.6
IM2
39.0
TS1
15.1
IM3
8.6
IM4
28.5
TS5
25.7
TS2
14.8
IM9
35.2
TS6
3.6
IM5
-0.1
IM13
20.6
TS3
2.4
IM7
28.3
TS4
-7.5
Alcohol
-18.7
Alkane
-13.8
Aldehyde

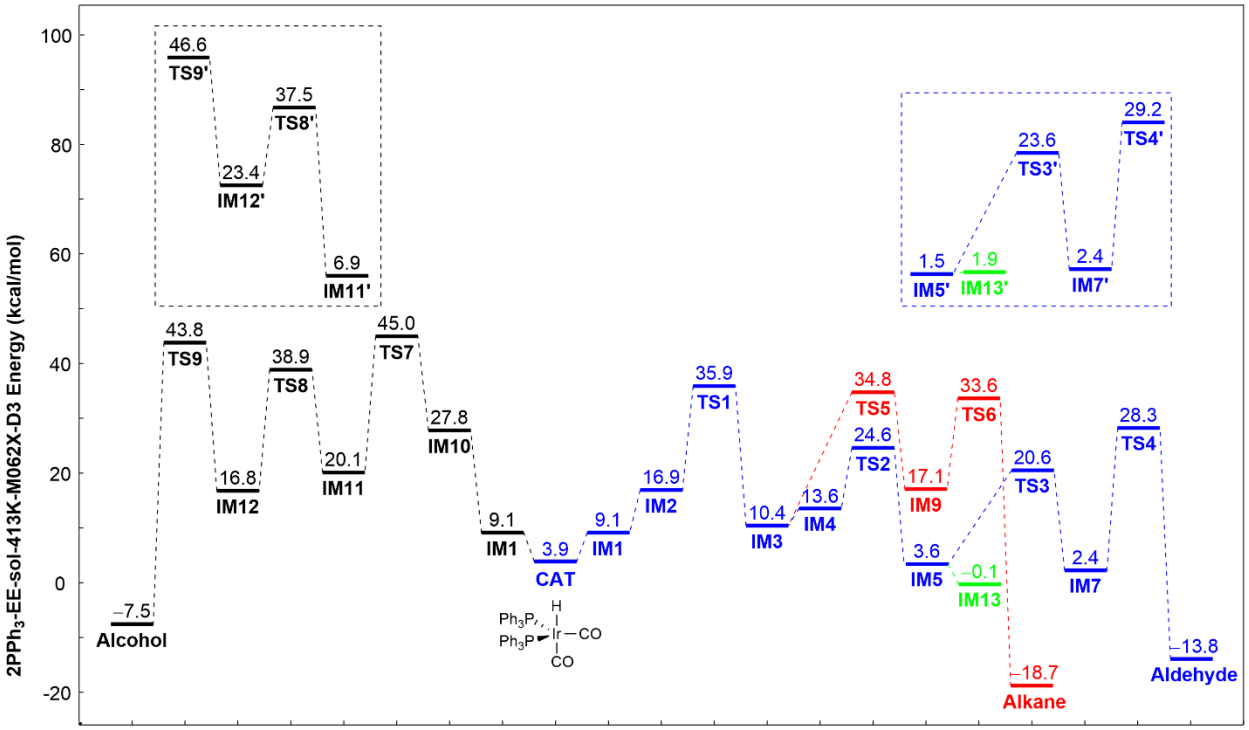
2PPh3-EE-sol-413K-M062X-D3 Energy (kcal/mol)
100
80
60
40
20
0
-20
46.6
TS9'
23.4
IM12'
37.5
TS8'
6.9
IM11'
1.5
IM5'
1.9
IM13'
23.6
TS3'
2.4
IM7'
29.2
TS4'
43.8
TS9
16.8
IM12
38.9
TS8
20.1
IM11
45.0
TS7
27.8
IM10
9.1
IM1
3.9
CAT
9.1
IM1
16.9
IM2
35.9
TS1
10.4
IM3
13.6
IM4
34.8
TS5
24.6
TS2
17.1
IM9
33.6
TS6
3.6
IM5
-0.1
IM13
20.6
TS3
2.4
IM7
28.3
TS4
-7.5
Alcohol
-18.7
Alkane
-13.8
Aldehyde

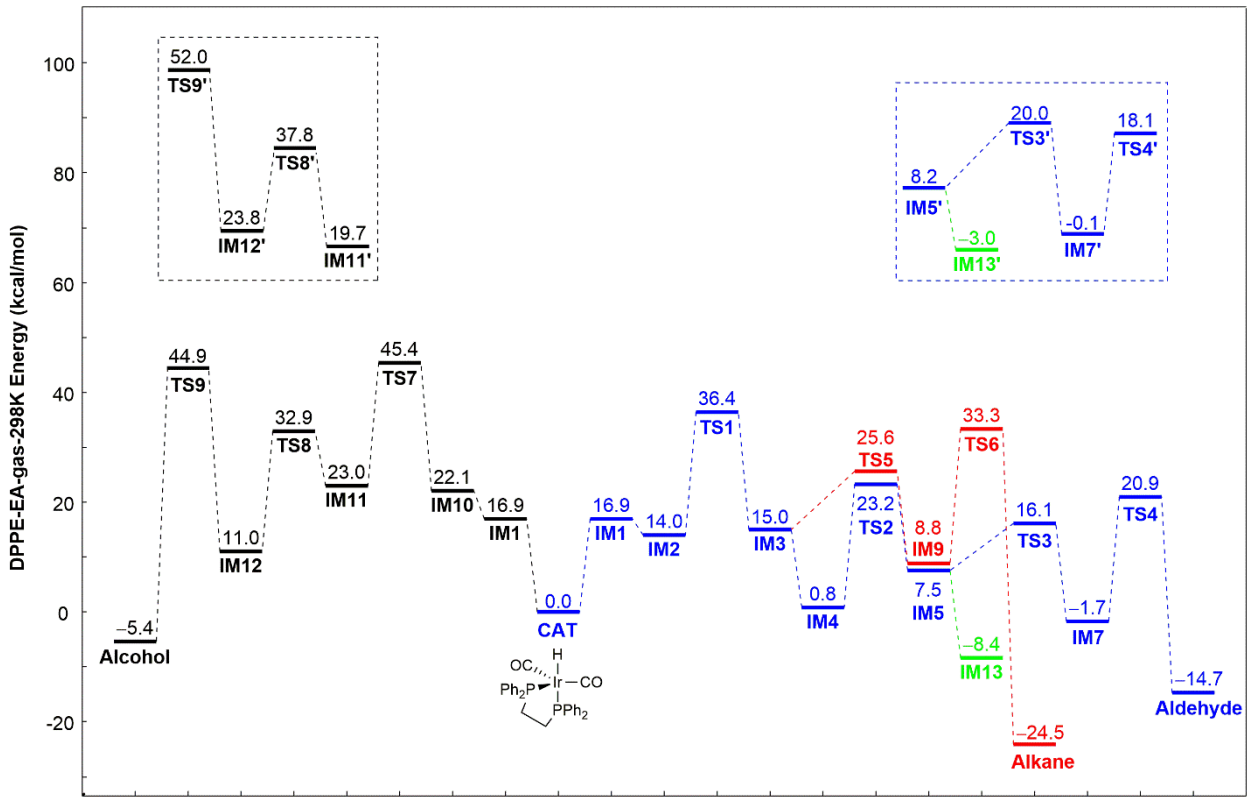
DPPE-EA-gas-298K Energy (kcal/mol)
100
80
60
40
20
0
-20
52.0
TS9'
23.8
IM12'
37.8
TS8'
19.7
IM11'
8.2
IM5'
20.0
TS3'
-3.0
IM13'
-0.1
IM7'
18.1
TS4'
-5.4
Alcohol
44.9
TS9
11.0
IM12
32.9
TS8
23.0
IM11
45.4
TS7
22.1
IM10
16.9
IM1
16.9
IM1
14.0
IM2
36.4
TS1
15.0
IM3
0.8
IM4
25.6
TS5
23.2
TS2
8.8
IM9
7.5
IM5
33.3
TS6
-8.4
IM13
16.1
TS3
-1.7
IM7
20.9
TS4
0.0
CAT
-14.7
Aldehyde
-24.5
Alkane

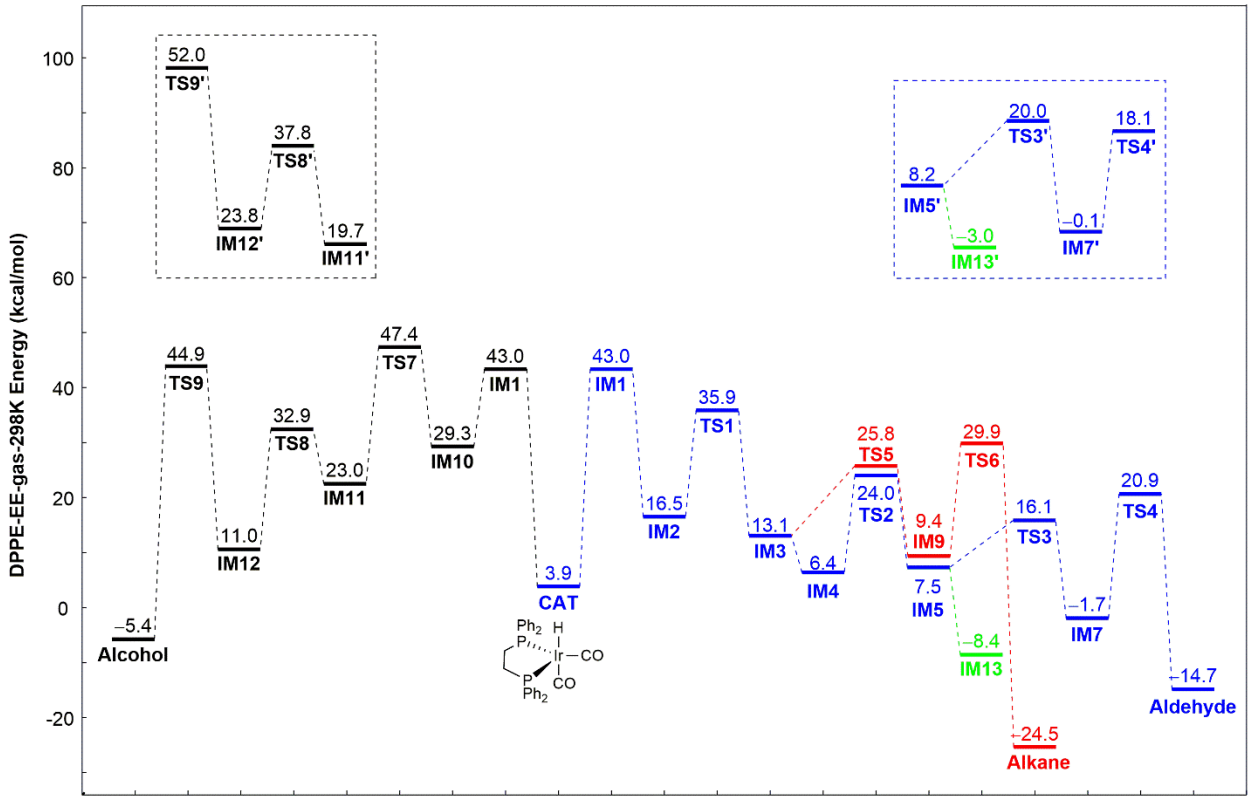
DPPE-EE-gas-298K Energy (kcal/mol)
100
80
60
40
20
0
-20
52.0
TS9'
23.8
IM12'
37.8
TS8'
19.7
IM11'
8.2
IM5'
20.0
TS3'
-3.0
IM13'
-0.1
IM7'
18.1
TS4'
-5.4
Alcohol
44.9
TS9
11.0
IM12
32.9
TS8
23.0
IM11
47.4
TS7
29.3
IM10
43.0
IM1
43.0
IM1
16.5
IM2
35.9
TS1
13.1
IM3
6.4
IM4
25.8
TS5
24.0
TS2
9.4
IM9
7.5
IM5
29.9
TS6
-8.4
IM13
16.1
TS3
-1.7
IM7
20.9
TS4
3.9
CAT
-14.7
Aldehyde
-24.5
Alkane

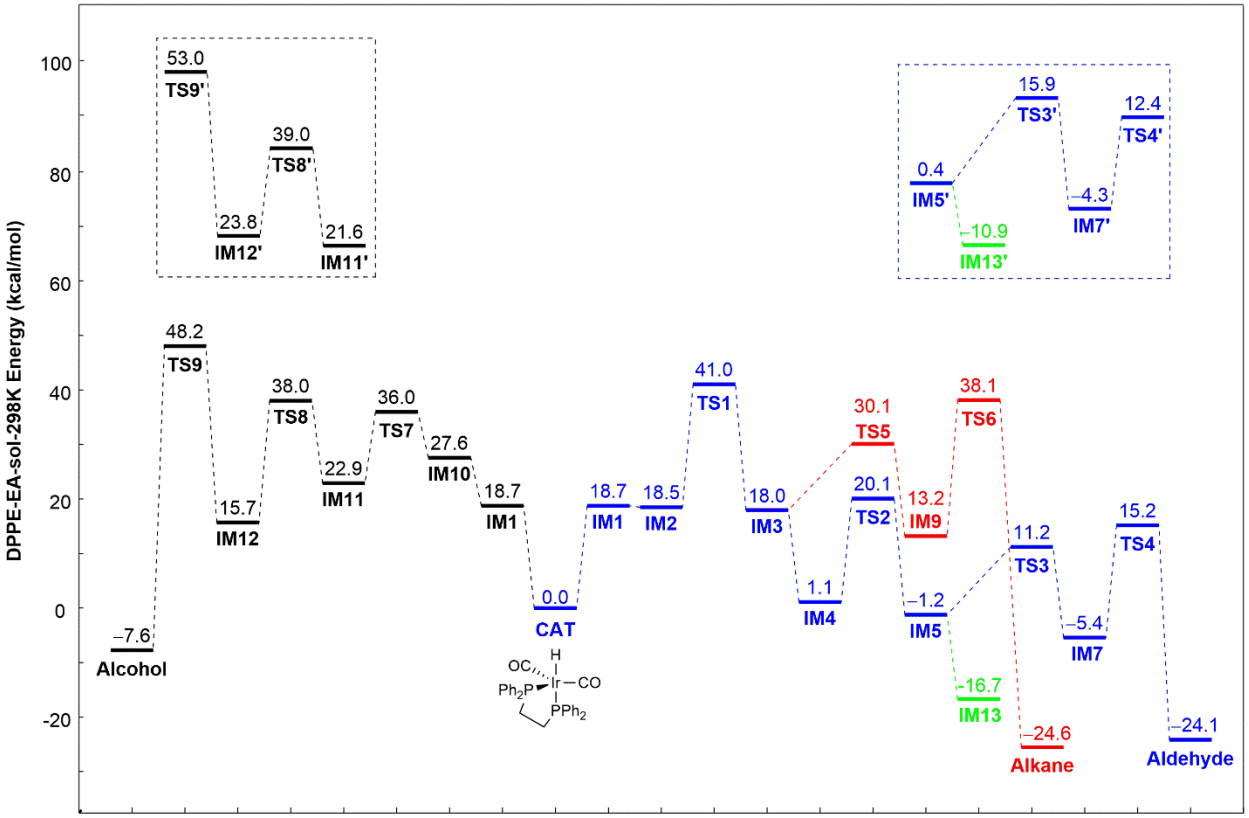
DPPE-EA-sol-298K Energy (kcal/mol)
100
80
60
40
20
0
-20
53.0
TS9'
23.8
IM12'
39.0
TS8'
21.6
IM11'
0.4
IM5'
15.9
TS3'
-10.9
IM13'
-4.3
IM7'
12.4
TS4'
-7.6
Alcohol
48.2
TS9
15.7
IM12
38.0
TS8
22.9
IM11
36.0
TS7
27.6
IM10
18.7
IM1
0.0
CAT
18.7
IM1
18.5
IM2
41.0
TS1
18.0
IM3
1.1
IM4
30.1
TS5
20.1
TS2
13.2
IM9
-1.2
IM5
38.1
TS6
-16.7
IM13
-24.6
Alkane
11.2
TS3
-5.4
IM7
15.2
TS4
-24.1
Aldehyde

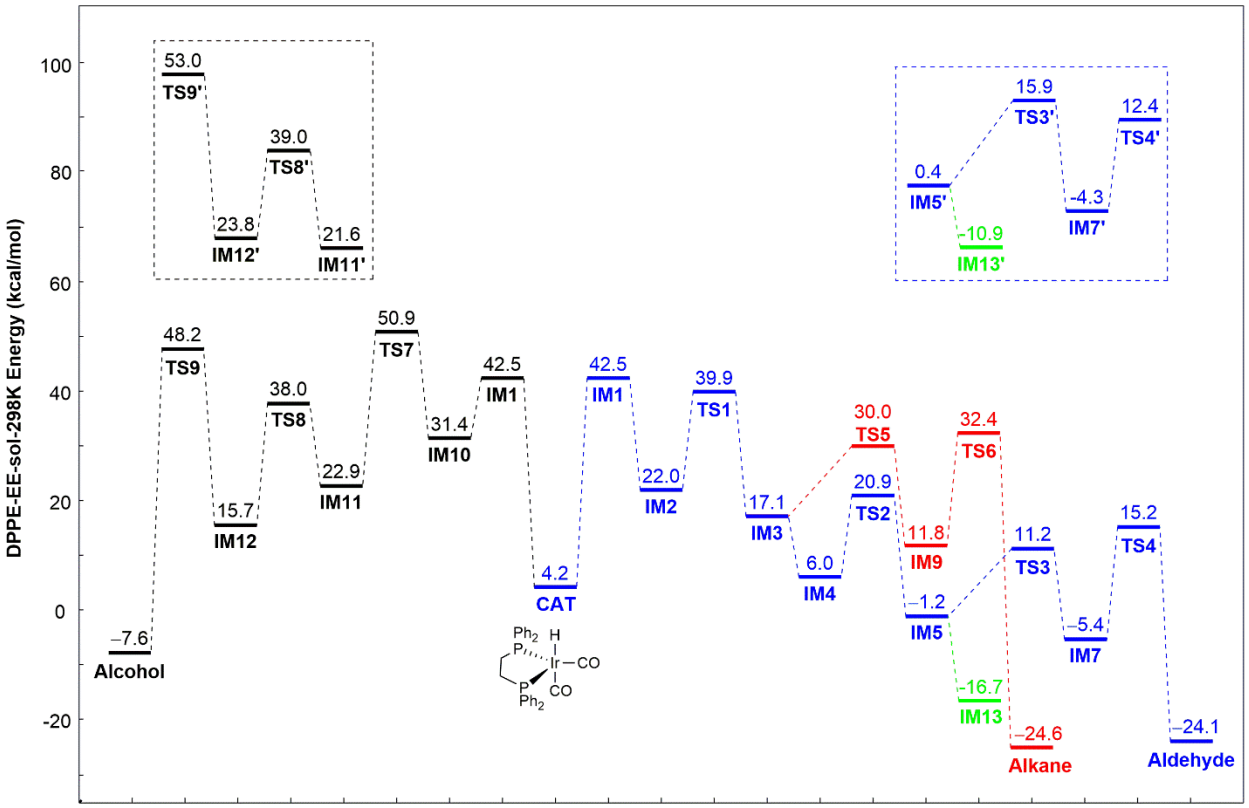
DPPE-EE-sol-298K Energy (kcal/mol)
100
80
60
40
20
0
-20
53.0
TS9'
23.8
IM12'
39.0
TS8'
21.6
IM11'
0.4
IM5'
15.9
TS3'
-10.9
IM13'
-4.3
IM7'
12.4
TS4'
-7.6
Alcohol
48.2
TS9
15.7
IM12
38.0
TS8
22.9
IM11
50.9
TS7
31.4
IM10
42.5
IM1
4.2
CAT
42.5
IM1
22.0
IM2
39.9
TS1
17.1
IM3
6.0
IM4
30.0
TS5
20.9
TS2
11.8
IM9
-1.2
IM5
32.4
TS6
-16.7
IM13
-24.6
Alkane
11.2
TS3
-5.4
IM7
15.2
TS4
-24.1
Aldehyde

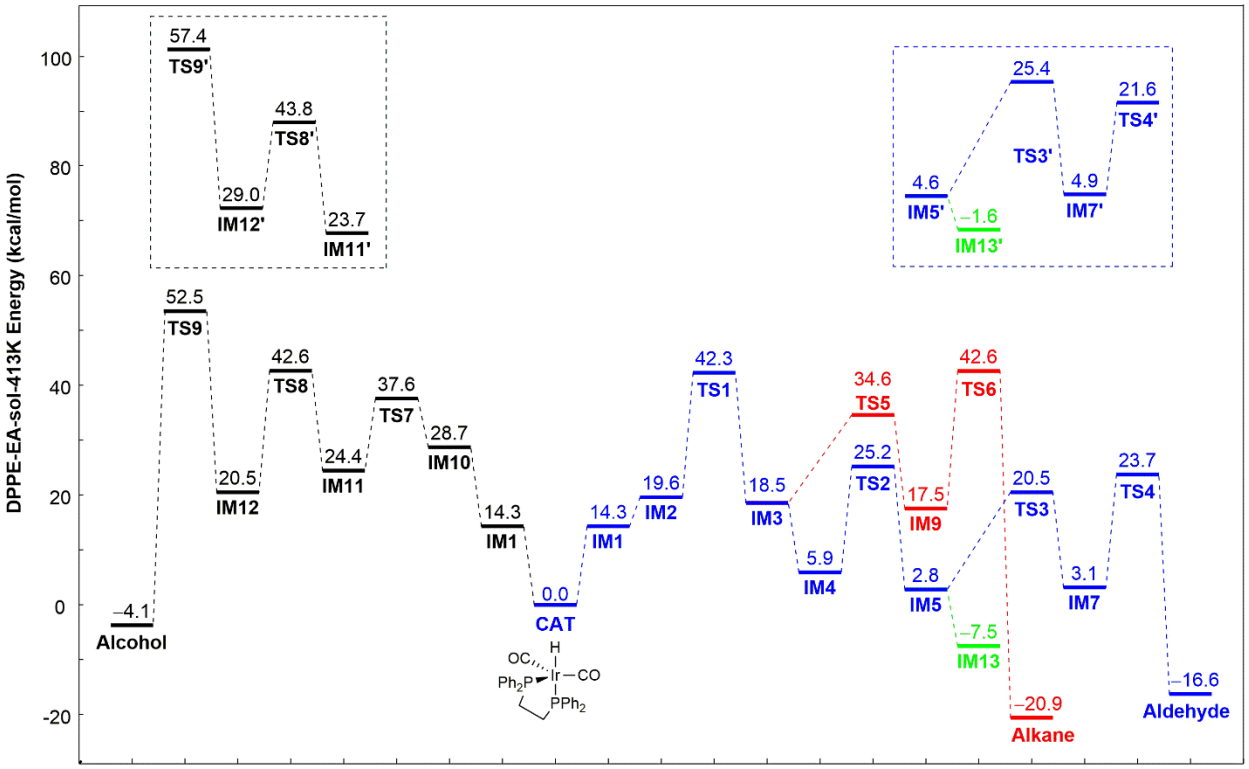
DPPE-EA-sol-413K Energy (kcal/mol)
100
80
60
40
20
0
-20
57.4
TS9'
43.8
TS8'
29.0
IM12'
23.7
IM11'
25.4
TS3'
21.6
TS4'
4.6
IM5'
-1.6
IM13'
4.9
IM7'
52.5
TS9
42.6
TS8
37.6
TS7
28.7
IM10
42.3
TS1
34.6
TS5
42.6
TS6
25.2
TS2
20.5
IM12
24.4
IM11
14.3
IM1
19.6
IM2
18.5
IM3
17.5
IM9
20.5
TS3
23.7
TS4
-4.1
Alcohol
0.0
CAT
5.9
IM4
2.8
IM5
3.1
IM7
-7.5
IM13
-20.9
Alkane
-16.6
Aldehyde

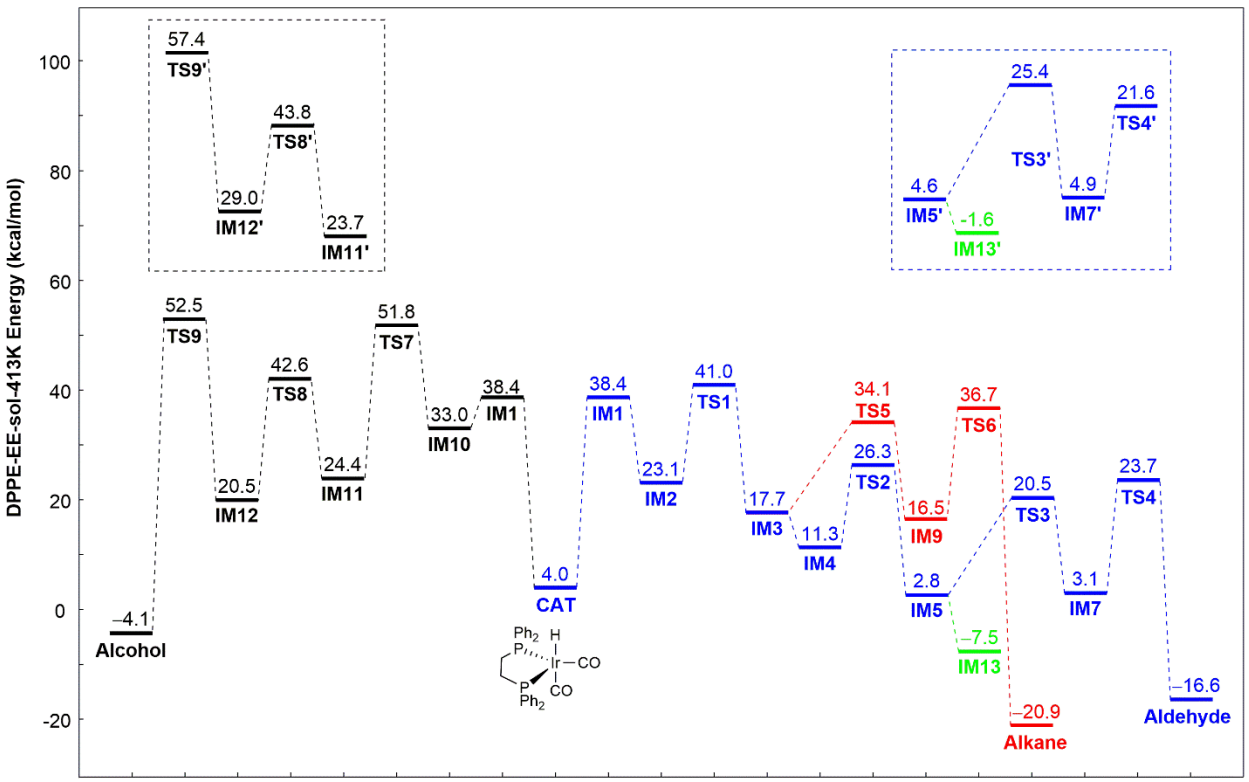
DPPE-EE-sol-413K Energy (kcal/mol)
100
80
60
40
20
0
-20
57.4
TS9'
43.8
TS8'
29.0
IM12'
23.7
IM11'
25.4
TS3'
21.6
TS4'
4.6
IM5'
-1.6
IM13'
4.9
IM7'
52.5
TS9
51.8
TS7
42.6
TS8
38.4
IM1
41.0
TS1
34.1
TS5
36.7
TS6
26.3
TS2
20.5
IM12
24.4
IM11
33.0
IM10
38.4
IM1
23.1
IM2
17.7
IM3
16.5
IM9
20.5
TS3
23.7
TS4
-4.1
Alcohol
4.0
CAT
11.3
IM4
2.8
IM5
3.1
IM7
-7.5
IM13
-20.9
Alkane
-16.6
Aldehyde

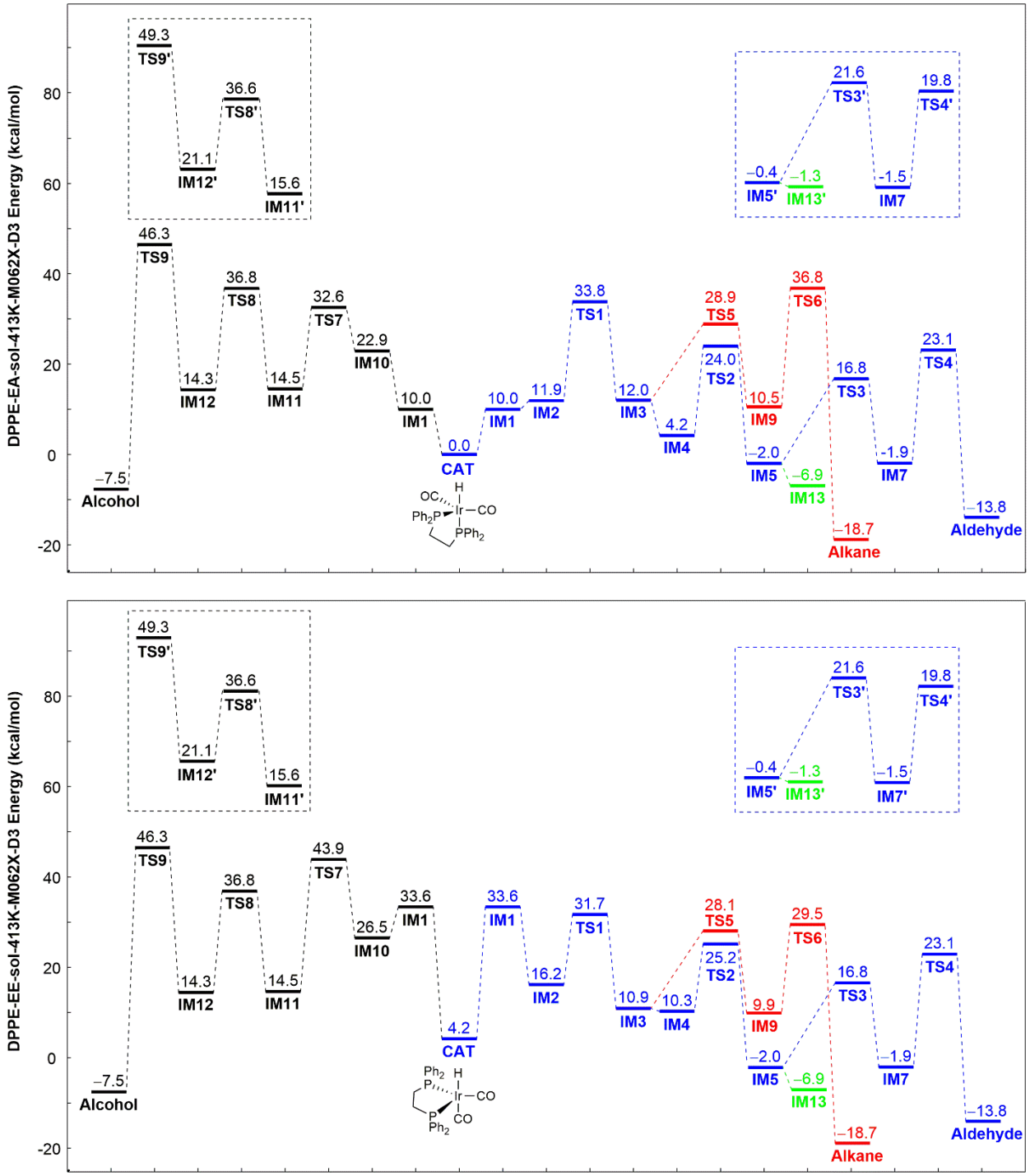

Figure DFT-S5. Free energy profile of the catalytic cycle shown in Scheme S1 catalyzed by different Iridium hydrides with pure carbonyl ligand or phosphine ligands.

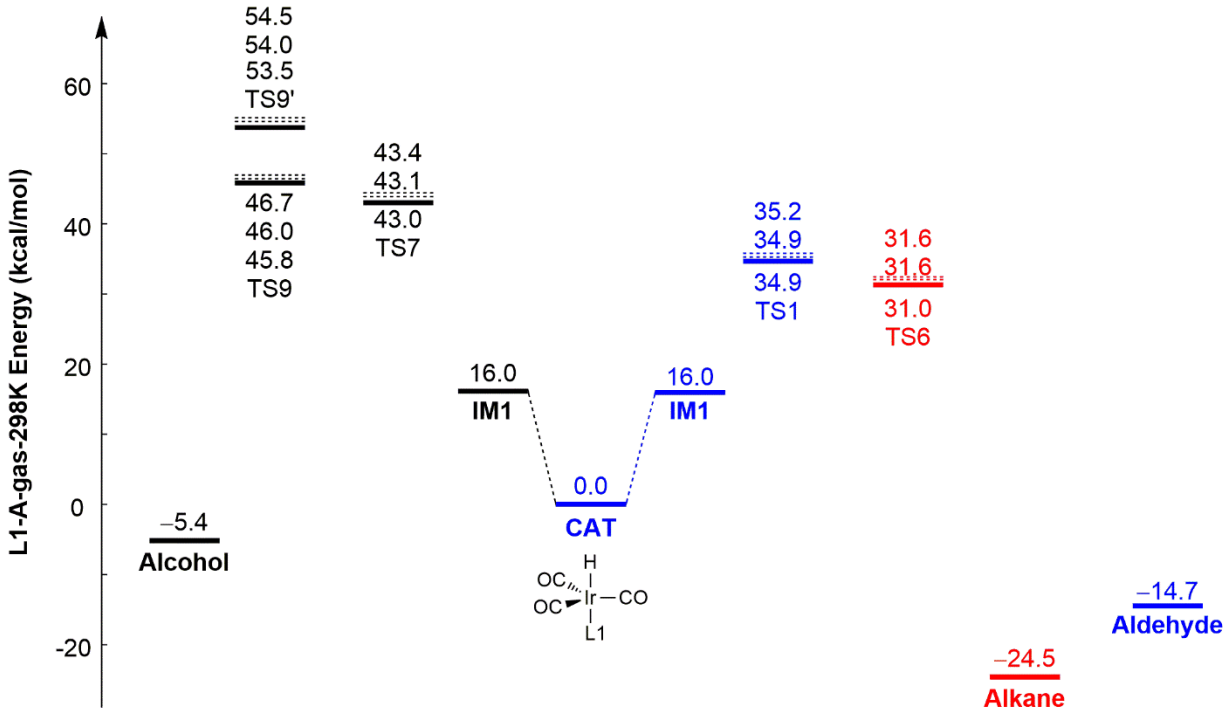
L1-A-gas-298K Energy (kcal/mol)
60
40
20
0
-20
54.5
54.0
53.5
TS9'
46.7
46.0
45.8
TS9
43.4
43.1
43.0
TS7
35.2
34.9
34.9
TS1
31.6
31.6
31.0
TS6
16.0
IM1
16.0
IM1
0.0
CAT
−5.4
Alcohol
−14.7
Aldehyde
−24.5
Alkane

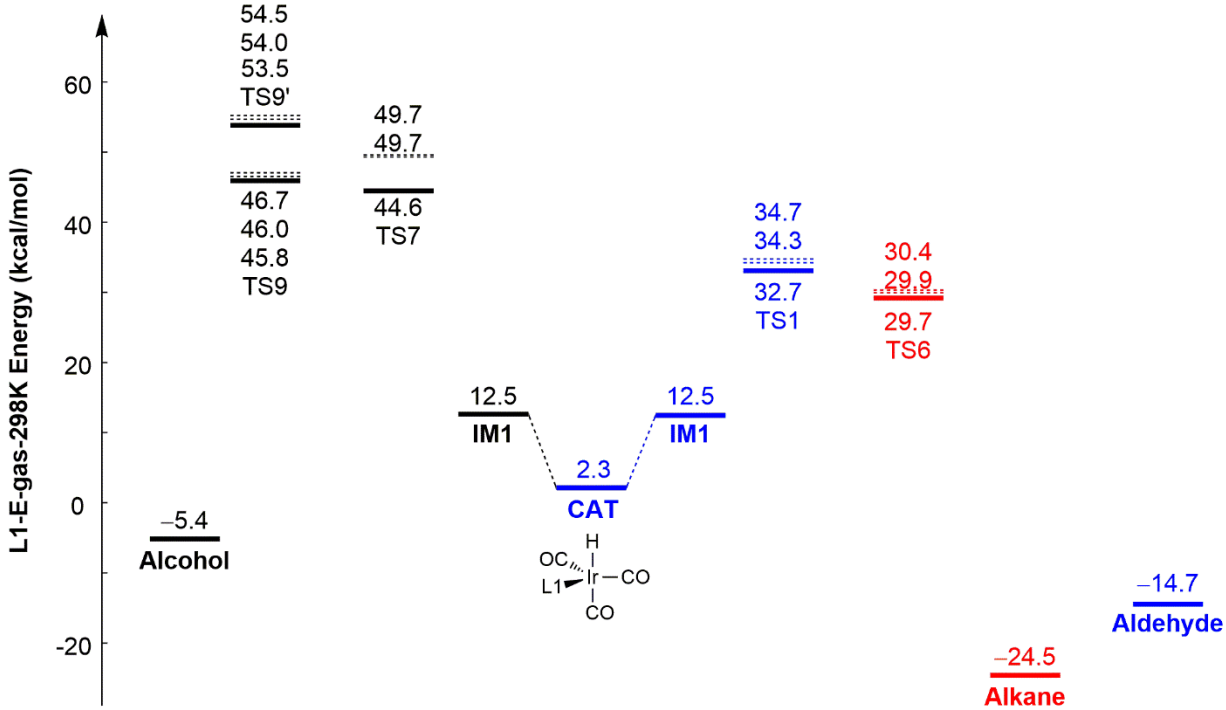
L1-E-gas-298K Energy (kcal/mol)
60
40
20
0
-20
54.5
54.0
53.5
TS9'
46.7
46.0
45.8
TS9
49.7
49.7
44.6
TS7
34.7
34.3
32.7
TS1
30.4
29.9
29.7
TS6
12.5
IM1
12.5
IM1
2.3
CAT
−5.4
Alcohol
−14.7
Aldehyde
−24.5
Alkane

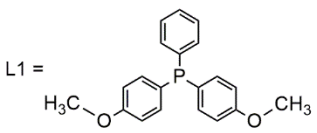
L1 =

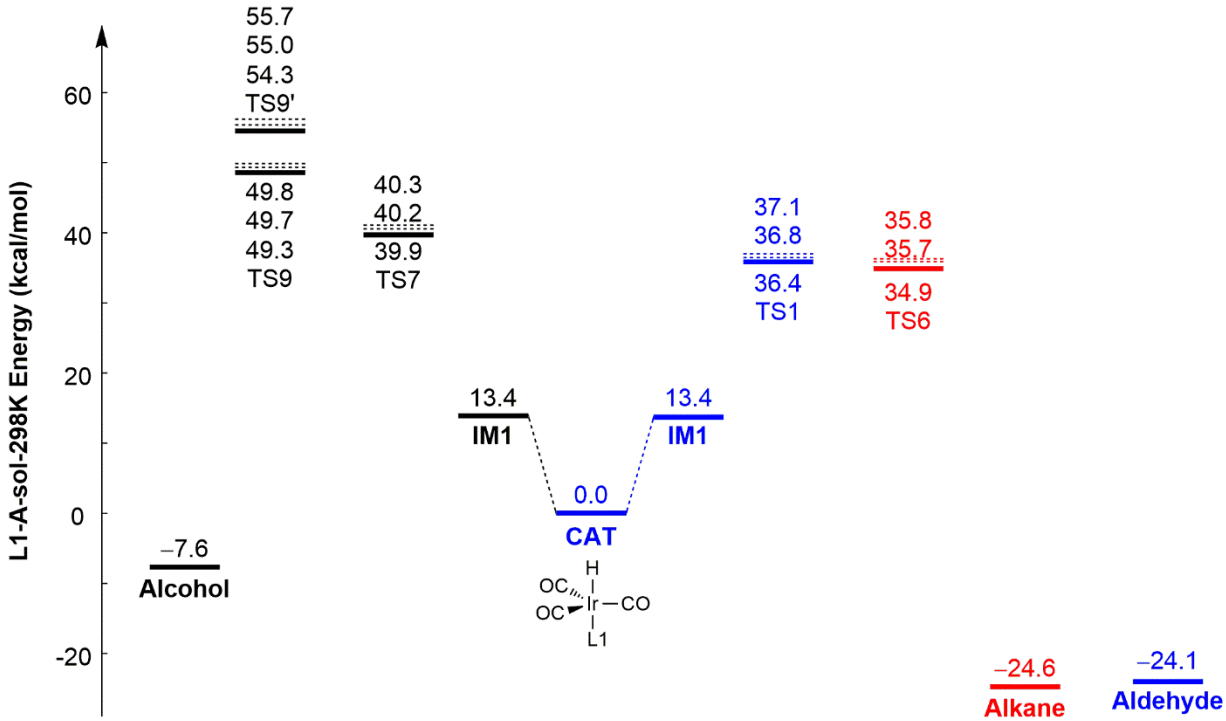
L1-A-sol-298K Energy (kcal/mol)
60
40
20
0
-20
55.7
55.0
54.3
TS9'
49.8
49.7
49.3
TS9
40.3
40.2
39.9
TS7
37.1
36.8
36.4
TS1
35.8
35.7
34.9
TS6
13.4
IM1
0.0
CAT
13.4
IM1
−7.6
Alcohol
−24.6
Alkane
−24.1
Aldehyde

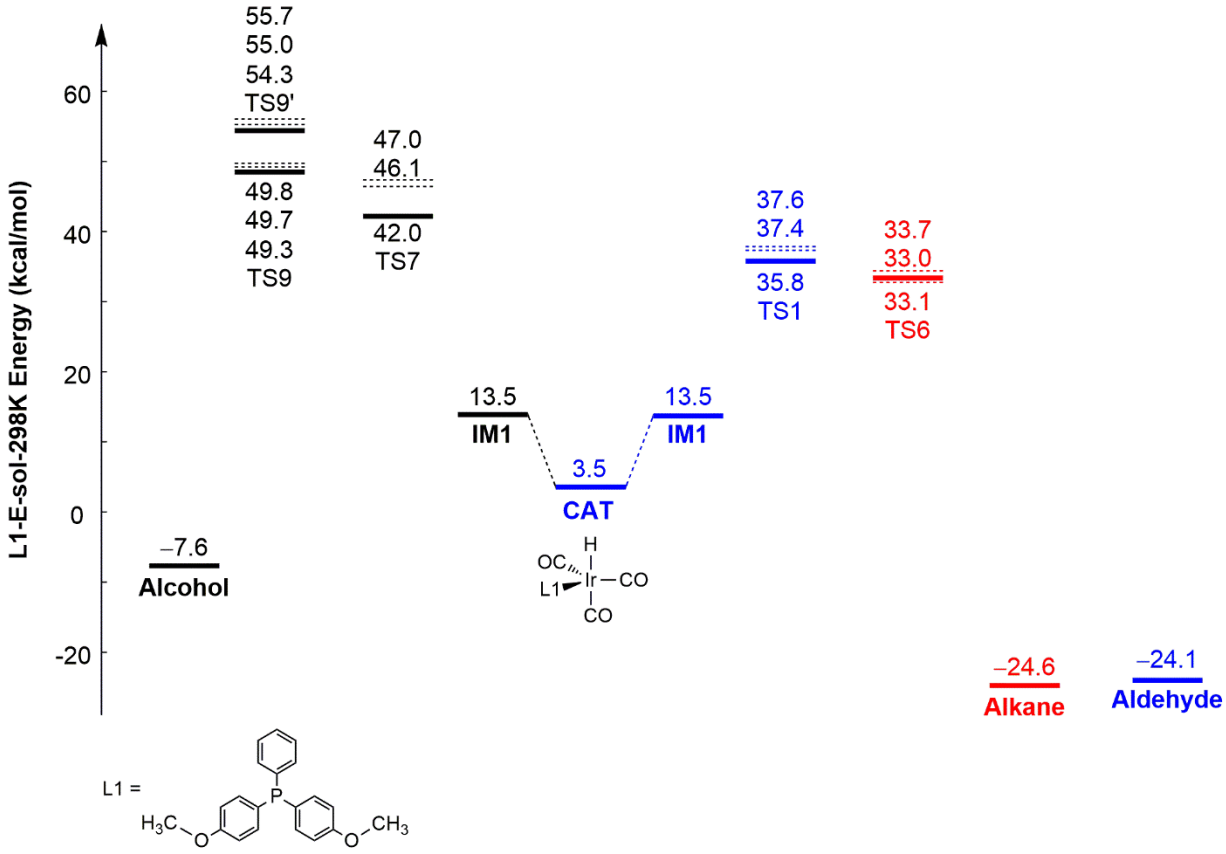
L1-E-sol-298K Energy (kcal/mol)
60
40
20
0
-20
55.7
55.0
54.3
TS9'
49.8
49.7
49.3
TS9
47.0
46.1
42.0
TS7
37.6
37.4
35.8
TS1
33.7
33.0
33.1
TS6
13.5
IM1
3.5
CAT
13.5
IM1
−7.6
Alcohol
−24.6
Alkane
−24.1
Aldehyde
L1 =

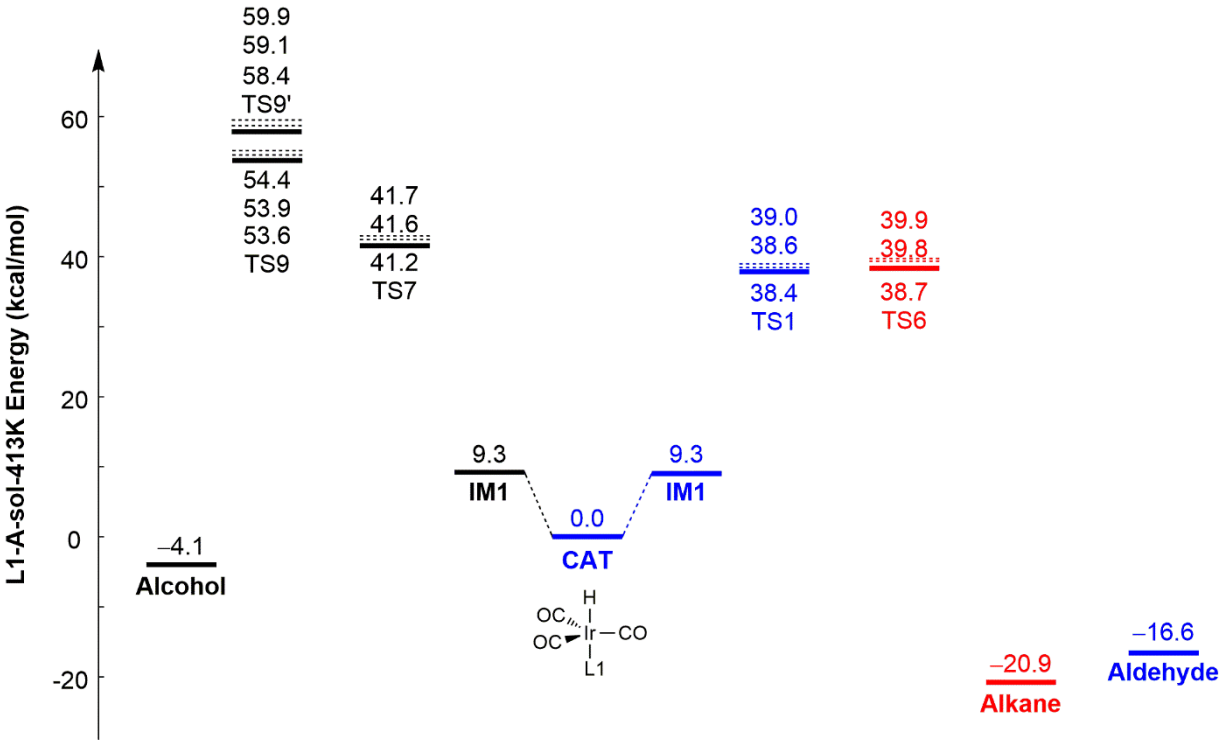
L1-A-sol-413K Energy (kcal/mol)
60
40
20
0
-20
59.9
59.1
58.4
TS9'
54.4
53.9
53.6
TS9
41.7
41.6
41.2
TS7
39.0
38.6
38.4
TS1
39.9
39.8
38.7
TS6
9.3
IM1
0.0
CAT
9.3
IM1
H
OC
OC
Ir—CO
L1
−4.1
Alcohol
−20.9
Alkane
−16.6
Aldehyde

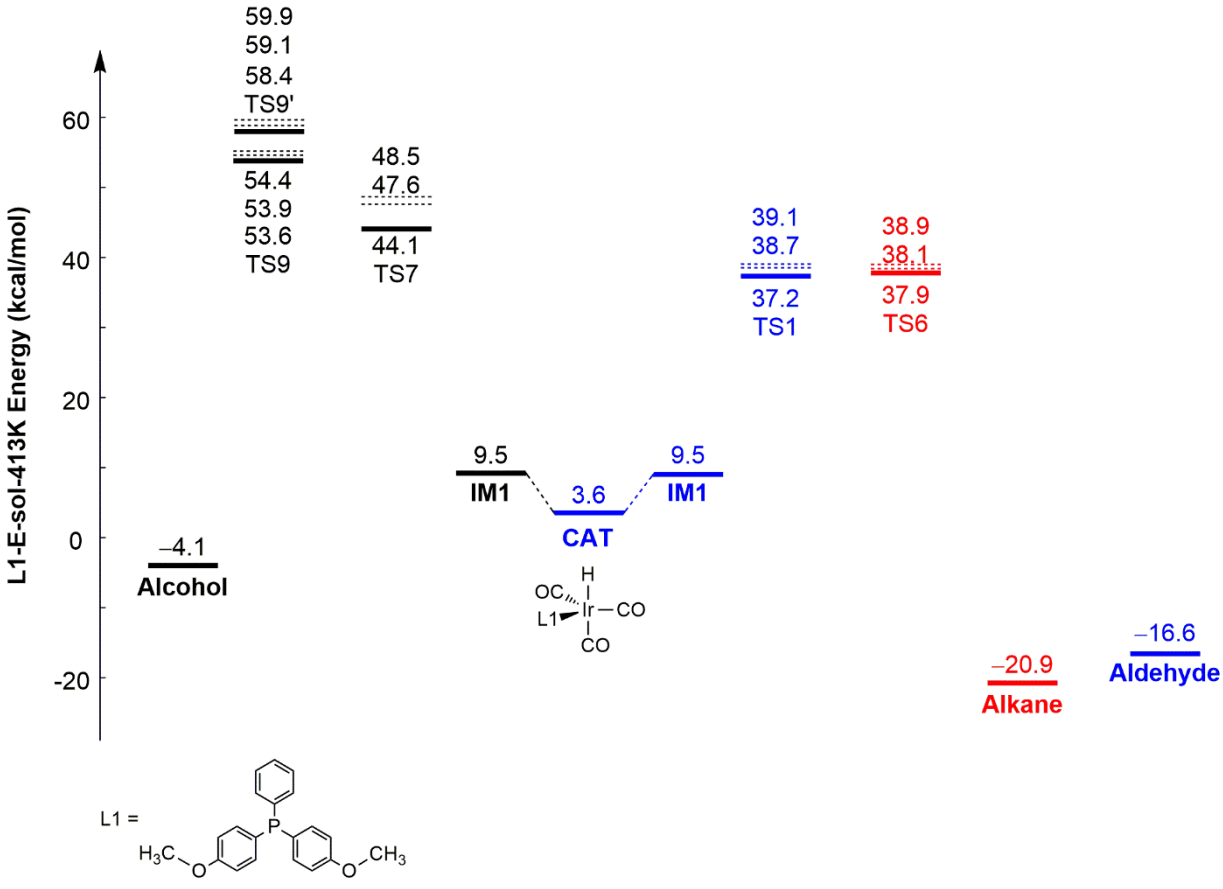
L1-E-sol-413K Energy (kcal/mol)
60
40
20
0
-20
59.9
59.1
58.4
TS9'
54.4
53.9
53.6
TS9
48.5
47.6
44.1
TS7
39.1
38.7
37.2
TS1
38.9
38.1
37.9
TS6
9.5
IM1
3.6
CAT
9.5
IM1
H
OC
L1
Ir—CO
CO
−4.1
Alcohol
−20.9
Alkane
−16.6
Aldehyde
L1 =
H3C
O
P
O
CH3

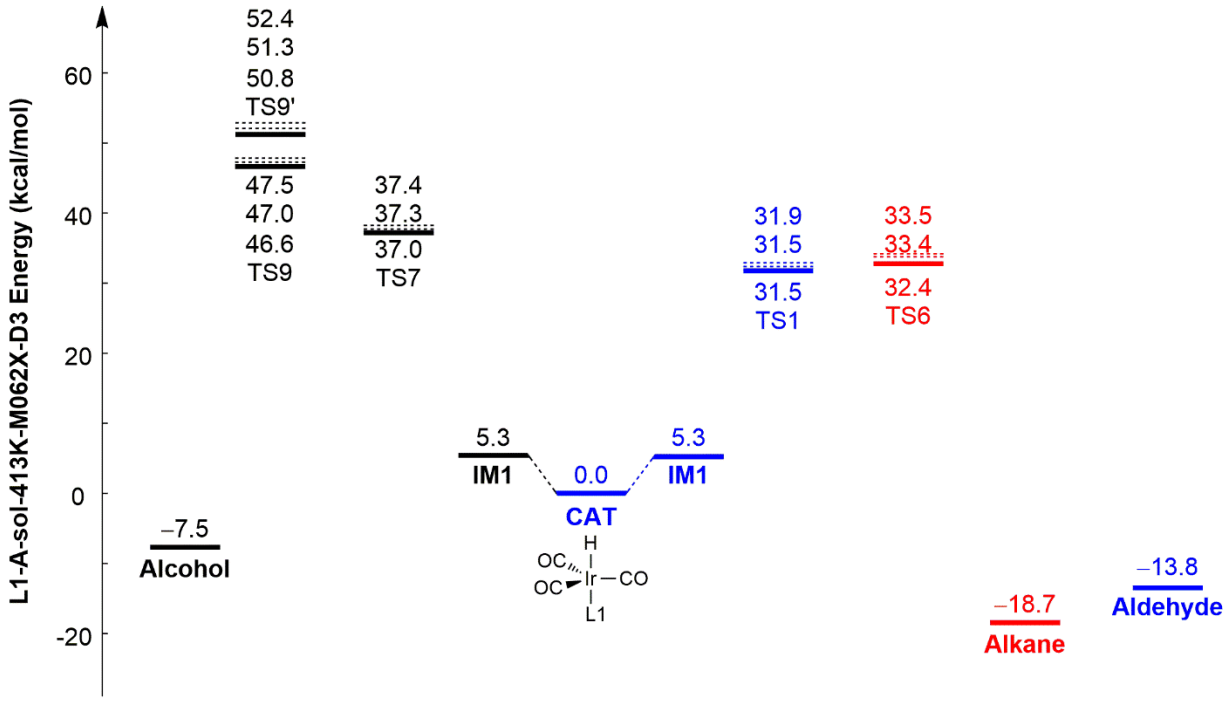
L1-A-sol-413K-M062X-D3 Energy (kcal/mol)
60
40
20
0
-20
52.4
51.3
50.8
TS9'
47.5
47.0
46.6
TS9
37.4
37.3
37.0
TS7
31.9
31.5
31.5
TS1
33.5
33.4
32.4
TS6
5.3
IM1
0.0
CAT
5.3
IM1
H
OC
OC
Ir—CO
L1
−7.5
Alcohol
−18.7
Alkane
−13.8
Aldehyde

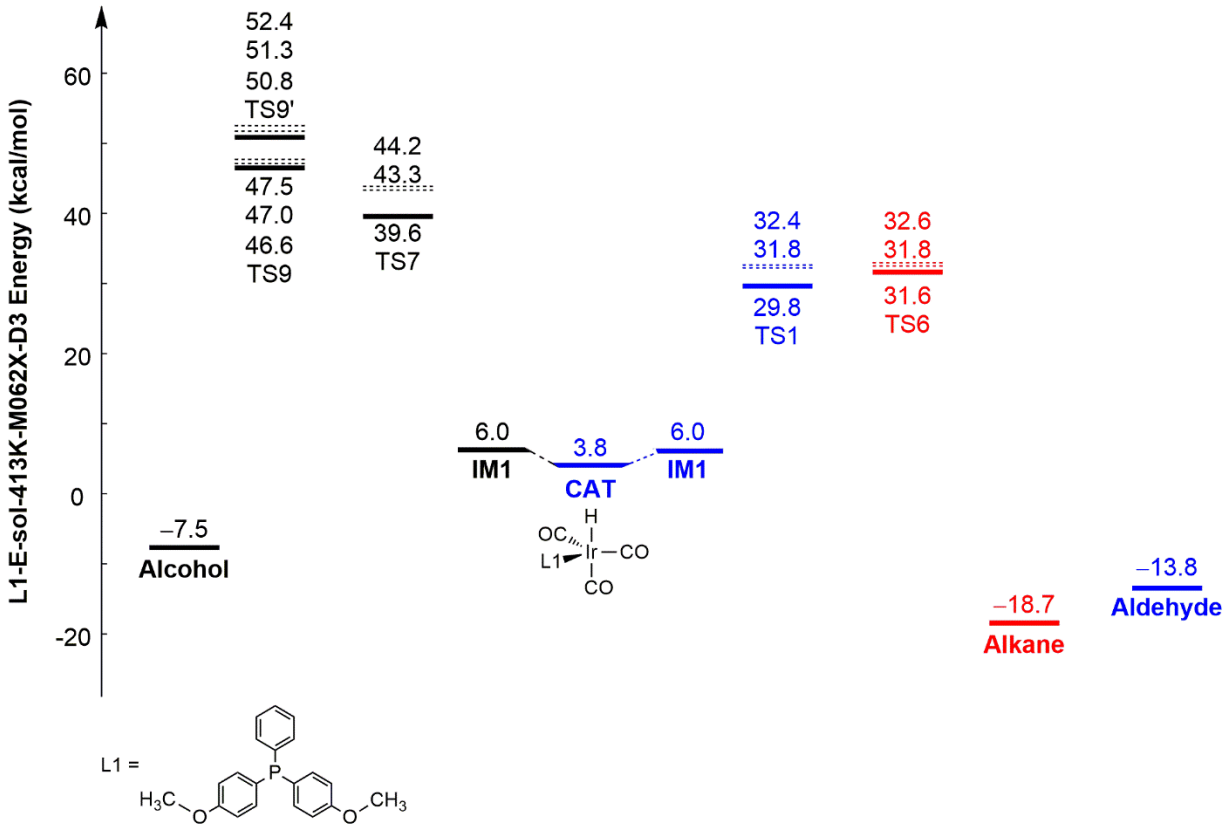
L1-E-sol-413K-M062X-D3 Energy (kcal/mol)
60
40
20
0
-20
52.4
51.3
50.8
TS9'
47.5
47.0
46.6
TS9
44.2
43.3
39.6
TS7
32.4
31.8
29.8
TS1
32.6
31.8
31.6
TS6
6.0
IM1
3.8
CAT
6.0
IM1
H
OC
L1
Ir—CO
CO
−7.5
Alcohol
−18.7
Alkane
−13.8
Aldehyde
L1 =
P
H3C
O
O
CH3

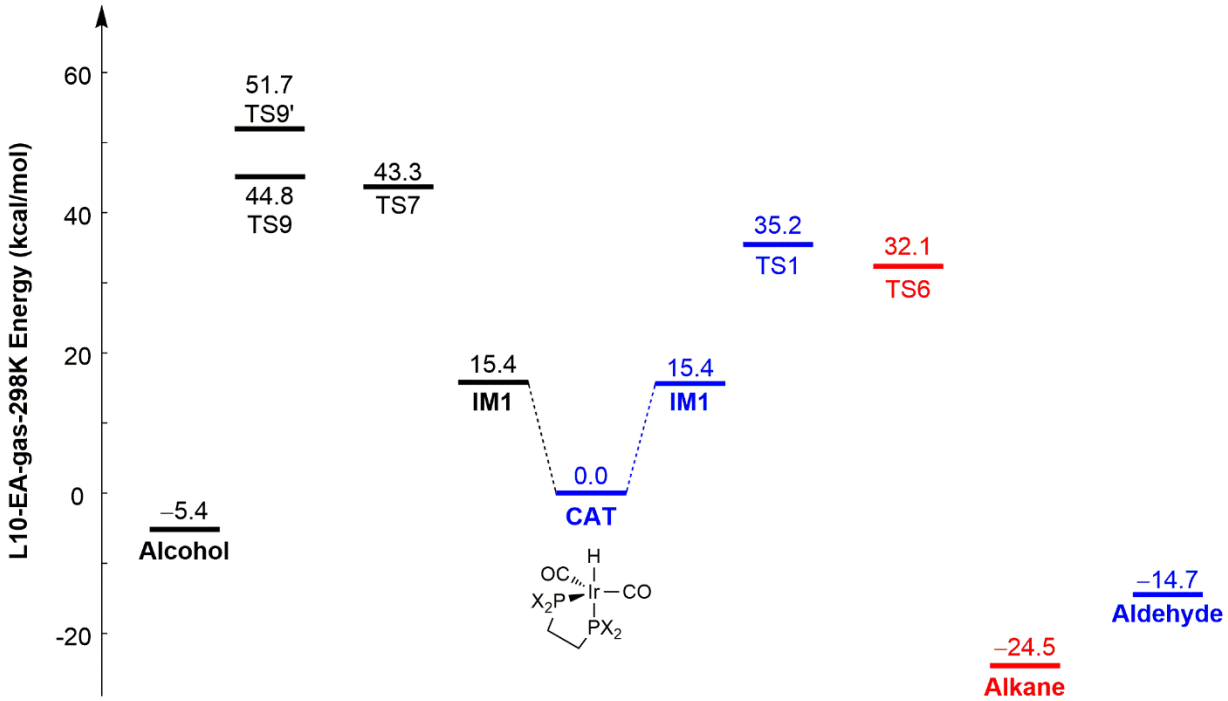
L10-EA-gas-298K Energy (kcal/mol)
60
40
20
0
-20
51.7
TS9'
44.8
TS9
43.3
TS7
35.2
TS1
32.1
TS6
15.4
IM1
15.4
IM1
0.0
CAT
−5.4
Alcohol
−14.7
Aldehyde
−24.5
Alkane

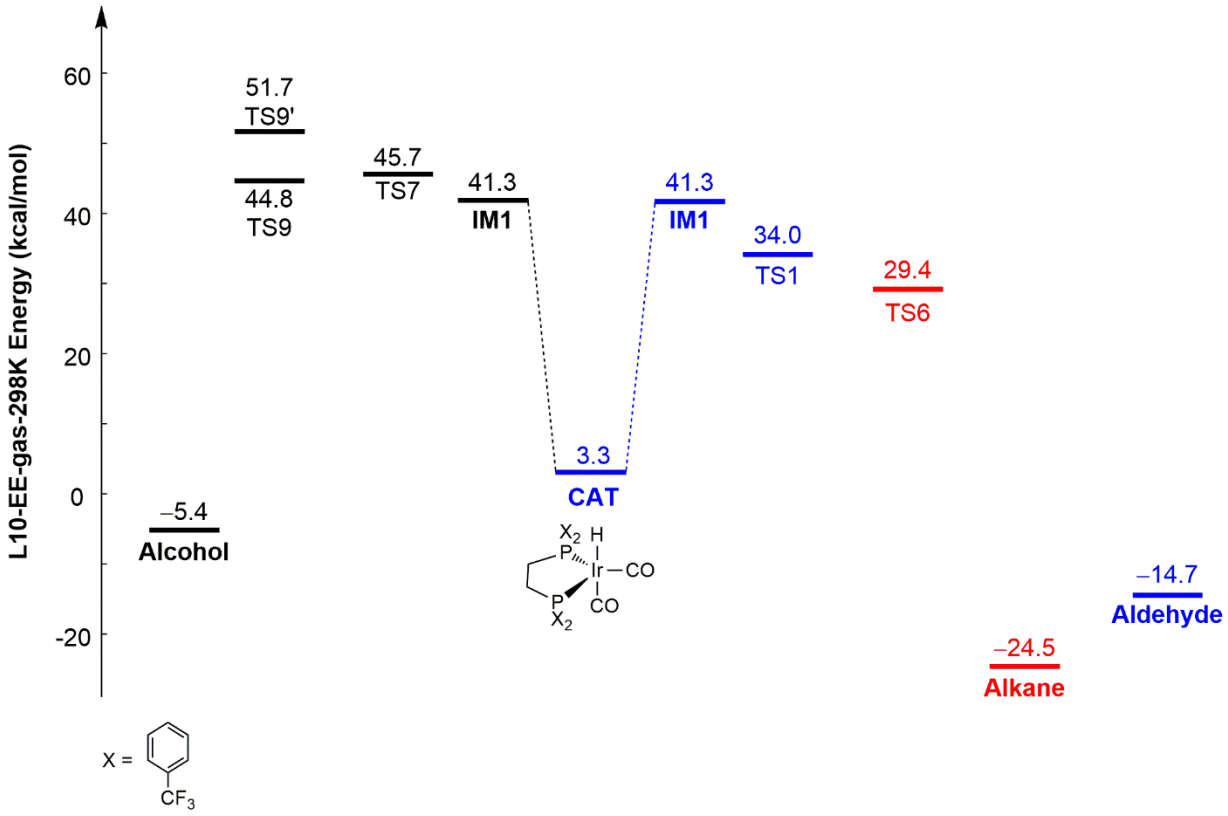
L10-EE-gas-298K Energy (kcal/mol)
60
40
20
0
-20
51.7
TS9'
44.8
TS9
45.7
TS7
41.3
IM1
41.3
IM1
34.0
TS1
29.4
TS6
3.3
CAT
−5.4
Alcohol
−14.7
Aldehyde
−24.5
Alkane
X =
CF3

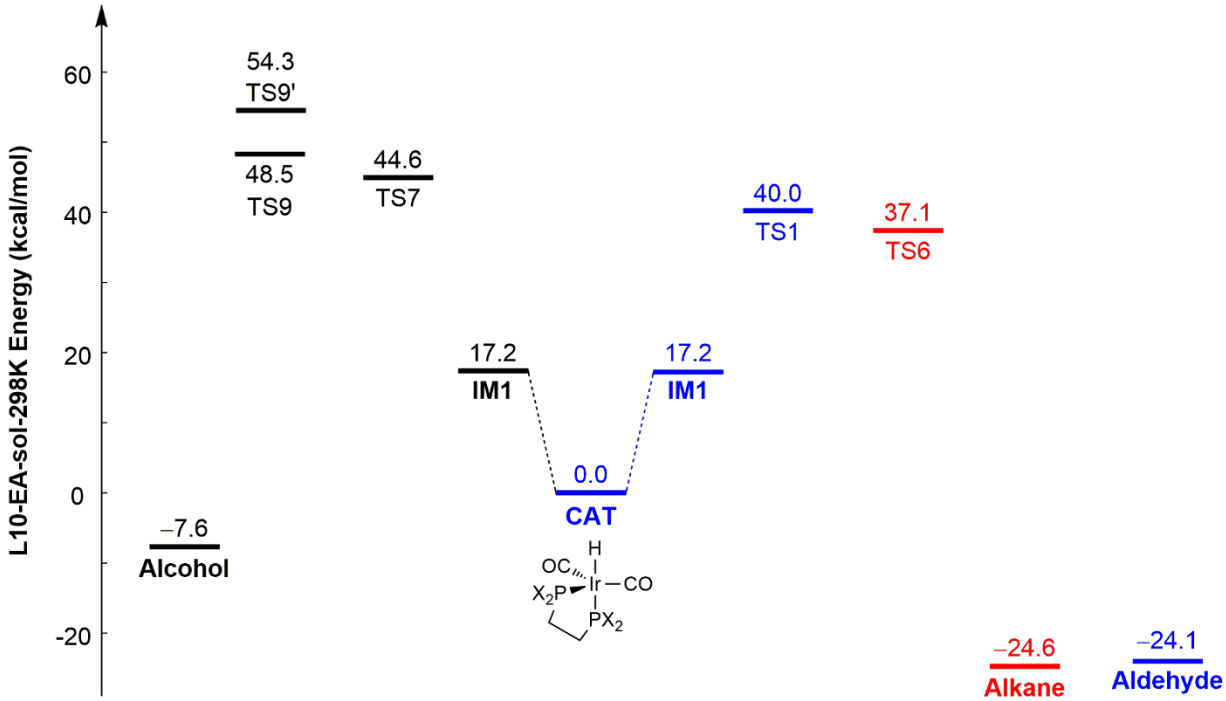
L10-EA-sol-298K Energy (kcal/mol)
60
40
20
0
-20
54.3
TS9'
48.5
TS9
44.6
TS7
40.0
TS1
37.1
TS6
17.2
IM1
17.2
IM1
0.0
CAT
−7.6
Alcohol
−24.6
Alkane
−24.1
Aldehyde

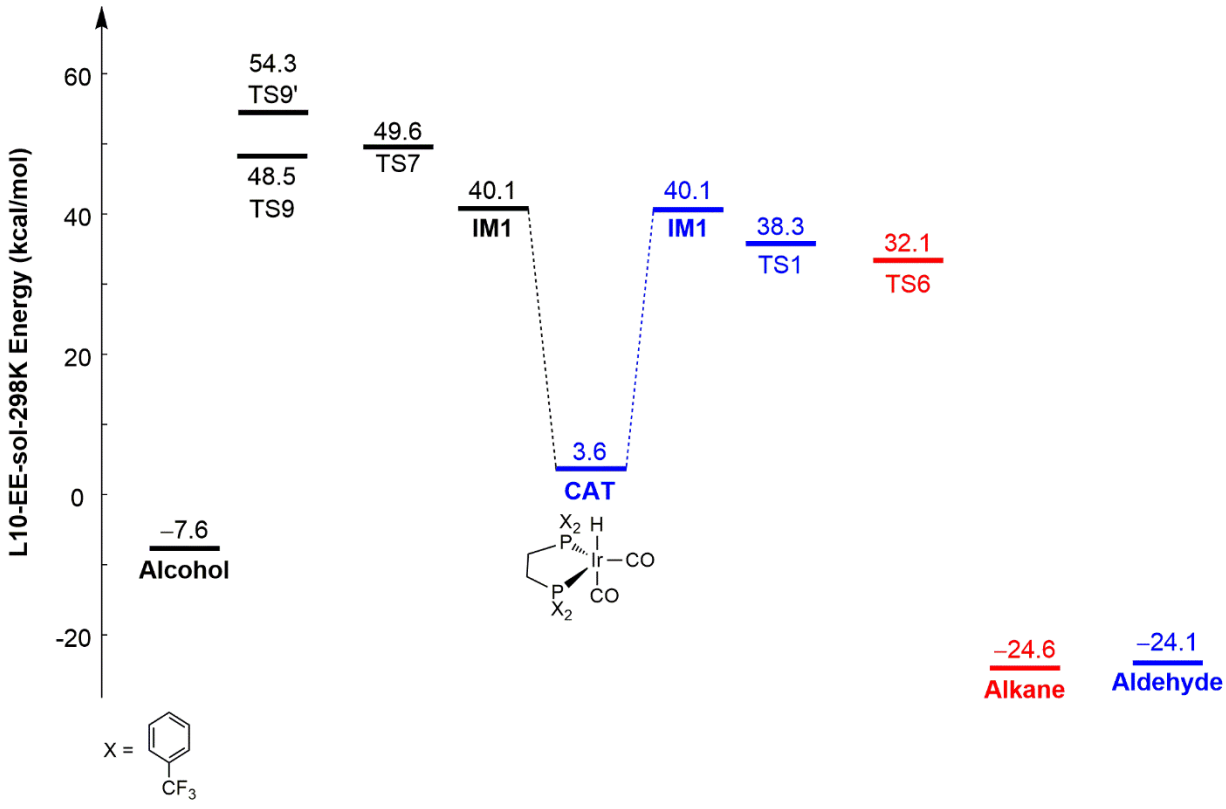
L10-EE-sol-298K Energy (kcal/mol)
60
40
20
0
-20
54.3
TS9'
48.5
TS9
49.6
TS7
40.1
IM1
40.1
IM1
38.3
TS1
32.1
TS6
3.6
CAT
−7.6
Alcohol
−24.6
Alkane
−24.1
Aldehyde
X =
CF3

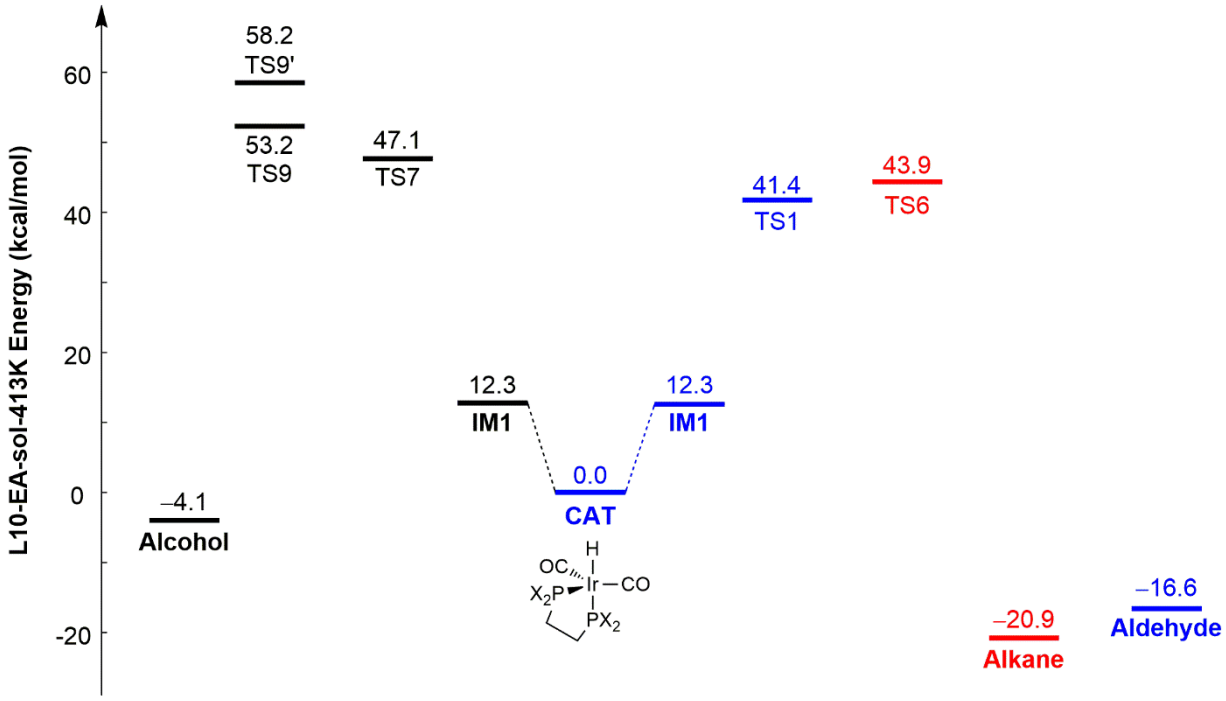
L10-EA-sol-413K Energy (kcal/mol)
60
40
20
0
-20
58.2
TS9'
53.2
TS9
47.1
TS7
41.4
TS1
43.9
TS6
12.3
IM1
0.0
CAT
12.3
IM1
−4.1
Alcohol
−20.9
Alkane
−16.6
Aldehyde

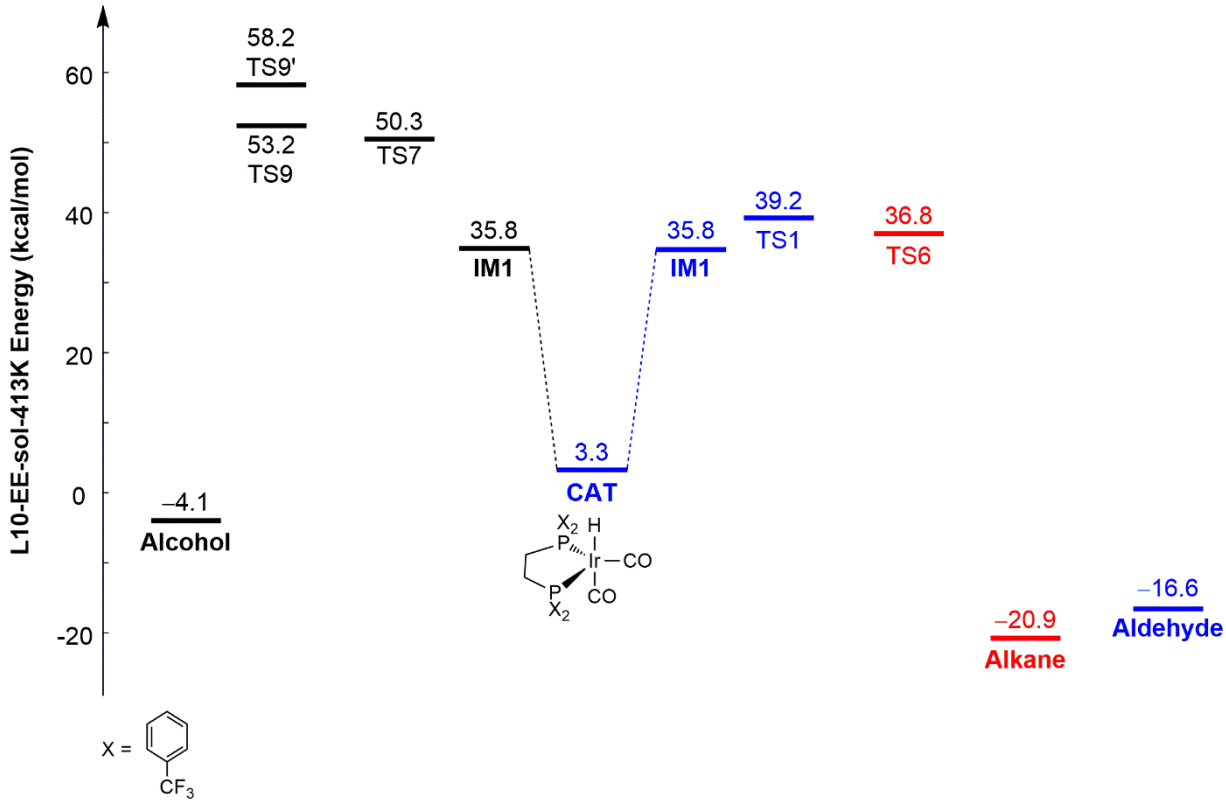
L10-EE-sol-413K Energy (kcal/mol)
60
40
20
0
-20
58.2
TS9'
53.2
TS9
50.3
TS7
35.8
IM1
3.3
CAT
35.8
IM1
39.2
TS1
36.8
TS6
−4.1
Alcohol
−20.9
Alkane
−16.6
Aldehyde
X =
CF3

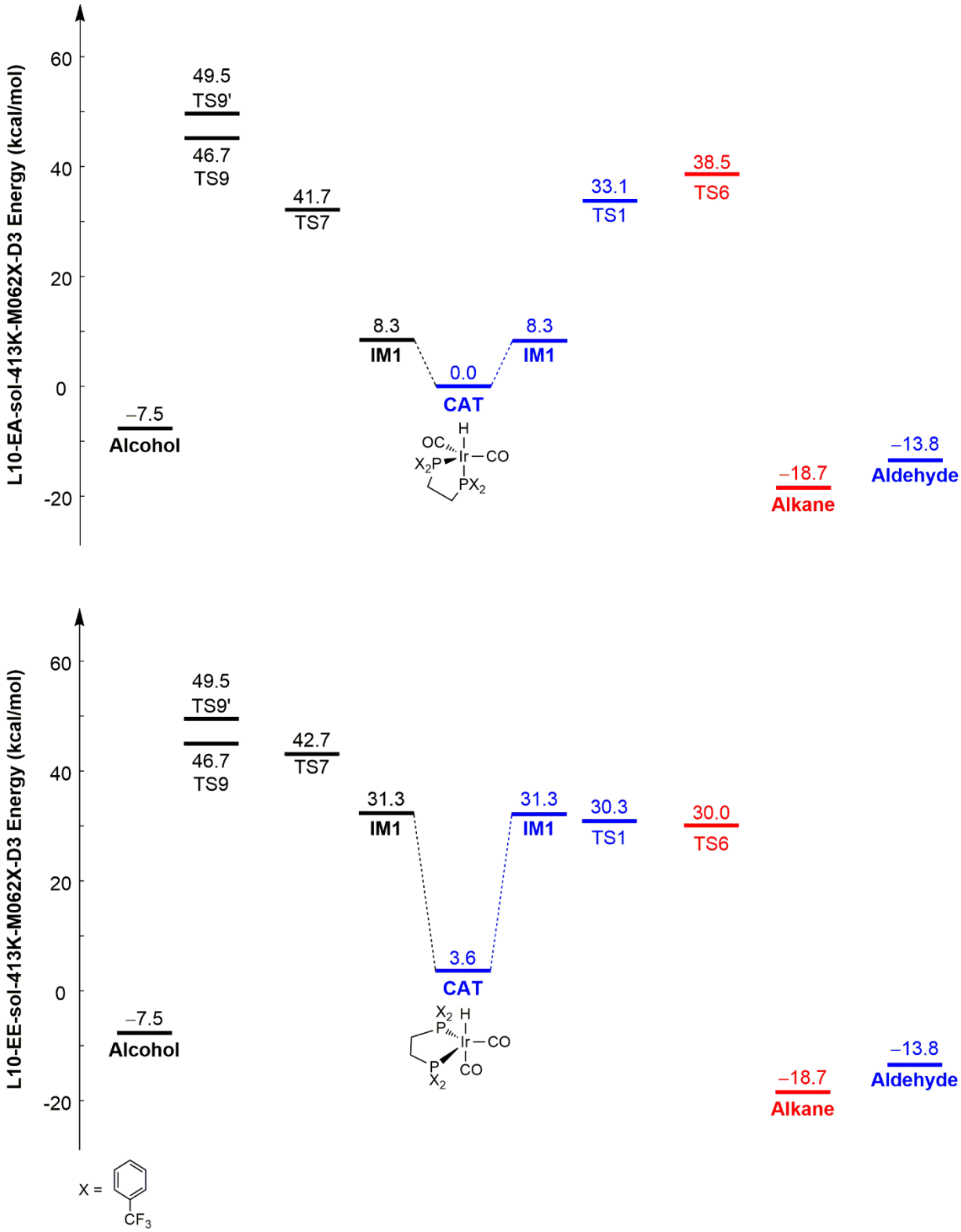

Figure DFT-S6. Free energy profile of the catalytic cycle shown in Scheme S1 catalyzed by L1 and L10 ligands (only the important transition states are listed). Dash line presents the isomers with different conformation.

Reference

[1] Purification of Laboratory Chemical (Eds: Perrin, D. D.; Armarego, W. L. F.-). Pergamon Press, Oxford, **1988** *3*.
[2] Mirabelli, K. Christopher, T. H. David, F. F. Leo, L. M. Francis, R. G. Gerald, B. B. Deborah, M. S. Blaine, O. L. B. Joan, T. C. Stanley, K. J. Randall, *J. Med. Chem.* **1987**, *30*, 2181-2190.
[3] E. P. Cappellani, S. D. Drouin, G. Jia, P. A. Maltby, R. H. Morris, C. T. Schweitzer, *J. Am. Chem. Soc.* **1994**, *116*, 3375-3388.
[4] Frisch, M. J. *et al*. Gaussian 16, Revision A.03. *Gaussian Inc. Gaussian, Inc., Wallingford CT, 2016*
[5] Y. Zhao, D. G. Truhlar, *J. Chem. Phys.* **2006**, *125*, 194101: 1-18.
[6] P. J. Hay, W. R. Wadt, *J. Chem. Phys.* **1985**, *82*, 299-310.
[7] A. Schaefer, C. Huber, R. Ahlrichs, *J. Chem. Phys.* **1994**, *100*, 5829-5835.
[8] A. V. Marenich, C. J. Cramer, D. G. Truhlar, *J. Phys. Chem. B* **2009**, *113*, 6378-6396.
[9] Y. Zhao, D. G. Truhlar, *Theor. Chem. Acc.* **2008**, *120*, 215-241.
[10] S. Grimme, J. Antony, S. Ehrlich, H. Krieg, *J. Chem. Phys.* **2010**, *132*, 154104.
[11] C. Kubis, W. Baumann, E. Barsch, D. Selent, M. Sawall, R. Ludwig, K. Neymeyr, D. Hess, R. Franke, A. Börner, *ACS Catal.* **2014**, *4*, 2097-2018.
[12] A. D. Becke, *J. Chem. Phys.* **2010**, *98*, 5648-5652.
[13] H. S. Yu, X. He, S. L. Li, D. G. Truhlar, *Chem. Sci.* **2016**, *7*, 5032-5051.
[14] I. Piras, R. Jennerjahn, R. Jackstell, A. Spannenberg, R. Franke, M. Beller, *Angew. Chem. Int. Ed.* **2011**, *50*, 280-284.
[15] H. C. Kang, C. H. Mauldin, T. Cole, W. Slegeir, K. Cann, R. Pettit, *J. Am. Chem. Soc.* **1977**, *99*, 8323–8325.